MYLONITE DEVELOPMENT IN THE WOODROFFE THRUST, NORTH OF AMATA, MUSGRAVE RANGES, CENTRAL AUSTRALIA

VOLUME 1

by

Timothy Hampton Bell,
B.Sc.(Hons), Adelaide

Department of Geology and Mineralogy
University of Adelaide

June, 1973

CONTENTS

Page

SUMMARY

The mylonitization of amphibolite and granulite facies acid gneisses lying respectively east and west of the Woodroffe Thrust, central Australia has been studied in detail in an area fifteen kilometres north of Amata. The macro, meso and microstructural effects of mylonitization on the structure of the country rock to either side, and the further development of the mylonitic rocks was examined. The microstructural study was confined to the major constituents within the rocks examined i.e. quartz, feldspar and mica. The development of host and new grain fabrics, and the angular relationships between host and new grains, and adjacent new grains, for quartz, was also studied in some detail.

The schistosity within the mylonitic rocks is axial plane to folds of country rock layering and schistosity, on both sides of the main mylonite belt. This is most apparent in the amphibolite facies gneisses east of the Woodroffe Thrust as they have been strongly penetrated by the mylonitization. Intrafolial folds of the mylonitic schistosity which refold the above folds, are also produced such that the axial planes of the later folds are parallel to the mylonitic schistosity outside them. Both the mylonitic lineation and the axes of these folds bend through large angles in the plane of the mylonitic schistosity. This phenomenon occurs on all scales, and there is evidence to suggest that it causes ductile rotation of relatively unmylonitized blocks several kilometres long of amphibolite facies acid gneiss (sitting within the mylonite) relative to one another about an axis normal to the mylonite schistosity.

The microstructural development of the mylonites is described in terms of ductile deformation and recrystallization. The only brittle

deformation present occurs about, and associated with, pseudotachylite formed on the granulite facies acid gneiss margin to the mylonitic rocks. The pseudotachylite forms as a late stage event and is often discordant with and intrusive into the mylonitic schistosity. It is thought to be a product of fusion after brittle failure due to an increased strain rate. Significant differences in recrystallization microstructures occur from the granulite to the amphibolite facies side of the mylonite zone (i.e. from west to east). The subgrain and new grain size in quartz and feldspar, the new grain size in mica, and the degree of recrystallization relative to strain is far greater on the amphibolite facies side. Subgrains were seen in highly deformed mica on the granulite facies side but not on the amphibolite facies side. In quartz, the nucleation sites for new grains differ across the zone with new grains growing on host grain edges on the amphibolite facies side but on host grain edges and deformation band boundaries on the granulite facies side. The nucleation mechanisms in quartz and feldspar include bulge, subgrain growth and coalescence, and in quartz on the amphibolite facies side, involve considerable subgrain rotation. The nucleation mechanisms in mica may involve subgrains on the granulite facies side but not on the other side.

Host grain - new grain angular relationships (from c - axes) for quartz also differ considerably from side to side across the main mylonite zone. On the granulite facies side there is an extremely strong angular relationship between host grains and new grains directly adjacent to them. On the amphibolite facies side there is no such relationship but instead a near-uniform angular distribution of new grains about the host. There is also a considerable difference in the fabric development relative to the degree of strain. On the amphibolite facies side of the

main mylonite zone the mylonite fabric is strongly developed within host grains with very little strain, whereas, on the granulite facies side the same degree of preferred orientation is not attained until there has been considerable strain. New grains also develop the mylonite fabric during syntectonic growth with relatively less strain on the amphibolite facies side. Hence there must be a radical difference in the combination of slip and climb systems operating from side to side across the main mylonite zone. These differences in nucleation, degree of recrystallization relative to strain and combination of slip and climb systems operating, can only be a result of a difference in the rate of climb of individual dislocations and/or the number of dislocations able to climb. The only significant chemical difference between the granulite and amphibolite facies acid gneisses which is known to affect dislocation generation and movement in such a way is the higher water content in the amphibolite facies acid gneiss. The only other factor which might be involved is a strain rate difference (which of course could be dependent on the water content difference).

The fabric, petrographic and chemical evidence suggests that the granulite and amphibolite facies rocks were initially in contact before or during the early stages of mylonitization at a point east of the Woodroffe Thrust where the microstructure shows an ultimate degree of development. The tectonic significance of this is discussed.

This thesis contains no material which has been accepted for the award of any other degree or diploma in any University nor, to the best of my knowledge and belief, does it contain any material previously published or written by another person, except where due reference is made in the text.

T.H. BELL

Acknowledgements.

Professor R.W.R. Rutland and Dr. T.P. Hopwood are gratefully acknowledged for suggesting mylonites for a thesis study. Professor Rutland, Dr. M.A. Etheridge and Dr. R.L. Oliver supervised the work and I thank them all.

I would especially like to thank Dr. Etheridge for time spent with me in discussion, the effort he put into reading the bulk of the numerous drafts and the suggestions for improvement of the thesis that he made.

I also thank the following people for help in the fields indicated: Mr. R. Barrett (photography), Mr. M. Bridges (statistics), Mr. D. Bruce (thin section preparation), Mr. R.J. Hill(computing), Miss M. McBriar (petrography), Mrs. K. Round (typing), Miss M. Swan (drafting advice), Mr. S. Trzichy (sodium, magnesium and water analyses), Mrs. D. Walker (typing) and Mr. R.G. Wiltshire (computing and general discussion).

Finally I thank my wife for her support and encouragement throughout my course of study and for her invaluable help with drafting and compilation of the thesis.

1.1 Mylonitization and Mylonites

'The old planes of schistosity become obliterated, and new ones are developed; the original crystals are crushed and spread out, and new secondary minerals, mica and quartz are developed. The most intense mechanical metamorphism occurs along the grand dislocation (thrust) planes, where the gneisses and pegmatites resting on those planes are crushed, dragged, and ground out into a finely laminated schist (Mylonite, Gr. mylon, a mill) composed of shattered fragments of the original crystals of the rock set in a cement of secondary quartz, the lamination being defined by minute inosculating lines (fluxion lines) of kaolin or chloritic material and secondary crystals of mica. Mylonites may be described as microscopic pressure-breccias with fluxion structure, in which the interstitial dusty siliceous, and kaolinitic paste has only crystallized in part.' (Lapworth, 1885, p.558-559). This was the first detailed description of mylonites and their formation. Lewis (1885) described similar rocks and attributed them partly to similar processes (for instance his descriptions of granulated and broken quartz). However, he considered the feldspar megacrysts and biotite in these rocks had recrystallized, the former from 'dusty' inclusion-full feldspars and the latter from hornblende in the adjacent massive country rock. The former of these two papers (which were presented on the same page in Nature ninety years ago) has profoundly influenced subsequent literature on mylonites. It is only recently that the importance of observations like those of Lewis on the recrystallization of feldspar and biotite has been realized.

This section summarizes the historical development of the interpretation of mylonitization and mylonite structures. The papers

discussed have been selected because they are widely referred to, and/or because they represent important stages in the development of the theory.

1.1.1 Brittle Deformation Theories

Until the last decade, the processes of brittle deformation that Lapworth described were considered the dominant processes of mylonitization (Waters and Campbell, 1935; Hsu, 1955; Christie, J.M., 1960, 1963). Recently (Higgins, 1971), more importance has been placed on recrystallization processes, but many people (including Higgins) apparently still believe that brittle deformation is the dominant process of mylonitization.

The microstructures which the above workers attributed to brittle deformation were fractures, aggregates of small grains of quartz or feldspar (breakage,granulation), small grains of quartz surrounding or cutting through a larger quartz grain (grinding),small grains of feldspar surrounding or cutting through a larger grain (grinding), and small grains of mica surrounding and within a strongly deformed larger grain (shredding).

In transitional mylonitic rocks (i.e. rocks in the transition zone between country rock and mylonite e.g. augen schist, mylonite gneiss and blastomylonite), many geologists (including those above) believed recrystallization processes played a more important part, but brittle deformation was still inherent.

1.1.2 Strain Theories

The intense flattening that occurs during mylonitization was noted by Johnson (1967), McLeish (1971) and Ross (1973). They proposed that

mylonitization was a product of irrotational strain rather than simple shear. The main evidence used by Johnson and McLeish to support irrotational strain apart from the above flattening was the orthorhombic symmetry of quartz fabrics of mylonites from the Moine Thrust (Christie 1963).

The validity of this symmetry argument, however, has not been fully tested. Experimentally deformed quartzites (Tullis, Christie and Griggs, 1973) and syntectonically recrystallized fine grained quartz aggregates (in which the recrystallized grains were strained and flattened; Green, Griggs and Christie, 1970), gave approximately orthorhombic fabrics with respect to the major stress axis and the microstructural anisotropy. However, the relationships of fabric to microstructural anisotropy in quartz aggregates deformed experimentally by simple shear, and shear combined with strong compressive stress, have not been determined. Simple shear experiments on metals (Williams, 1962) and ice (Kamb, 1972) produced asymmetric fabrics about the microstructural anisotropy and the shear plane. Hence by analogy it is possible that asymmetric fabrics could form in quartz deformed by simple shear. In fact the quartz fabrics measured by Ramsay and Graham (1970) on what they considered to be simple shear zones in metagabbro, appear to be asymmetric with respect to the shear plane and the schistosity (though this could be due to insufficient data). However, no fabric data is available for the case of shear combined with a strong flattening strain. The quartz fabrics from such a deformation could quite conceivably be orthorhombic and this style of deformation is a distinct possibility for that which occurs during mylonitization. Apart from this, quartz fabrics measured

in other mylonites (Moore, 1970; Ross, 1973; and this thesis chapter 3) often show monoclinic symmetry with respect to the mylonitic schistosity suggesting rotational or shear strain (using the symmetry argument of Johnson and McLeish).

McLeish does not consider the possibility of simple shear combined with flattening. Hence his arguments against such a possibility are not known.

The variation in strain that occurs in shear belts was considered by Ramsay and Graham (1970). They concluded that, provided the walls of the shear zone were undeformed and volume change unimportant, such zones could only be formed by the process of heterogeneous simple shear. If mylonites are formed in such shear zones, because the strain in mylonitic rocks is so great, the mylonitic schistosity would be effectively parallel to the shear direction. However Ramsay and Graham showed that the schistosity within and due to the shear zone, should always curve into the country rock across the transition (between shear zone and country rock). This has not been recorded as typical of mylonite zones. In fact Ross (1973) recorded axial planes of folded country rock compositional layering parallel to mylonitic schistosity in adjacent mylonites. He also correlated folded compositional layering within these mylonites (with mylonitic schistosity axial plane) with that in adjacent country rock.

1.1.3 Experimental Work

Carter, Christie and Griggs (1964) compared microstructures in experimentally deformed and recrystallized quartzite with those in

naturally deformed quartzites from beneath the Moine Thrust (Plate 9) and quartz rich rocks of mylonite zones (Plate 10). They stated that petrologists have commonly attributed the origin of such microstructures to 'crushing' or 'granulation' of quartz grains, and concluded that since textures such as those in their Plate 9A,B,C and Plate 10B were solely a result of recrystallization due to deformation that, like textures in naturally deformed quartzites, perhaps had a similar origin.

One of the main microstructural features of the mylonites described by Lapworth which led him to interpret them as a product of brittle deformation was what he considered to be shattered fragments of original quartz set in a cement of secondary quartz. The ductile deformation and recrystallization microstructures experimentally produced in quartz aggregates by Carter et al. (op cit) and subsequently by Tullis et al. (op cit) are very similar to those described by Lapworth (and figured by Teall, 1918) for quartz. Similar microstructures have been experimentally produced by ductile deformation and recrystallization in olivine (Blacic, 1972). Hence the processes of mylonitization envisaged by Lapworth are questionable.

1.1.4 Ductile Deformation and Recrystallization Theories

Although a number of people recognized the significance of the work of Carter, Christie and Griggs (1964) with respect to ductile deformation and recrystallization in mylonites (e.g. McLaren and Hobbs, 1972; Green and Radcliffe, 1972; Ross, 1973), many still considered mylonites to be dominantly formed by processes such as Lapworth

envisaged (e.g. Hsu, 1966; Higgins, 1971; Belliere, 1971; Krupicka and Sassano, 1972). Thus to date it is only McLaren and Hobbs (1972), Green and Radcliffe (1972) and Ross (1973) who have considered the microstructures seen in mylonites in terms of ductile deformation and recrystallization. In fact, McLaren and Hobbs were able to show that the substructures they observed by transmission electron microscopy in mylonitic quartzites, indicated that the rocks had been plastically deformed by mechanisms involving generation, motion and interaction of dislocations. Green and Radcliffe, and Ross, considered that small grains adjacent to large strained grains of olivine-bronzite and quartz respectively, had formed by syntectonic recrystallization during the mylonitization.

1.2 Aim of Thesis

The preceding section shows that the origin of mylonites is still in doubt with regard to the internal changes which take place and the strain involved.

This thesis is a detailed study of these changes across the mylonite zone associated with the Woodroffe Thrust, in an area within the Musgrave Ranges, Central Australia. A structural analysis of the mylonites and the country rock to either side was accomplished. Specimens were collected from country rock on one side through the mylonite zone to country rock on the other side. These specimens were then subjected to detailed microstructural and preferred orientation studies.

The remainder of this introductory chapter is a summary of ductile deformation, recovery and recrystallization and their effect on microstructure and preferred orientation.

1.3 Microstructure and Preferred Orientation Development

The microstructures and preferred orientation(s) observed in polycrystalline materials depend on the deformation, recovery and recrystallization that these materials have undergone.

1.3.1 Ductile Deformation

Deformation experiments on single crystals (Schmid 1925) have shown that deformation occurs by slip or twinning on specific crystallographic planes in specific directions. Slip occurs at a critical resolved shear stress (the Schmid Law). Schmid found that the single active slip system was that for which the stress (resolved on the slip plane and in the slip direction) was the highest amongst the equivalent slip systems available.

A grain within a polycrystalline aggregate however, cannot freely change its shape during deformation of the aggregate because of the constraints of its neighbours. A minimum of five independent slip systems is needed for an arbitrary shape change (Von Mises, 1928). Taylor (1938) considered homogeneous strain (under uniaxial tension or compression) of a polycrystalline aggregate. He postulated that amongst all combinations of five independent slip systems capable of accomodating a given strain, the active combination would be that one for which the sum of the absolute values of the glide shears is minimum.

The work done (computed from the above principle which assumes that an aggregate deforms uniformly) is identical to that calculated from a maximum work principle advanced by Bishop and Hill (1951a, 1951b). This principle considers that the work done is as if the aggregate

deforms uniformly. Bishop (1954) extended this principle to produce a theory of preferred orientation development. This theory is essentially equivalent to that of Taylor but the labours involved in choosing the five slip systems necessary for an arbitrary strain, are minimized through application of the maximum work principle.

The disadvantages of Taylors theory were considered by Calnan and Clews (1950) to be;

a) that homogeneous deformation rarely occurs in practice.

b) that the heavy computation makes its application to metals other than those which are face centred cubic, virtually impossible.

They proposed an ingenious theory which considers deformation to be inhomogeneous. They introduced the concept of an effective stress axis upon a grain which differs from the applied stress axis due to constraints of surrounding grains. As the applied stress increased, the resolved shear stress would increase until slip would occur in some grains if they were isolated. However grains around them provide constraints which prevented the resolved stress from reaching the critical value. They postulated that the effective stress axis changes its orientation because of the above constraints (and so that the critical resolved shear stress is not exceeded for the principal slip system) until it is parallel to [100], [111] or [110] (for f.c.c. metals). At these positions there are many slip systems available and deformation can occur without violating conditions of continuity across grain boundaries. This however, would not produce preferred orientations, as the slip systems are symmetric about the above orientations. This difficulty was overcome by assuming that the development of preferred orientation was confined to surface grains which would be less constrained and

grains for which large constraints would be necessary to prevent single or duplex slip.

Both Bishop and Hill (1951) and Taylor (1956) objected to the above theory on the grounds of lack of preservation of continuity across grain boundaries after deformation. However Calnan and Clews did consider this (for f.c.c. and b.c.c. metals) as they proposed continuity of grain boundaries could be preserved by those grains undergoing multiple slip. This may not be applicable to adjacent surface grains however, though their theory does predict textures for many crystal structures which are in fair accord with those observed.

The availability of computers removed one objection of Calnan and Clews to Taylors theory. Using linear programming methods Chin and Mammel (1967) and Chin, Mammel and Dolan (1967) applied Taylors theory. They found that one of their results was practically identical to that obtained by a Bishop and Hill analysis (Hosford and Backofen, 1964). Chin and Mammel (1969) then showed that the method of Bishop and Hill was in fact completely equivalent to Taylors theory.

The other objection of Calnan and Clews was refuted by Wonsiewicz and Chin (1970). They deformed a number of individual metal crystals of varying composition by plane strain compression. According to the Taylor theory two distinct combinations of slip systems were favoured at the initial orientation. They found that shear stresses, set up by friction due to the surroundings, favoured one of the combinations depending on the sign of the shear. The sign changed from one portion of the crystal to another, and as a result it separated into macroscopically distinct regions which deformed according to that combination of slip systems favoured by the sign of the shear. Hence if lattice rotation during

deformation caused instability such that the crystal separated into regions of different orientation, the analysis must be based on the current rather than the initial orientation with each region considered as a separate homogeneously deformed body. Thus, although the Taylor theory is based on homogeneous deformation, it remains essentially valid for inhomogeneous deformation.

Groves and Kelly (1963, 1969) discussed the problem of strain in materials which do not satisfy the Von Mises criterion for ductile deformation of an aggregate, (i.e. materials which do not have five independent slip systems). These materials cannot ductilely deform as crystal aggregates by slip alone. They suggested that polycrystals which even at high temperatures posses too few independent slip systems to undergo general dilatation free strain by glide alone can deform by dislocation climb and/or cross slip occuring in association with slip. Twinning can also provide another effective and independent deformation system and the Taylor analysis was modified to cover preferred orientation development by this means (Chin, Mammel and Dolan, 1969).

Cross slip and climb of dislocations however, are also essential processes in recovery (Jonas, McQueen and Wong, 1968; Jonas Sellars and Tegart, 1969).

1.3.2. Recovery

Cross slip and climb of dislocations are essential processes in recovery, which includes all annealing phenomena that occur before the appearance of recrystallized grains. When cross slip and climb operate concurrently, the screw and edge components of dislocations are able to surmount barriers and rearrange themselves into lower energy configurations (Jonas et al, 1968, op cit). This leads to polygonization which

includes a lowering of the overall dislocation density and the formation of subgrains.

Recovery can be static or dynamic. Static Recovery is polygonization driven by internal stresses (i.e. cross slip or climb of individual dislocations in response to the stress fields of other dislocations) and thermal activation. Dynamic Recovery is polygonization during deformation driven by external as well as internal stresses and thermal activation.

Dynamic recovery proceeds more rapidly than static recovery due to the accelerating effects of shear stresses and strains associated with deformation. The resolved shear stress components of the external stress close up extended dislocations which increases the rate of cross slip and climb (Seeger, 1957; Wong, McQueen and Jonas, 1967) and deformation produces intersection jogs and vacancies which promote climb (Shoeck, 1961).

1.3.3 Recrystallization

Beck and Hu (1966) define primary recrystallization as a process in which stored energy of deformation (stored strain energy) is released through migration of high angle grain boundaries. This is essentially the same as the classical picture of recrystallization which according to Beck (1954) involves nucleation and growth of new strain free grains at the expense of a deformed matrix. Normal grain growth and secondary recrystallization also involve movement of high angle grain boundaries but take place after primary recrystallization has occured. They are driven by the tendency to reduce grain boundary energy rather than stored strain energy.

Crystallization is regarded as the growth of discrete crystals from their chemical constituents (Etheridge, 1971). Obviously these definitions overlap. However for the purpose of the following discussion crystallization is considered to include the nucleation and growth of a radically different chemical phase with respect to the host (e.g. nucleation and growth of mica within feldspar or on a grain boundary in a quartz aggregate).

The development of preferred orientation due to recrystallization depends on the two processes, nucleation and growth, and these will be considered separately below.

1.3.3.1 Nucleation

The Classical Theory of Nucleation

This theory was formulated by Gibbs in 1877. It was first applied quantitatively to experiment by Volmer and Weber (1926) and was then modified by Becker and Doring (1935) who applied it to liquid-solid and gas-solid phase changes. However it was initially applied to the condensation of a pure vapour to form liquid. The basic notion was that local random fluctuations of energy or density causes condensation of a group of vapour atoms to a liquid embryo. The stability of this embryo would be dependent on the balance between the surface free energy (i.e. the energy needed to form an interface between the two phases) and the volume free energy decrease which would favour the embryo's growth. The surface free energy increases as the second power of the embryo radius, but the volume free energy increases as the third power. Hence at a critical radius, the embryo becomes a stable (viable) nucleus. Above this radius it would tend to grow but

below this radius it would tend to disappear.

Becker (1938) made the first attempt to modify the above theory for the more complicated case of a transformation within a solid phase (compositional changes only). He also considered the surface energy and certain crystallographic aspects of nuclei in solid-solid transformations.

Later workers showed that nucleation in solid-solid transformations is not homogeneous or random as the above model suggests. That is, it takes place preferentially on grain boundaries (Burke and Turnbull, 1952; Cahn, 1956) and individual dislocations (Cahn 1957). The possibility of nucleation on impurity particles was also suggested. These localities enhance nucleation because they help reduce the surface free energy factor, and, in the case of dislocations and grain boundaries, provide stored energy for the nucleation process to release.

Orowan (1954) pointed out that classical nucleation theory cannot apply to the formation of recrystallization nuclei in pure metals and perhaps also in impure metals. He showed that the energy required to create a thermal fluctuation in copper from which a recrystallization nucleus could form, was much larger than that needed for the nucleation process (i.e. the critical radius is too large and the activation energy too high). Hence, even allowing for a decrease in the surface free energy factor due to heterogeneous nucleation, it appears for relatively pure metals that the theory does not predict experimental results.

In alloys however, for certain compositions of the nucleus with respect to the host (these compositions are dependent on the temperature

at the time of nucleation) there is a substantial contribution to the driving force for nucleation from the free energy change of the whole assembly (Becker, 1938; Uhlmann and Chalmers, 1965; Burke, 1965). In the initial stages of nucleation there is also a contribution from the change in free energy per atom of the nucleus from the moment of nucleation until it reaches its optimum free energy for that temperature (Uhlmann and Chalmers, 1965).

A classical nucleation mechanism could theoretically produce a nucleus of any orientation with respect to the host. However if a change in volume of the nucleus occurs with respect to the host material, elastic energy considerations may play a part in determining the orientation of the nucleus.

Spinodal decomposition - the Cahn-Hilliard non-uniform model of nucleation in two component systems.

An objection to the classical theory of nucleation is the implied assumption that a sharp interface exists between nucleus and matrix, at which the composition and/or structure changes abruptly. Gibbs (1887) recognized two classes of phase change;

a) Those changes small in degree but large in spatial extent.

b) Those large in degree but small in extent.

Classical nucleation considers only the latter.

Cahn and Hilliard (1959 b) considered the former type exemplified by a small composition fluctuation spread over a large volume. They found that, as supersaturation increases, the following changes occur in the properties of the critical nucleus;

a) The work required for its formation becomes progressively less than

that given by the classical theory, and approaches continuously to zero at the spinodal (the point of inflexion on the free energy versus composition curve).

b) The interface with the exterior phase becomes more diffuse until finally no part of the nucleus is even approximately homogeneous.

c) As the spinodal is approached the radius increases to infinity.

Thus between the spinodals no work is required to form a critical nucleus, and an initial compositional fluctuation in a homogeneous phase quenched to within the spinodal, can grow because even a small change in composition lowers its free energy (Yund and McAllister, 1970; p.12). A supersaturated phase cooled to within the spinodal would therefore spontaneously decompose at a rate limited only by diffusion. The critical wavelength for a fluctuation which will grow is determined by the gradient energy (a term analogous to surface energy and which is proportional in a first approximation to the composition gradient Cahn and Hilliard, 1958). The critical wavelength approaches infinity at the spinodal.

Cahn (1962 c) modified the spinodal decomposition theory to cope with solid-solid nucleation. He considered the effect of strain energy produced by a change in size of the nucleus with respect to the host (Cahn, 1962 a) and predicted preferred orientations that would arise from this. He also showed that the effect of strain is to decrease the driving force for decomposition.

Thus, for alloy systems, spinodal decomposition is a viable nucleation mechanism, provided that the composition of the host at the temperature of nucleation falls between the spinodals. Whether it is feasible kinetically will depend (as mentioned above) on the rate

of diffusion.

Nucleation by subgrain growth or coalescence

This theory and those following are only applicable to recrystallization whereas the first two theories are applicable to crystallization also.

Beck (1949) and Cahn (1950) proposed that polygonization of a region with a high density of one type and size of dislocation, would provide subgrains, of which one would be a viable nucleus and grow into the surrounding matrix. That is, relatively dislocation free cells surrounded by diffuse dislocation rich boundaries form, and when one cell becomes large enough that part of its periphery is a high angle boundary the latter will begin to migrate rapidly and recrystallization starts.

Hu (1963) concluded that subgrains coalesce. He postulated that succesive subgrains bodily rotate and become merged with and indistinguishable from their neighbours. Li (1962) analysed the dislocation motions and energetics of this model.

Subgrain growth and subgrain coalescence produce nuclei related in orientation to the host. There is a possible range in orientation however because both models require sharp local deviations in orientation of the host.

Bulge Nucleation

The bulge nucleation model was proposed by Bailey (1960) and Bailey and Hirsch (1962). Bulge nucleation depends on pre-existing high angle (grain) boundaries, or the formation of high angle boundaries (such as kinks) by deformation. If there is a dislocation

density difference across such a boundary, the boundary will bulge between where it is pinned by subgrain boundaries, impurities etc., into the region of higher strain energy (i.e. dislocation density). The driving force is the stored strain energy difference because bulge of a high angle boundary in such a manner leads to lower energy configurations.

The orientation of new grains produced in such a way must be directly related to the host grain which is bulging. Hence the orientations of new grains produced by this mechanism are also roughly predetermined. There is a possible range in orientations due to the steep variation in dislocation density required by this model. These are consistent with sharp curvatures in the host material.

There is one important difference between bulge nucleation and the two previously mentioned models. That is, bulge nucleation can occur in deformed aggregates of materials with a low stacking fault energy, in which subgrain growth and coalescence are inhibited because of the relative difficulty of subgrain formation.

Dynamic Recrystallization

The replacement of the substructure within original grains by new grains which nucleate and grow during the deformation process is called dynamic recrystallization (Honeycombe and Pethen, 1972). Greenwood and Worner (1939) showed that lead could recrystallize during creep and since then dynamic recrystallization during high temperature creep has been shown to occur in many other face centred cubic materials such as gold, copper, gamma iron and nickel (Feltham, 1953; Gifkins, 1958-59; Hardwick, Sellars and Tegart, 1961-62; Richardson, Sellars and Tegart, 1966).

Rossard and Blain (1959, 1960) showed that dynamic recrystallization occurs in gamma iron during hot working (hot torsion). Dynamic recrystallization during hot working (other than creep) has subsequently been shown to occur in gold, copper, lead, nickel and certain stainless steels (Hardwick and Tegart, 1961; Richardson, Schnable and Stuwe, 1969; Honeycombe and Pethen, 1972; McQueen and Bergerson, 1972).

Dynamic recrystallization by a bulge nucleation mechanism has occured in aggregates deformed by high temperature creep and hot torsion (Richardson, Sellars and Tegart, 1966; Luton and Sellars, 1969; Honeycombe and Pethen, 1972). It is suggested that metals such as aluminium do not dynamically recrystallize because they have a high stacking fault energy. This gives rise to well defined sub boundaries which do not have as much energy to pin a migrating grain boundary as do the more tangled boundaries characteristic of alloys with low stacking fault energies.

McQueen and Bergerson (1972) performed hot torsion experiments on copper at relatively high strain rates and to large strains. This caused dynamic recrystallization. They stated that 'the observation that nuclei are only slightly larger than the subgrains, and that fairly high misorientations are present within the more heavily worked grains, indicate that high angle boundaries form from cell walls through the accumulation of dislocations.' This therefore is a mechanism involving pure subgrain rotation of some sort.

1.3.3.2 Growth

Thermodynamic Theories on Preferred Orientation Development

Many papers have been written which give a theoretical

thermodynamic treatment for the development of preferred orientation during crystallization and recrystallization under stress. The most important are those of Kamb (1959, 1961), and little advance has been made since his work. He applied Gibbs' (1906) thermodynamic conditions for solids under non-hydrostatic stress to 'linearly elastic crystals under infinitesimal strain.....For equilibrium across a given interface between crystal and fluid, the preferred orientation under any non hydrostatic stress is in most cases that for which the elastically weakest direction in the crystal is perpendicular to the interface. When recrystallization takes place by solution and redeposition, the preferred orientation is that which minimizes the chemical potential required for equilibrium across the plane normal to the greatest principle pressure axis'. Kamb recognized that his theory did not take account of 'annealing recrystallization after plastic flow'.

Macdonald (1960) suggested a somewhat similiar treatment but he assumed that the elastic strain energy is a maximum for crystals in the preferred orientation. Kamb (1961) however, showed that Macdonalds theory was invalid.

Paterson (1973) reviewed work in this field. He showed that two assumptions are generally used.

1) The internal state of the crystals except in regard to elastic strain, is the same before and after recrystallization.
2) All crystals in the aggregates are assumed to be under the same homogeneous stress as the aggregate as a whole.

The first condition (as recognized by Kamb) ignores annealing recrystallization. The second condition is untenable even as an approximation;

1) Because of implied discontinuities in strain across grain boundaries.
2) Where a fluid phase is assumed to exist, because shear stress cannot be transmitted across solid-fluid boundaries.
3) Heterogeneity of the stress field on a local scale might mean new grains nucleate under stress conditions markedly different from the average.

Paterson concluded that 'there are serious reservations about the usefulness of the homogeneous shear hypothesis, and.....both stress distribution and orientation are probably variables to be solved for calculating the thermodynamically (and/or kinetically) most favoured situation'.

Another problem with these thermodynamic treatments is that none of them consider nucleation and its effect on preferred orientation with the exception of Parlange (1968). He predicted preferred orientations of recrystallized nuclei by minimizing a quantity chosen according to a criterion of minimum work. However Paterson considers Parlange's treatment to be faulty because it'involves thermodynamic considerations which are defective in the treatment of the work term'.

Etheridge, Paterson and Hobbs (1973) suggest an empirical mechanism for experimental crystallization of phlogopite from its oxide constituents under load. This mechanism is an interaction of orientation dependent 'pressure solution' and anisotropic growth rate. This still does not consider nucleation (though the constraints on material movement discussed by Etheridge et al (op cit) will have an effect on nucleation) but it is a more realistic approach to crystal growth.

Coincidence Lattice - Kronberg-Wilson Relationships

Kronberg and Wilson (1949) noted textures from which the

orientation relationships of new and old grains could be determined. They found that these relationships showed that the new and old grains have a common sublattice of a special kind (referred to as a coincidence lattice) which consists of an array of atoms that lie on the lattices of both grains. A certain degree of lattice coincidence can be found for any orientation relationship between two grains. This orientation relationship however is only significant when the density of coincidence sites is relatively high (called Kronberg-Wilson relations).

Kronberg and Wilson (op cit) suggested that boundaries having a high coincidence site density are intrinsically high mobility boundaries. They suggested that since atom movements necessary for grain boundary migration may only be fractions of an atomic distance for these boundaries, atomic movements may be partly cooperative in nature and thus have low activation energies.

Aust and Rutter (1959a, 59b, 60a, 60b, 62) and Aust (1961) used Kronberg-Wilson relations to explain growth of new grains in the various metals on which they performed experiments. Aust (1969, and Simpson and Aust, 1972) is still a strong proponent of exact Kronberg-Wilson relation control on growth of new grains with respect to the host.

This mechanism predicts strong orientation relationships between host and new grains due to growth of recrystallized nuclei.

The orientation of the actual grain boundary can vary within a coincidence lattice. This can effect the degree of coincidence along the actual boundary which may have important effects on grain boundary mobility.

Orientation - impurity effect on grain boundary mobility

A number of anomalies occur concerning Kronberg-Wilson relations in

various metals, for example;

Aust and Rutter's (op cit) experiments on extremely pure metals show that new grains had nearly random orientation relationships with respect to the matrix. Graham and Cahn (1956) obtained a similiar result in impure Aluminium.

Lucke and Ibe (1964) examined orientation relationships between 1200 recrystallized grains and the deformed single crystal matrices in Al. They found that although Kronberg-Wilson type boundaries were favoured, there was considerable scatter from ideal Kronberg-Wilson relationships, and the rotation axes of dominant grains deviated on the average by 12° from Kronberg-Wilson boundaries.

Brandon, Ralph, Rangonathan and Wald (1964) proposed that deviations of several degrees in coincidence relationship could be accomodated by the presence of dislocations in the coincidence sublattice along the boundary plane. This means that boundaries can still exhibit appreciable atomic fit even when they deviate several degrees from ideal Kronberg-Wilson relationships. The introduction of dislocations of this sort not only rotates the two lattices with respect to each other, but also widens the boundary, introducing considerable porosity. Field-ion microscope work by Hren (1965) corroborates this.

Gordon and Vandermeer (1966) noted these anomalies. They examined the Kronberg-Wilson orientation relationship and Aust and Rutters subsequent work on it in considerable detail. For an ideal Kronberg-Wilson relationship they stated that the concept of lower activation energies in relatively 'tight' boundaries is difficult to understand - both intuitively and because it appears contrary to the well established fact of lower activation energies for diffusion in grain boundaries as

compared with grain bulk. The latter is presumably due to the 'looseness' or porosity of the grain boundary structure as compared with the 'tight' bulk structure.

They advance the view advocated by Li (1961,63) that boundaries between grains with Kronberg-Wilson orientation relationships, i.e. high coincident densities 'are in fact low mobility boundaries because their porosity is low and that only when grains deviate appreciably from the ideal Kronberg-Wilson relations is the boundary mobility high'. They find support for the above view also from the experimental fact that the most frequently observed high mobility boundary types are not the boundaries of highest coincidence site density. In addition to this, a coherent twin boundary can be considered as a Kronberg-Wilson boundary of the highest coincidence-site density and these twin boundaries are virtually immobile.

Thus Gordon and Vandermeer (1966) postulate;

1) The mobility of a grain boundary in pure materials depends on porosity in the boundary and is higher when porosity is greater because energy barriers to atomic diffusion are low when porosity is high.
2) The mobility of a grain boundary in an impure material depends also on the segregation of solute impurities at the boundary and tends to be lower when segregation is greater.
3) The porosity varies with the density of coincidence sites in the boundary and consequently with the orientation, type and perfection of the coincidence-site relationship.

They thus propose for very pure materials that 'random or near random boundaries having the highest mobilities should be preferred

rather than special boundaries of the K-W type' (they suggest that K-W boundaries should also actually be avoided).

When impurities are present, for boundaries of high to medium coincidence site density there is less segregation of solute atoms. With increasing porosity of the grain boundary there is increasing impurity drag due to increased segregation of impurities to boundaries. This causes lower grain boundary mobility. This relationship of mobility to concentration of impurities at the boundary means that there is a region of low segregation and high mobility and a region of high segregation and low mobility. Thus the mobility of boundaries with a medium to high coincidence site density goes through a maximum as misorientation from coincidence increases and then decreases, the highest overall mobility corresponding to that of some boundary of intermediate coincidence density for which the relative grain and boundary orientations are not quite ideal.

Thus this mechanism predicts random or near random host - new grain orientation relationships in pure materials, and preferred orientation of host - new grain orientation relationships about the Kronberg-Wilson relation in impure materials, for growth during recrystallization.

1.4 Preferred orientation of quartz [0001] in mylonitic rocks.

The [0001] quartz fabrics of mylonitic rocks have been attributed to brittle deformation (Christie, 1963), ductile deformation (Balk, 1952; Christie, 1963; Ross, 1973), post kinematic crystallization (Christie, 1963), and syntectonic recrystallization (Shelley, 1971; Ross, 1973). The actual mechanisms for development of preferred orientation (e.g. slip systems involved, orientation controls on recrystallized grains) have never been satisfactorily delineated. Most authors reasoned that not enough was known about the mechanisms by which quartz acquires a preferred orientation and hence attention focused on the symmetry of the fabric. In the following sections therefore, the quartz fabrics of mylonitic rocks will just be briefly described for deformed and recrystallized grains.

1.4.1 Fabrics of deformed quartz grains

Shelley (1971, fig. 9) shows a quartz fabric which he refers to as the fabric of a typical mylonite. Similar fabrics were obtained by Christie (1963, fig. 23 D1, D2, D3) from mylonitized quartzites which contained highly strained grains. This fabric is a girdle (or near girdle) normal to the lineation within the mylonites, which generally contains two maxima symmetrically oriented about the mylonitic schistosity.

Two maxima are not always present however. Balk (1952, fig. 15, 18) and Ross (1973, fig. 8) found deformed quartz grain fabrics, in quartzites near thrusts and in mylonites respectively, which had only one of the two maxima developed changing the symmetry with respect to the mylonitic schistosity from orthorhombic to monoclinic.

1.4.2 Fabrics of recrystallized quartz grains

Ross (1973) recorded fabrics obtained from small strain free inequant to polygonal grains within aggregates which lay between the strained quartz used in the above mentioned fabrics. These grains, considered by Ross to be a product of syntectonic recrystallization during mylonitization, have orthorhombic fabrics with respect to the mylonitic schistosity but tend to lie in two girdles at high angles to the mylonitic lineation rather than one girdle normal to it. Christie (1963) obtained somewhat similar fabrics in mylonitized quartzites which he considered had suffered 'post kinematic crystallization'.

Shelley (op cit) considered that the fabric he attributed to a typical mylonite, was due to preferential growth during syntectonic recrystallization of those quartz grains with the most stable orientations with respect to the slip systems operating during deformation. However he considered that the preferred orientation was related to the stress field rather than the strain and hence took no account of the effect of strain on orientation (his photographs and description show that much of the quartz in his mylonites is strongly strained).

1.4.3 Fabrics of experimentally produced mylonite like rocks.

Tullis, Christie and Griggs (1973) produced mylonitic microstructures in experimentally deformed quartzites. The fabric they recorded from deformed grains in a specimen shortened by 60% (at a strain rate of 10^{-5}/sec and 1000°C, fig. 9A), is somewhat similar to that found in natural mylonites by Christie (fig. 23 D2, D3). The similarity is that two maxima within the former fabric lie on or close to the

primitive circle and they are connected by a flattened small circle distribution. The difference is the extra maximum within the small circle. Tullis et. al. (op cit) attribute their fabric to mechanical reorientation of the c-axes by Dauphine twinning and intra granular slip. These processes may also be important during the development of preferred orientation of deformed quartz grains in natural mylonites.

1.4.4. The typical mylonite fabric

It is apparent from the above discussion that at least for deformed quartz grains in mylonites, there is a fairly typical fabric developed. This consists of a partial girdle normal to the mylonitic lineation which generally contains two maxima situated either side of the mylonitic schistosity. Sometimes, however, only one of these maxima is developed changing the symmetry of the fabric from orthorhombic to monoclinic. An example of the ultimate development of this fabric is shown in Figure 3 - 5 j.

2.1 Introduction

2.1.1 Location and broad geological relationships

This study was conducted in an area which lies along the South Australia - Northern Territory border between longitude 131°03' and 131°10' (see map). The rock outcrops in this area form part of the Musgrave Ranges.

The regional geological map of the Musgrave Ranges (Major, et al, 1967) shows that the above area contains granulite facies acid gneisses with some intermediate and basic inter bands on the west (fig 2-1a). These are separated from granulites and altered granulites (amphibolite facies rocks) to the East by the Woodroffe Thrust and the mylonitic rocks associated with it.

Three bands of mylonitic rocks are shown on the regional map. (See also fig 2-1a). Those furthest to the West are steeply dipping and associated with a fault which is later than and displaces the Woodroffe Thrust. The two bands to the East are shallow dipping to the West and associated with the Woodroffe Thrust. They are shown on the regional map to anastomose to the south of the area mapped. The plane of the Woodroffe Thrust is shown by Major et al (op cit) to lie at the contact of the granulites to the West with the central band of mylonites.

These regional observations differ only slightly from those of the author. The rocks between the anastomosing mylonite bands are amphibolite facies acid gneisses and not granulite facies, as they contain horneblende and biotite but no pyroxene.

2.1.2 Rock Types

The rock types west of the Woodroffe Thrust are mainly granulite facies acid gneisses which consist dominantly of quartz and feldspar with minor ortho pyroxene, clinopyroxene, garnet, apatite, biotite, opaque and sometimes a little horneblende. In the far west a few basic interbands and thick quartzites occur but they are rare in the monotonous acid gneiss sequence. The cross cutting dolerite dykes shown on the map dip steeply West on this side of the thrust. Some pseudotachylite occurs amongst the mylonitic rocks in Opparinna Creek.

The amphibolite facies country rocks East of the Woodroffe Thrust are also mainly acid gneisses but they contain a few granitic bodies in which the gneissosity is not as well developed, and which have discordant contacts with the foliated gneiss. These rocks however are similar in composition (fig 2.10, 791A and 791B). The acid gneisses east of the thrust are composed dominantly of quartz and feldspar, with minor biotite, horneblende, garnet, opaque and sphene. Dolerite dykes occur within these gneisses. They often intrude along the mylonite schistosity but are not mylonitized.

Pseudotachylite occurs at the contact of the granulite facies country rock to the West with the mylonites associated with the Woodroffe Thrust; i.e. at the position of the thrust plane as mapped by Major, et al (1967).

Due to the relative constancy of rock type within each of major zones of country rock, the mapping in these zones was mainly structural. The only mappable rock variations are the quartzites in the far west and the dolerite dykes (see map). The mylonitic rocks were differentiated on the basis that some were gneissic and others more schistose. These

contacts were mapped and they delineate the trend of the mylonitic schistosity.

2.1.3 Structural relationships across the Thrust

The relationship between country rocks either side of the Woodroffe Thrust is not known. They are structurally different and, although the chronology of deformation events on each side can be determined, time relationships from one side to the other are not known. The major penetrative schistosity in the granulite facies rocks is the first deformational event recognizable there. The dominant schistosity in the amphibolite facies rocks is the second deformational (or later) event.

Thus schistosity and lineation subscripts have time significance only within their respective sides of the Thrust. They imply no time relationships across the thrust.

2.2 Structural Analysis

The structure of the mylonitic rocks associated with the Woodroffe Thrust will be described first in this section even though the mylonitization is a late event in the deformation sequence. This is done to avoid repetition as the structure of the amphibolite facies country rock east of the Woodroffe Thrust has been strongly effected by the mylonitization and cannot be understood without prior knowledge of the deformation effects of mylonitization.

2.2.1 The mylonitic rocks associated with the Woodroffe Thrust (Sub areas 1, 2, 3 & 4).

The mylonitic rocks east of the Woodroffe Thrust are sporadically penetrative through much of the amphibolite facies country rock. They surround pods of relatively unmylonitized country rock in an anastomosing manner. There are however, two major belts of mylonitic rocks (i.e. sub areas 2 & 4), one of which (sub area 2) divides the amphibolite facies country rock into two main areas. In contrast with the amphibolite facies country rock, the granulites contain no mylonitic rocks associated with the Woodroffe Thrust beyond its main contact with them (the mylonites of sub area 6,occur along a vertical fault later than the Woodroffe Thrust).

The two major belts of mylonitic rocks are sub areas 2 and 4. However, thin (3 metres) bands of mylonitic rock penetrate the amphibolite facies country rock in sub areas 1 and 3 in an anastomosing manner. Structurally the mylonitic rocks of sub areas 1, 2, 3 and 4 are very similar.

2.2.1.1 Structural elements and style

The mylonitic schistosity (S_M) forms axial plane to folds of country rock schistosity (S_2) and layering (S) in sub areas 1 and 3. A good example of this is shown in fig 2.3C. These folds are relatively open where the mylonitic schistosity is not strongly developed, but tighten and become isoclinal once the mylonitic schistosity begins to dominate. Figs. 2.2b and 2.3a show such a fold, which is a flattened version of those shown in fig. 2.3C (These folds are referred to as $BS_2^{S_M}$ folds).

The schistosity (S_M) is defined by alignment of flattened quartz and feldspar grains and aggregates, and (001) of micas. As the folds tighten, the original schistosity and layering of the country rock is rotated into near parallelism with the mylonitic schistosity in the limbs, giving the latter a layered appearance. However, much of the apparently strong layering in these mylonites is due to the extremely strong mylonitic lineation (L_M: a table listing the structural elements in chronological order is shown in fig 2.8). L_M forms parallel to the axes of these $BS_2^{S_M}$ folds in the plane of S_M. It is partly due to extreme elongation of quartz and feldspar grains or aggregates and partly due to an intersection of S_2 with S_M. This extremely strong lineation results in an apparent layering in any section except that perpendicular to L_M.

Within the mylonites, another type of fold referred to as $BS_M^{S_M}$, folds the mylonitic schistosity (S_M) so that the axial plane remains parallel to the mylonitic schistosity outside it. In fact another weak mylonitic schistosity often develops in the hinges. Such a fold is shown in figs. 2.2c and 2.3 b. The fold shown contains a refolded $BS_2^{S_M}$ fold also. These folds are intrafolial and apparently contemporaneous with

the mylonitization. They can form adjacent to $BS_2^{S_M}$ folds. They sometimes have a weak elongation lineation developed parallel to their hinges.

The axes of both $BS_2^{S_M}$ and $BS_M^{S_M}$ folds are often folded through large angles in the plane of the mylonitic schistosity. They are folded in such a manner that the axial plane remains planar. The mylonitic lineation L_M (which is parallel to $BS_2^{S_M}$ fold axes) is also often folded in such a manner. Fig 2-4a shows L_M on one schistosity (S_M) surface bent through an angle greater than 90^o while on a lower schistosity surface it is undistorted and trends in the direction about which the lineation on the upper schistosity surface is bent. This phenomenon was observed on all scales (see orientation data).

Finally, there is a deformation later than the mylonitization which always folds the mylonitic schistosity with a sinistral sense looking north west (fig 2-2d). These folds $BS_M^{S_3}$ generally developed an axial plane schistosity (S_3) in their hinge defined by allignment of (001) of muscovites. These folds occur mainly in the north-eastern corner of the area mapped but they outcrop sporadically throughout sub areas 1, 2, 3 and 4 though they diminish considerably in frequency towards the south west of sub areas 3 and 4.

2.2.1.2 Orientation of Structural Elements

The orientations of the principal structural elements within the mylonitic rocks of sub areas 1, 2, 3 and 4 are shown in figure 2-5.

The mylonitic schistosity (S_M) in each sub area plots in a single maximum except in sub area 3 where the lower percentage contours are drawn out into a girdle (fig 2-5, $1S_M$, $2S_M$, $3S_M$, $4S_M$). The thin

mylonites which penetrate the country rocks in sub area 3, anastomose considerably (apparently they follow the weaknesses in the country rock to a certain extent). This produces the girdle in the lower percentage contours. Hence the mylonites are effectively planar.

The mylonitic lineation (L_M) is distributed in each sub area on a girdle which is the plane of S_M (fig 2-5 $1L_M$, $2L_M$, $3L_M$, $4L_M$). There is a strong maximum in sub areas 2 and 4 (the sub areas containing mainly mylonitic rocks) which plunges at a shallow angle to the south west. Thus, although S_M is planar, the mylonitic lineation is folded through 180^o in the plane of S_M (see earlier description of deformed $BS_2^{S_M}$, $BS_M^{S_M}$, and L_M; see also fig 2-4a). This spread is due to variation of the maximum elongation direction during deformation, and this in itself would also contribute to the spread of orientations.

The $BS_2^{S_M}$ fold axes (fig 2-5 $1BS_2^{S_M}$, $2BS_2^{S_M}$, $3BS_2^{S_M}$, $4BS_2^{S_M}$) also tend to be distributed in the plane of S_M. Not enough measurents were made to delineate their distribution clearly but whenever $BS_2^{S_M}$ folds were observed, L_M was always parallel to their axes and hence their distribution should simulate that of L_M. Very few $BS_M^{S_M}$ folds were measured (fig 2-6, $2BS_M^{S_M}$, $4BS_M^{S_M}$) and hence their distribution is meaningless. However as already stated, their axes also were seen to fold in the plane of S_M.

The orientations of the sinistral (looking NW) $BS_M^{S_3}$ folds which deform the mylonitic schistosity are shown in fig 2-7, $BS_M^{S_3}$. They plunge at shallow angles to the north west and have a fairly constant axial plane orientation (fig 2-7, S_3).

2.2.2 The amphibolite facies country rock (sub areas 1 & 3)

As mentioned at the beginning of the previous section, these rocks

(fig 2-1a, sub areas 1 & 3) consist of a number of ovoid blocks which are relatively un-affected by the mylonitization. They are surrounded by mylonitic rocks in a manner analogous to porphyroblasts in a schist. However a few thin mylonites penetrate even the largest of these blocks of country rock (see map).

2.2.2.1 Structural elements and style

The dominant schistosity (S_2) in the amphibolite facies country rock is defined by alignment of ellipsoidal quartz and feldspar grains and (001) of micas. It is generally parallel to a compositional layering (S). In the few localities where this is not so, tight to isoclinal folds of the layering (S) occur (fig 2-2a), with S_2 axial plane. An earlier schistosity S_1 can sometimes be seen in the hinges of these folds parallel to the layering. In the limbs of these folds S, S_1 and S_2 are effectively parallel (fig 2.8 lists the structural elements in chronological order).

A lineation L_2 defined by elongate grains and aggregates lies in the plane of S_2 parallel to $BS_1^{S_2}$ (or $B_S^{S_2}$) fold axes.

S_2 has been deformed by three different types of folds. The first of these are broad open folds which show up mainly in the orientation data and were rarely observed on a relatively small scale: Such a fold is shown in fig 2-2a. They have no axial plane structures and hence are denoted by the symbol BS_2. The second type of fold is that associated with the mylonitization. They have been previously described in the section on mylonites. These $BS_2^{S_M}$ folds are mesocoscopically developed (fig 2-3c) and have mylonitic schistosity developed as axial plane. The BS_2 folds are apparently earlier in time than the $BS_2^{S_M}$ folds because they

do not deform the mylonitic schistosity. They are unlikely to be contemporaneous because their statistical orientation differs substantially from sub area 1 to sub area 3 (see later).

The third type of fold is associated with the deformation which also deforms the mylonitic schistosity (i.e. the $BS_M^{S_3}$ folds). These folds ($BS_2^{S_3}$) are contemporaneous with the $BS_M^{S_3}$ folds and deform S_2 so that the folds have a sinistral sense looking northwest (this deformation affected S_M in the same manner). The $BS_2^{S_3}$ folds have an axial plane schistosity developed in their hinges which is defined by alignment of (001) of muscovite (fig 2-2a, & 2-2d).

2.2.2.2 Orientation of structural elements

The orientation of the principle structural elements within the relatively unmylonitized amphibolite facies country rock are shown in Fig 2-6. From sub areas 1 and 3, which are mainly country rock it can be seen that S_2 has a complex distribution. This is due to the overprinting effects of the three fold types described above. The effects of the $BS_2^{S_3}$ folds can be neglected as they are a small scale fold with a constant asymmetry and as readily seen from sub area 2, their equivalents within the mylonites did not effect the planar distribution of S_M (see map) greatly. Hence the S_2 distribution can be dominantly attributed to the overprinting effects of BS_2 and $BS_2^{S_M}$ folds. An attempt was made to determine the constancy of the distribution over the whole of the two sub areas. This was done by dividing each of sub areas 1 and 3 up into a number of smaller sub areas. The girdles marked were found to be penetrative over the whole of each sub area respectively. Since the mylonitization effects are non penetrative throughout the amphibolite

facies country rock, and the statistical fold axes for these two girdles are not related to any L_M or $BS_2^{S_M}$ maxima (fig 2-5), they can be attributed to the BS_2 folds. Measurements around individual large BS_2 folds and individual smaller $BS_2^{S_M}$ folds confirm this.

The remainder of the distribution can be attributed to the effects of the $BS_2^{S_M}$ folds. The distribution is additionally complicated by the fact that these folds are distributed in the plane of the mylonitic schistosity (see earlier section on mylonites).

The distribution of the country rock lineation L_2 has also been affected by these later deformations. Again the effects of $BS_2^{S_3}$ folds will be neglected for the reasons mentioned above. The distribution of L_2 is somewhat similar to the distribution of L_M in sub areas 1 and 3 (figs 2-5 & 2-6). This similarity is not as great in sub area 3 where there is a weak tendency for L_2 to be distributed in tight small circles around L_M concentrations. The statistical BS_2 fold axes also lie close to the statistical plane of the mylonitic schistosity in each sub area and hence to the L_M and $BS_2^{S_M}$ distributions. It appears that the initial orientation of L_2, before either deformation occured, was close to the statistical BS_2 fold axes (within 20^o). Hence the BS_2 folds did not affect the L_2 distribution greatly. The subsequent mylonitization redistributed L_2 in the plane of S_M.

2.2.2.3 The relationship of sub area 1 to sub area 3

The mylonitic rocks of sub area 2 lie between the amphibolite facies country rock of sub areas 1 and 3 (fig 2.1a). The mylonitic schistosity of sub area 2 is statistically planar (fig 2-5, $2S_M$). The mylonitic lineation (L_M) and $BS_2^{S_M}$ folds are both distributed through more

than 90^{o} in the plane of the mylonitic schistosity (see section 2.2.1.2.). This indicates considerable ductile rotation in the plane of S_M. Since this rotation is macroscopic in extent it is feasible that sub areas 1 and 3 may be related by a rotation in the plane of S_M, across sub area 2.

The above conclusion can be easily tested. If sub areas 1 and 3 were initially the same block of country rock before mylonitization, but have been rotated by the mylonitization, constant linear structures within them prior to mylonitization should lie on the same small circle about the pole to the statistical plane of the mylonitic schistosity after rotation. The only such structure available is the statistical BS_2 fold axis. When the above test was conducted on the statistical BS_2 orientation for sub areas 1 and 3, and showed that they do lie on the same small circle (fig 2-4c). However, this might just be coincidence, or more data may reveal that the statistical BS_2 fold axis for each sub area does not quite lie on the same small circle about the statistical pole to S_M.

If sub areas 1 and 3 were initially one block of country rock, then it is possible that BS_2 folds homogeneously affected both areas so that the structure in both was the same. Then if the BS_2 fold axis of sub area 1 was rotated on the above mentioned small circle to coincide with the BS_2 fold axis of sub area 3, and the limits of the girdle distribution of S_2 poles (which defined BS_2) were similarly rotated on their appropriate small circles about the statistical S_M pole, the distribution of S_2 poles obtained should be similar to that for sub area 3. This was done (fig 2-4c) using the 4% contour limits for sub area 1 and it was found that

on rotation they coincide almost exactly with the limits of the 3% contour in sub area 3 (see fig 2-4c). This strongly suggests that the mylonite deformation has rotated sub area 1 relative to sub area 3 through approximately 90^{o}.

2.2.3 The granulite facies country rock

The structure of these rocks is relatively simple. Sub areas 5 and 7 are the two areas of granulite facies rocks (fig 2-1a). They are separated by a thin belt of mylonitic rocks (sub area 6) which displaces the Woodroffe Thrust East side North by 200 - 300 metres. In granulite facies rocks further to the northwest, beyond the area mapped, there are a number of these faults, all of which displace the Woodroffe Thrust in the same sense and by approximately the same amount.

The structure of sub areas 5 and 7 is practically identical as would be expected if the mylonite zone between them lies on a simple displacement as evidenced by the shift in the Woodroffe Thrust. Hence they will be dealt with simultaneously.

2.2.3.1 Structural elements and style

The country rock schistosity (S_1) is homogeneous and penetrative, and defined by ellipsoidal quartz and feldspar grains. It is parallel to a weak compositional layering (S) except within the thick (15 metres) quartzites in the far west of sub area 7 (see map). Close examination of schistosity and layering in these quartzites shows that the schistosity has an equal or slightly greater dip than the layering. However S_1 is effectively parallel to the compositional layering within the quartzites.

The lineation L_1 lies in the plane of S_1 and is defined by an

extremely strong mineral elongation (i.e. elongation of quartz and feldspar grains). A few small isoclinal folds of compositional layering S were found preserved in quartzite in sub area 7 (fig 2-1b) but they were not measurable and hence the relationship of L_1 to their axes is not known. S_1 is parallel to the axial plane of these folds which have the same sense (i.e. sinistral looking north) as the cross cutting relationship seen between S and S_1 in the thick quartzites.

2.2.3.2 Orientation of structural elements

The orientations of the principle structural elements in sub areas 5 and 7 are shown in Figure 2-7. The schistosity S_1 has the same constant orientation in both sub areas (fig 2-7, $5S_1$, $7S_1$) as would be expected if the mylonite zone between them (sub area 6, fig 2-1a) lies on a non-rotational displacement. There is no significant evidence of deformation of S_1 in the area mapped. There is some gentle warping throughout the area but it is insignificant and does not show up on the stereo plots. This warping has horizontal axes trending slightly west of north.

The lineation (L_1) in both sub areas is drawn out slightly in the lower contour intervals within the plane of S_1. This effect is only slight and probably due to minor variation in the long axis of the strain ellipsoid during S_1 formation. The distribution in sub areas 5 and 7 is very similar.

2.2.3.3 Boulder, xenolith or relict early structure?

In one locality within sub area 7 (see map) a block of folded gneissic rock was found within granulite facies gneiss (figs. 2.1c, 2.4b). The block contains a well preserved gneissic layering and a

schistosity which is oblique to this layering and the schistosity in the surrounding granulite facies country rock. Both the gneissic layering and the schistosity are folded with the country rock schistosity S_1 as axial plane. The block has a higher mafic content (garnet and biotite) than, and sharp contacts with the surrounding gneiss.

The possibilities for its origin are a boulder, xenolith or relic early deformation structure. This of course depends on the original nature of the surrounding gneiss. If the block is a relic deformation structure or a xenolith, the presence of at least one deformation and possibly two within it prior to the granulite facies deformation is of considerable importance as no deformation structures earlier than the formation of S_1 were observed. If the block is a boulder its significance is decreased, but it indicates a deformed gneissic terrain as a sediment source.

The sharp boundaries of the block and its higher mafic content than the surrounding gneiss perhaps indicate that a relic early structure is not as likely as the other possibilities. Just how it has managed to survive a granulite facies deformation is difficult to envisage and hence differentiating between the other two possibilities is virtually impossible.

2.2.3.4 The mylonitic rocks of sub area 6

These mylonites are very fine grained. The mylonitic schistosity (S_M) is well developed and has a layering parallel to it. The schistosity is defined by alignment of flattened and inequidimensional minerals and the layering is due dominantly to grain size and some compositional variation. The layering is sometimes emphasized by pseudotachylite

developed parallel to it. The belt of mylonites is very narrow and discontinuous. They merge with pseudotachylite on one side and sharply with granulite facies gneiss on the other (see map).

The mylonitic lineation (L_M) is extremely strong and defined by an intense elongation of quartz and feldspar grains and aggregates. No folds were observed associated with the mylonite formation except a general rotation of the country rock schistosity close to the mylonite belt (see map).

Fig 2-7 shows the orientation of L_M and poles to S_M. The mylonitic schistosity fans about the vertical on an axis which trends parallel to the approximately horizontal mylonitic lineation.

2.2.4 A brief summary of the structural events

2.2.4.1 The deformation events in chronological order East of the Woodroffe Thrust.

1) Formation of S_1 - no folds associated with this deformation were seen.
2) Deformation of S_1 (and S) and formation of S_2 axial plane to $BS_1^{S_2}$ ($B_S^{S_2}$) folds.
3) Mild deformation of S_2 forming BS_2 folds.
4) Mylonite deformation of S_2 forming S_M axial plane to $BS_2^{S_M}$ folds and the contemporaneous folding of S_M into $BS_M^{S_M}$ folds.
5) Deformation of S_2 and S_M forming S_3 axial plane to $BS_2^{S_3}$ and $BS_M^{S_3}$ folds.
6) Mostly brittle deformation of S_M associated with formation of pseudotachylite and probable formation of the Woodroffe Thrust (see chapter 3 for evidence regarding this).

West of the Woodroffe Thrust

1) Deformation of S, and formation of S_1 axial plane to $B_S^{S_1}$ folds.
2) Mylonite deformation of S_1 adjacent to pseudotachylite (see also chapter 3).
3) Deformation of S_1 associated with the formation of pseudotachylite and the Woodroffe Thrust.
4) Mylonite deformation of S_1 associated with displacemtnt of the Woodroffe Thrust.

2.2.4.2 The mylonite deformation associated with the Woodroffe Thrust

The deformation associated with the mylonitization is complex. S_M forms axial plane to $BS_2^{S_M}$ folds. S_M is subsequently folded and $BS_2^{S_M}$ folds refolded, by intrafolial $BS_M^{S_M}$ folds which have a weak new S_M developed in their hinges parallel to S_M outside the fold. $BS_2^{S_M}$ and $BS_M^{S_M}$ folds form adjacent to one another and their axes and L_M are often folded through large angles in the plane of S_M. This indicates an exceedingly ductile but heterogeneous deformation the tectonic significance of which is discussed in the final chapter.

2.2.5 Comparison with other work

The work of Collerson, Oliver and Rutland (1972), and Collerson (1972) is the only previous structural analysis accomplished in the Western Musgrave Ranges. Their results differ in a number of ways from the results of this work, but they are both compatible. Important differences occur however in the mylonitization structures observed and their effects on the amphibolite facies country rock. This however is predictable as this work concentrated on the effects of mylonitization on the surrounding rocks. Their orientation data for the amphibolite

facies rocks, reinterpreted in the light of the effects of mylonitization on them evident from this work, becomes compatible with these results.

Collerson (1972) did not recognize that much of the schistosity he saw within the amphibolite facies terrain was mylonitic. If his aL_2 and aL_3 lineations are therefore the same lineation and equivalent to L_2 in this work, the structural relationships seen in the amphibolite facies country rock in both areas are very similar.

2.3 The fabric study

The structural analysis was accomplished to provide a basis for detailed fabric and microstructural analysis of the development of mylonites from their host rocks. It showed however, that there was a deformation later than the mylonitization (which produced the $BS_M^{S_3}$ and $BS_2^{S_3}$ folds). This deformation has strong effects on the mylonite microstructures and fabrics (fig 2.9). However it only approaches a penetrative distribution in the northeast corner of sub areas 1 and 2 (fig 2.1 a). Its effects decrease strongly towards the south west and no $BS_M^{S_3}$ or $BS_2^{S_3}$ folds were seen in the south west of sub areas 3 and 4. Hence specimens for detailed fabric work were collected in a section from granulite facies country rock through mylonite to amphibolite facies country rock in this region (see map).

Specimens were also collected from a section passing from country rock (sub area 3) through mylonite to country rock (sub area 1) in the northeast corner of the map (see map). This was done to determine the effects of the $BS_M^{S_3}$ deformation on the mylonitization microstructures so that any effects of this deformation on microstructures in rocks from the section to the southwest could be readily recognized if present (the effects of this deformation are shown in fig 2.9).

2.3.1 The petrography of the rocks used in the fabric study

At the approximate midway position between granulite and amphibolite facies country rock in this section, occurs a mylonitic rock which shows an ultimate microstructural development with respect to the mylonites on either side (see chapters 3, 4 and 5). This mylonite is referred to as the central mylonite. Those mylonites on the granulite facies facies country rock side of this are referred to as being on the granulite

facies side. Those mylonites on the amphibolite facies country rock side of this central mylonite are referred to as amphibolite facies side mylonites.

In the following sections the petrography of the country rock on either side of the central mylonite is described briefly in terms of major, minor (between 1% and 5%) and accessory (less than 1%) constituents. The changes which take place towards the central mylonite are then delineated for each mineral.

2.3.1.1 Granulite facies side

The major constituents of the granulite facies acid gneiss (stage 1A, chapter 3) are quartz and feldspar (orthoclase, microcline, and some plagioclase (An 44)). The minor constituents are orthopyroxene, clinopyroxene, garnet, apatite and opaque with accessory biotite, hornblende and zircon. The orthopyroxene and clinopyroxene often have garnet and opaque (magnetite) coronas. Clinopyroxene sometimes has hornblende associated with it.

Quartz: The deformation and recrystallization of quartz is described in chapter three. The amount of quartz remains approximately constant at around 45% from the granulite facies rocks to the central mylonite. There is less in the pseudotachylite rich rocks due to the bulk of the pseudotachylite but there is an equivalent drop in the feldspar content in these rocks.

Feldspar: The deformation and recrystallization of feldspar is described in chapter 5. The feldspar content (initially around 52%) decreases gradually and then more rapidly towards the centre mylonite (which contains 17% feldspar). This is due dominantly to the breakdown of feldspar to biotite. There is some breakdown of feldspar to muscovite near the

central mylonite.

Biotite: The deformation and recrystallization of biotite is described in chapter 4. The biotite content increases from an accessory to a major constituent (18%) at the central mylonite. It forms in pyroxene cleavage in the early stages of mylonitization and within feldspar. It becomes a major constituent once quartz has wholly recrystallized (stage 4A, chapter 3).

Apatite: Apatite occurs up to and within the pseudotachylite zone. It is not present once the rock has a mylonitic appearance.

Orthopyroxene: Orthopyroxene is present until the pseudotachylite zone is reached but shows increased breakdown towards this zone to hornblende, opaque and garnet. Biotite nucleates and grows along its cleavage during this stage.

Clinopyroxene: Augite is present in decreasing amounts at all stages of mylonitization except the slaty mylonite stage (it changes to an accessory constituent at stage 3.2 ; chapter 3). Initially it breaks down to hornblende but east of the pseudotachylite zone it mainly breaks down to a fine grained brownish material which is generally associated with opaque surrounded by granular garnet. From within this fine grained brownish material and the opaque, sphene nucleates. In the mylonites east of the pseudotachylite belt, the augite is often deformation twinned, ellipsoidal and aligned parallel to S_M.

Garnet and Opaque: These minerals occur at every stage of mylonitization. However there is a slight increase in opaque and garnet content until the quartz is wholly recrystallized partly due to the pyroxene breakdown.

Zircon: Zircon occurs as an accessory mineral at all stages of mylonitization.

Hornblende : Hornblende is never more than an accessory constituent. It forms mainly as a breakdown product of pyroxene but then itself breaks down to biotite so that it has disappeared a stage before the quartz has wholly recrystallized (i.e. by stage 3.3A, chapter 3).

Sphene: Sphene initially appears directly after the pseudotachylite zone (i.e. east of the pseudotachylite belt). It appears to be strongly associated with the breakdown of clinopyroxene as it mainly forms within the brownish pyroxene alteration products. It is present as an accessory or minor constituent from then on (i.e. eastward).

Clinozoisite: Clinozoisite initially appears at the mica growth stage of mylonitization (stage 5A, chapter 3). It nucleates on the grain boundaries of other minerals as small ellipsoidal grains which are aligned parallel to S_M. It increases in size and amount towards the central mylonite (the central mylonite contains 1% clinozoisite).

Muscowite: At this stage muscovite also appears (nucleates within feldspar) and it is a major constituent (17%) at the central mylonite stage (stage 7, chapter 3).

Pseudotachylite: Pseudotachylite occurs sporadically within the rocks up to a distance of forty metres (normal to S_M) either side of the mapped pseudotachylite belt.

2.3.1.2 Amphibolite facies side

The major constituents of the amphibolite facies and gneiss (stage 1B, chapter 3) are quartz and feldspar (orthoclase, microcline and some plagioclase) and biotite. The minor constituents are opaque and garnet with accessory hornblende and zircon.

Quartz: The deformation and recrystallization of quartz is described in chapter three. The amount of quartz remains approximately constant

at around 45% from the amphibolite facies rocks to the central mylonite.

Feldspar: The deformation and recrystallization of feldspar is described in chapter five. The feldspar content (initially around 46%) drops gradually and then more rapidly towards the central mylonite (which contains 17% feldspar). This is dominantly due to the breakdown of feldspar to biotite and muscovite.

Biotite: The deformation and recrystallization of biotite is described in chapter four. The biotite content (initially around 7%) increases towards the central mylonite.

Garnet and Opaque: These minerals occur at every stage of mylonitization as minor constituents.

Zircon: Zircon occurs as an accessory mineral at all stages of mylonitization.

Hornblende: Hornblende is an accessory mineral but breaks down to biotite and has disappeared by the time quartz has wholly recrystallized (i.e. by stage 4B, chapter 3).

Muscovite: Muscovite initially forms as a breakdown product in feldspar. It becomes a minor constituent before the quartz wholly recrystallizes and the amount gradually increases until it becomes a major constituent at the central mylonite.

Sphene: Sphene initially appears at the stage of mylonitization where the quartz has wholly recrystallized and is present as an accessory constituent from then on (westward) to the central mylonite.

Clinozoisite: Clinozoisite initially appears as small ellipsoidal grains which nucleate on the grain boundaries of other minerals at the quartz wholly recrystallized stage of mylonitization. It increases in size and quantity towards the central mylonite by which stage it has become

a minor constituent.

2.3.2 The chemistry of the rocks used in the fabric study

2.3.2.1 The whole rock analyses

The whole rock analyses are shown in figure 2-10, together with the rubidium strontium ratios. The water content was determined by the Penfield method. The specimens are arranged in sequential order from granulite facies country rock to the West, through mylonite to amphibolite facies country rock in the east. The specimen numbers containing A or B indicate those specimens used in the fabric study. They coincide with the numbers used in chapter three.

The two largest relative changes by far are the changes in water content and rubidium strontium ratio. The amphibolite facies country rock has over five times more water and an over seven times greater rubidium strontium ratio than the granulite facies country rock. Both the water content and the rubidium strontium ratio show a sharp change at the central mylonite. The significance of this is discussed in section 3.3.3.3 and section 6.1.2.

2.3.2.2 Cluster analysis

A cluster analysis (fig. 3.3f: Lance and Williams, 1966a, 66b; Rhodes, J.M., 1969) was conducted on the whole rock analyses and the rubidium strontium ratios to quantitatively determine rock relationships. It shows that the two rocks collected containing dominantly pseudotachylite (these come from the location (according to Major et al, 1967) of the thrust plane) are far more different in composition from the other rocks collected than even the difference between the granulite and amphibolite facies country rocks. It is evident from

fig. 2-10 that this separation in the cluster analysis is due to the pseudotachylite rich rocks containing slightly higher Al_2O_3, Fe_2O_3 (total Fe as Fe_2O_3), MgO, CaO, TiO_2 and MnO and significantly less SiO_2. Even so, apart from SiO_2, these changes are not very great. This indicates that the remainder of the rocks collected are fairly similar in composition. In fact the clustering can be mainly attributed to the rocks having formed from initially granulite or amphibolite facies country rock (see chapter 6.1).

2.3.3 The metamorphic grade of the mylonites.

The absence of mylonitized basic rocks in the area studied precludes their use as a indicator of metamorphic grade. From section 2.3.1 it is apparent that the mylonite mineral assemblage is quartz, feldspar (orthoclase, microcline and plagioclase), biotite, muscovite, clinozoisite, garnet, sphene and opaque (magnetite). This assemblage represents a grade of metemorphism between upper greenschist and upper amphibolite facies (Winkler, 1965). However, microcline is recrystallizing as microcline and orthoclase appears to be recrystallizing as orthoclase (the new grains contain no crosshatch twinning c.f. Crawford and Oliver, 1968, p.301). This may indicate that the grade of metamorphism is closer to upper amphibolite facies than upper greenschist facies (c.f. Heier, 1961; Crawford and Oliver, 1968, p.301).

CHAPTER 3

THE MICROSTRUCTURAL AND FABRIC CHANGES OF QUARTZ ACROSS THE MYLONITES ASSOCIATED WITH THE WOODROFFE THRUST.

3.1 Introduction

3.1.1 Procedure

The changes in quartz microstructures and fabrics due to mylonitization can be readily delineated by describing a sequence of fourteen rocks collected from the section (discussed in chapter 2.3) which passes from granulite facies country rock eastward across the Woodroffe Thrust, through mylonite to amphibolite facies country rock. Two rocks collected from the next large block of amphibolite facies country rock to the east were used to supplement this study.

The rocks are described under the following headings which denote their particular character.

1A Slightly affected country rock

2.1A Strongly affected country rock

2.2A Pseudotachylite

3.1A Coarse quartz-feldspar mylonite

3.2A Medium quartz-feldspar mylonite

3.3A Fine quartz-feldspar mylonite

4A Quartz wholly recrystallized

5A Mica growth

6A Homogenization

7 Slaty Mylonite

6B Homogenization

5B Mica Growth

4B Quartz wholly recrystallized

3B Coarse quartz-feldspar mylonite

2B Strongly affected country rock

1B Slightly affected country rock.

The symbol A shows the rock is on the granulite facies side of the central ultimate mylonite and the symbol B shows the rock is on the amphibolite facies side. The same numbers relate equivalent stages in degree of microstructural development on either side.

All microstructural descriptions and fabric measurements were made from the N-section, i.e. the section normal to lineation. The microstructures, quartz fabrics and angular relationships between grains are described stage by stage. This is followed by discussion of the development of these features and the differences from the granulite to the amphibolite facies side of the central ultimate mylonite.

3.1.2 Measurement techniques

The fabric plots and graphs of angular relationships between grains were made from universal stage measurements of [0001] of host and new grains. New grains were generally measured in groups of three or more adjacent grains directly adjacent to their associated host remains. This was done to remove operator bias in choosing a grain for measurement, to ensure that the new grains were directly related to the measured host and not some other kinked portion of it, and so that host-new grain and new-new grain angular relationships could be determined.

In some cases, new grains were also measured on the edge of aggregates containing host grain remains. This was done to determine the effects of ductile deformation and growth. To test whether the measurement of three or more new grains per host caused some effect on the new grain fabric, test measurements were made of one grain per host so that orientation data was obtained from a greater range of hosts.

In two cases on the amphibolite facies side only a few host grain

remains occured. Hence many new grains were measured per host. To test whether this had any bias on the new grain fabric, separate measurements were made on new grains in aggregates containing no host grain remains for a wide spread of aggregates.

3.2 Microstructure and fabric description

3.2.1 Slightly affected country rock

3.2.1 A Granulite facies side

Mesostructure

The rock shows no signes of mylonitization. It contains a strong schistosity S_1 and lineation L_1. L_1 is defined by alignment of elongate quartz grains in S_1.

Microstructure

S_1 is defined by ellipsiodal quartz and feldspar grains and rare aligned biotites. The only signs of mylonitization are two sets of weak non-penetrative microstructures. One set is parallel to the trend of the mylonitic schistosity S_M. This microstructure passes straight across the slide, cutting across grains and following grain boundaries with equal frequency. It is observed in quartz as:

a) a line of minute new quartz grains (diameter 4 μm; fig. 3.7a).

b) a line of minute opaque inclusions (fig. 3.7b).

c) a line of minute biotite grains (fig. 3.7c).

d) a thin line of local variation in birefringence (a narrow kink zone) with or without a), b) and c) along it (fig. 3.7c, 3.7d).

e) hairline fractures which in many cases do not pass the whole width of the grain (fig. 3.8a).

The other set of microstructures is almost perpendicular to the trend of S_M (average angle 80°; varies from 60° to 90°). This set is similar to the above but microfractures and in some cases micro shears (i.e. microfractures along which there has been slip) are much more common (fig. 3.8b, 3.8c). These fractures are generally filled with opaque material.

Away from these non-penetrative microstructures, the quartz grains (average length 500 μm) are strain shadowed.

Fabric plots

Figure 3.4a.

3.2.1B Amphibolite Facies Side

Mesostructure

The rock shows no signs of mylonitization. The schistosity S_2 is parallel to a compositional layering S. The lineation L_2 is difficult to observe as these rocks rarely break or weather along S_2.

Microstructure

The schistosity S_2 is defined by some ellipsoidal feldspars and aligned (001) of biotite grains (fig. 3.8d). There are however early signs of mylonitization and the mylonitic schistosity S_M can be readily recognized. The effects of mylonitization on the quartz are:

a) Strain shadowed host grains which sometimes contain weak deformation bands with diffuse boundaries,and many contain polygonal subgrains (fig. 3.9a) with an average diameter of 20 μm.

b) Strain shadowed hostgrains occur with new grains growing along the host grain edges. The boundaries of these new grains are often rounded (average diameter 45 μm; fig. 3.9b).

c) Aggregates of new grains occur in which there are no host remains. Grain boundaries range from rounded to gently curved to straight. A number of triple point boundaries at about 120° occur. The average diameter of these new grains is 60 μm (fig. 3.9c).

d) New grains are absent along deformation band boundaries within the host, but where such boundaries meet host grain edges there is

sometimes a slightly increased number of new grains.

e) New grains are of a similar to slightly larger size than adjacent subgrains within the host grain (figs. 3.9a, 3.9d).

f) New grains on the aggregate edges are often slightly strain shadowed.

g) Quartz aggregates and host grains are only sometimes elongate parallel to S_M (average length 1 mm) and host grains and aggregates generally have at least one boundary in direct contact with unrecrystallized feldspar grains.

Fabric plots and angular relationships between grains.

Figs. 3.4c, e, g and figs. 3.1a, c, e, g.

3.2.2 Strongly affected country rock

3.2.2.1 A Granulite facies side

Mesostructure

The rock shows no signs of mylonitization but the schistosity S_1 is difficult to pick and the lineation L_1 is extremely weak.

Microstructure

S_1 is weakly defined by a few aligned ellipsoidal quartz, feldspar and pyroxene grains. It has been considerably disturbed by increased mylonitization. The microstructures parallel to the trend of the mylonitic schistosity S_M previously described for the slightly affected country rock, have developed considerably. In many cases they are now microshears. Quartz grains adjacent to and cut by these microshears show:

a) Multiple strain shadows.

b) Fractures with or without opaque infill (fig. 3.10a).

c) New grain growth in some of the strongly strain shadowed grains along deformation band boundaries (average diameter 4 μm; fig. 3.10b).

d) New grains associated with subgrains of a similar or smaller size, occur away from the deformation band boundaries in host grains the same or similar to those described above (fig. 3.10b).

Away from the microshears, quartz grains (average diameter 600 μm) are commonly strain shadowed and contain blocky subgrains. These quartz grains are also commonly fractured, and the fractures infilled with fine grained sericitic material (fig. 3.10c).

This rock contains a small amount of pseudotachylite along some of the microshears. It develops in the microshears where the adjacent grains show strong ductile deformation.

Fabric plot

Figure 3.4b.

3.2.2 B Amphibolite facies side

Mesostructure

This rock resembles a medium grained acid gneiss with a schistosity defined by alignment of biotites.

Microstructure

In thin section, the above schistosity is seen to be distinctly mylonitic. This probably means that the mylonitic schistosity S_M has formed parallel to the original trend of the country rock schistosity S_2. Quartz shows the following characteristics:

a) Host grain remains are strain shadowed, sometimes contain weak deformation bands with diffuse boundaries and often contain subgrains (average diameter 30 μm).

b) Most host grains show new grain growth on their edges adjacent to subgrains (fig. 3.10d). The new grains have gently curved boundaries and vary considerably in size from 30 μm to 200 μm.

c) The only old quartz grains which show no new grain growth are some of those which are completely surrounded by feldspar.

d) Many aggregates of new grains occur in which there are no host grain remains. Grain boundaries range from gently rounded to straight (fig. 3.11a). A number of triple point boundaries at about 120° occur. The average diameter of these new grains is 80 μm.

e) New grains on the aggregate edge are sometimes slightly strain shadowed.

f) Quartz aggregates and host grains are sometimes elongate parallel to S_M (average length 1.1 mm) and generally have one boundary in direct contact with unrecrystallized feldspar.

Fabric plots and angular relationships between grains

Figs. 3.4d, f, h, i and figs. 3.1b, d, f, h.

3.2.2.2 A Pseudotachylite - Granulite facies side

Mesostructure

The rock contains a large amount of dark, very fine grained material which occur in lenses parallel to the trend of the mylonitic schistosity S_M.

Microstructure

No remains of the country rock schistosity S_1 are visible and the slide contains a large amount of pseudotachylite. It also contains numerous microfractures and microshears. The pseudotachylite occurs as thick streams, blebs, and thin streams and these streams are approximately aligned parallel to the trend of the mylonitic schistosity S_M. Thin streams of pseudotachylite often occur in zones of intense ductile deformation. At the contact of the pseudotachylite with the highly strained host grains either side there is considerable growth of minute

(less than 2 μm) new grains (fig. 3.11b). The thick streams and blebs of pseudotachylite however generally have sharp contacts with the minerals around them. Quartz shows the following characteristics:

a) Old grains are commonly fractured and the fractures infilled with opaque (fig. 3.11c).

b) Microshearing is common with significant displacement in some cases (fig. 3.11d).

c) Grains adjacent to thin streams of pseudotachylite often show strong strain shadowing and growth of minute new grains (fig. 3.12a).

d) Some new grains are visible along deformation band boundaries (fig. 3.12a, average diameter less than 5 μm).

e) Old grains are generally clouded by opaque, strain shadowed and motley.

The rocks either side of the pseudotachylite zone

The pseudotachylite zone is three to five metres wide but pseudotachylite occurs sporadically as blebs in the rocks either side. It occurs as far into the mylonite as the wholly recrystallized quartz stage of mylonitization, a distance of 40 metres normal to the mylonitic schistosity, and a similar distance west into granulite facies country rock.

There is a considerable amount of brittle fracturing in the rocks either side of the pseudotachylite zone. This intensifies towards the zone. On the east side of the main pseudotachylite zone, this brittle fracturing is later than the formation of S_M (as the fractures cut and displace S_M) and pseudotachylite intrudes down a number of these fractures (fig. 3.12b). On the west side, due to the microstructural inhomogeneity, it is impossible to define the chronology of the brittle and ductile

deformation.

B Amphibolite facies side

There is no pseudotachylite on the amphibolite facies side.

3.2.3 Coarse quartz feldspar mylonite

3.2.3.1 A Granulite facies side

Mesostructure

The mylonitic schistosity S_M and mylonitic lineation L_M are both very strong in this rock. L_M is defined by elongate quartz and feldspar grains and aggregates in the plane of S_M.

Microstructure

S_M is defined by aligned ellipsoidal quartz and feldspar grains. Quartz exhibits the following features :

a) Host grains are strongly strain shadowed and deformation banded and many contain polygonal subgrains away from deformation bands (average diameter 10 μm) and smaller rounded subgrains along deformation bands (average diameter 4 μm). The deformation bands are aligned about S_M (fig. 3.12c).

b) Host grains are elongate parallel to the trend of S_M (average length 1.2 mm; average length to width ratio 6) and generally have one long boundary in direct contact with unrecrystallized feldspar.

c) Some old grains occur surrounded by a single feldspar. They are strain shadowed the exhibit no new grain growth (fig. 3.12d).

d) Many host grains contain new grains growing along deformation band boundaries. These new grains have highly rounded boundaries. Figure 3.13a shows a deformation band boundary which is straight at one end (subgrains occur but new grains are rare; average diameter 5 μm) and becomes highly serriate (new grains are more abundant - the

boundary bulges around them and adjacent subgrains; average new grain diameter 10 μm), until it disappears into a mass of new grains at the other end (new grains have a more uniform size and average 16 μm in diameter).

e) New grains also form on host grain edges and are associated with subgrains (fig. 3.13b) shows subgrains (average diameter 7 μm) which are larger (10 μm) near the new grains (average diameter 14 μm). These new grains have rounded boundaries (fig. 3.13c).

f) Some host grains have been almost entirely converted to an aggregate of new grains. New grains surrounded by new grains have gently curved to straight boundaries (fig. 3.13d).

Fabric plots and angular relationships between grains

Figs. 3.5a, b, c and figs. 3.2a, h, b.

3.2.3 B Amphibolite facies side

Mesostructure

Freshly broken rock surfaces show a mylonitic schistosity S_M. The mylonitic lineation L_M is not as strong as in the equivalent rock on the granulite facies side.

Microstructure

S_M is defined by ellipsoidal quartz aggregates and feldspar grains. Quartz shows the following characteristics:

a) There are only a few host grain remains even where wholly included in feldspar. Some contain subgrains and the host remains generally occur in the centre of larger quartz aggregates (average diameter of subgrains is 30 μm; fig. 3.14a).

b) There is only a weak tendency for quartz aggregates to be elongate parallel to S_M. However the aggregates rarely have one boundary in

direct contact with unrecrystallized feldspar (average length of aggregates 900 μm; average length to width ratio 2).

c) The new grains range in size from 50 μm to 300 μm (average diameter 150 μm) and grain boundaries are rounded but vary from strongly rounded to gently curved (fig. 3.14b). They are generally equidimensional but some are slightly elongate parallel to S_M.

d) The larger slightly elongate new grains are strain shadowed and a few show deformation bands at angles around 45° to S_M (fig. 3.14c).

Fabric plots and angular relationships between grains

Figs. 3.5d, e, f and figs. 3.2c, d.

3.2.3.2 Medium quartz - feldspar mylonite

3.2.3.2 A Granulite Facies Side

Mesostructure

The mylonitic schistosity S_M and mylonitic lineation L_M in this rock are both strongly developed. L_M is again defined by elongate quartz and feldspar grains and aggregates.

Microstructure

S_M is strikingly developed and is defined by thin, elongate quartz hosts and aggregates and ellipsoidal feldspars. Quartz exhibits the following characteristics:

a) Host grains are strongly strain shadowed and deformation banded and often contain subgrains (average diameter 7 μm away from deformation band boundaries) which have polygonal boundaries away from, but rounded boundaries along deformation band boundaries (fig. 3.14d).

b) Host grains and aggregates are strongly elongate parallel to S_M (average length 1.0 mm; average length to width ratio 9) and only about 20% have one long boundary in direct contact with

unrecrystallized feldspar.

c) All host grains exhibit prolific new grain growth. New grains form on deformation band boundaries (average diameter 10 μm) and have rounded boundaries (fig. 3.15a). They also form adjacent to subgrains on the remains of host grain edges (average diameter of new grains 11 μm; fig. 3.15b).

d) New grains in aggregates containing no host grain remains have gently curved to straight boundaries (average diameter 25 μm). Triple point boundaries at around 120° are not common (fig. 3.15c).

e) Some new grains are slightly elongate parallel to S_M trend. These grains may or may not be strain shadowed (fig. 3.15d).

A small amount of pseudotachylite has formed in one or two zones of extremely high strain. New grain size in these zones is extremely fine (less than 2 μm). These zones are parallel to the trend of S_M.

Fabric plots and angular relationships between grains

Figs. 3.5g, h, i and figs. 3.2e, f.

3.2.3.2 B Amphibolite facies side

There is no rock on the amphibolite facies side equivalent to the above rock, as decrease in grain size takes place after the quartz has wholly recrystallized, a stage not yet reached on the granulite facies side.

3.2.3.3 Fine quartz - feldspar mylonite

3.2.3.3 A Granulite facies side

Mesostructure

The mylonitic schistosity S_M and the mylonitic lineation L_M are both extremely strong in this rock.

Microstructure

S_M is extremely well developed and is defined by ellipsoidal quartz host grains and aggregates and markedly ovoidal feldspars. Quartz exhibits the following characteristics:

a) Host grain remains are strongly strain shadowed and deformation banded. They contain subgrains (average diameter 4 μm) and exhibit prolific new grain growth (fig. 3.16a).

b) Host grain remains and aggregates are highly elongate parallel to S_M (average length 600 μm; average length to width ratio 12) and rarely have one boundary in contact with unrecrystallized feldspar.

c) New grains with rounded boundaries form on deformation band boundaries (average diameter 2 μm ; fig. 3.16b). New grains also form adjacent to subgrains on host grain edges (average diameter 6 μm). They have rounded to polygonal boundaries.

d) New grains in aggregates containing no host grain remains (average diameter 10 μm) have gently curved to straight boundaries.

Pseudotachylite occurs in zones of high strain which cut across S_M at about twenty five degrees. The quartz and feldspar aggregates within these zones are highly elongate parallel to them (fig. 3.16c). Subgrains and new grains within these aggregates are considerably smaller than those forming in adjacent un-affected mylonite. Locally the grain size decreases to zero into pseudotachylite which is developed in thin streams parallelto the length of these zones of intense deformation.

The pseudotachylite can occur as discordant blind protuberances into undisturbed mylonite (fig. 3.16d). Much of the pseudotachylite contains a schistosity defined by elongate minute blebs of quartz. It is generally isotropic and sometimes contains microlites.

Fabric plots and angular relationships between grains

Figs. 3.5j, k and fig. 3.2g.

3.2.4 Quartz wholly recrystallized

3.2.4 A Granulite Facies Side

Mesostructure

The mylonitic schistosity S_M and the mylonitic lineation L_M are both extremely strong.

Microstructure

S_M is extremely well developed and is defined by ellipsoidal quartz and feldspar aggregates. Quartz exhibits the following characteristics:

a) There are no host grain remains. The quartz aggregates are entirely made up of new grains.

b) The quartz aggregates have an average length of 600 μm and width of 50 μm, and are never in contact with unrecrystallized feldspar.

c) Grains within aggregates (average diameter 25 μm) have straight to gently curved boundaries and a few triple point boundaries at 120° occur. The frequency of these boundaries decreases with decreasing aggregate width. Grains tend to be rectangular in aggregates one and two grains wide (fig. 3.17a).

d) Strain shadowed new grains are rare. A few however are slightly elongate parallel to S_M.

Fabric Plot

Figure 3.6a.

3.2.4 B Amphibolite facies side

Mesostructure

The mylonitic schistosity S_M and mylonitic lineation L_M are both well developed.

Microstructure

S_M is defined by ellipsoidal quartz aggregates, coarse feldspar grains and feldspar aggregates. Quartz exhibits the following characteristics:

a) There are no host grain remains. The quartz aggregates are entirely made up of new grains.

b) The aggregates have an average length of 1.0 mm, an average width of 250 μm and are never in contact with unrecrystallized feldspar.

c) Grains within aggregates (average diameter 90 μm) have straight to gently curved boundaries and a few triple point boundaries at 120° occur. Long thin aggregates contain grains which tend to be rectangular (fig. 3.17b).

d) Grains within the aggregates are often strain shadowed and elongate parallel to S_M.

Fabric plot and angular relationships between grains

Figure 3.6b and fig. 3.3a.

3.2.5. Mica growth

3.2.5.A Granulite facies side

Mesostructure

The mylonitic schistosity S_M is extremely strong but the mylonitic lineation L_M is considerably weaker than at the quartz wholly recrystallized stage.

Microstructure

S_M is defined by highly ellipsoidal quartz aggregates, feldspars, and feldspar aggregates, and alignment of mica (001). Mica growth is very strong and markedly influences the microstructure. Quartz exhibits the following characteristics:

a) Quartz aggregates are highly elongate and rarely more than two grains

wide (average length 600 μm; average width 35 μm).

b) Grain boundaries are straight to gently curved. Triple point boundaries at 120° are rare and grains tend to be rectangular often giving four point boundaries at 90° in two grain wide aggregates (fig. 3.17c).

c) The average grain size within aggregates is 35 μm but grains range in size from 8 μm to 100 μm in diameter.

d) Mica growth along grain boundaries in quartz aggregates is quite common (fig, 3.17d). Some feldspar growth in similar sites also occurs.

Fabric plot and angular relationships between grains

Figure 3.6c and fig. 3.3b.

3.2.5 B Amphibolite facies side

Mesostructure

The mylonitic schistosity S_M and the mylonitic lineation L_M are both well developed.

Microstructure

S_M is defined by aligned ellipsoidal quartz and feldspar aggregates, feldspars and (001) of mica. Quartz exhibits the following characteristics:

a) Quartz aggregates are highly elongate and most are only one or two grains wide (average length 700 μm; average width 60 μm).

b) Grain boundaries are straight to gently curved. Triple point boundaries at 120° are rare and grains tend to be rectangular with boundaries parallel or perpendicular to S_M trend.

c) The average grain size within aggregates is 90 μm but grains range in size from 25 μm to 200 μm in diameter.

d) Mica and feldspar growth along grain boundaries in quartz aggregates is common (fig. 3.18a).

e) Some grains are elongate parallel to S_M and show strain shadowing.

Fabric plots and angular distribution between new grains

Figs. 3.6d, e and fig. 3.3c.

3.2.6 Homogenization

3.2.6.A Granulite facies side

Mesostructure

The mylonitic schistosity S_M is extremely strong but the mylonitic lineation L_M is weak.

Microstructure

S_M is defined by strong alignment of (001) of mica and ellipsoidal feldspar host grain remains. Quartz exhibits the following characteristics:

a) Only occasional remains of elongate quartz aggregates occur (fig. 3.18b). They are almost indistinguishable from the surrounding matrix.

b) Grain boundaries within aggregate remains are gently curved and no longer show rigid geometric relationships to the trend of S_M (fig. 3.18b).

c) The average grain size within the aggregate remains is 50 μm.

d) The mica growing on grain boundaries within the aggregate remains is muscovite while that in the surrounding matrix is dominantly biotite.

e) Some grains within the aggregate remains are strain shadowed.

f) The matrix dominates and is a quartz-feldspar mica schist (fig. 3.18c). The quartz grains are generally fairly equidimensional but some are slightly elongate parallel to S_M (average grain size 40 μm).

g) Quartz-quartz, quartz-feldspar and quartz-mica boundaries are all

common in the matrix and most grains are strain shadow free. The quartz-quartz and quartz-feldspar boundaries are generally gently curved, the angles between these boundaries are variable and triple point boundaries at 120^{o} occur only rarely.

Fabric Plot

Figure 3.6f.

3.2.6 B Amphibolite facies side

Mesostructure

This rock is identical mesoscopically with that at the homogenization stage on the granulite facies side.

Microstructure

This rock is similar microscopically to that at the homogenization stage on the granulite facies side. However the degree of homogenization is not as great and hence there are more quartz aggregate remains and the matrix is not as homogeneous (fig. 3.18d, 3.19a; c.f. fig. 3.18b,c). Many grains within the aggregate remains are strain shadowed and have small rounded new grains (average diameter 12 um) growing on their boundaries. Finally the average size of quartz grains within the matrix is slightly larger than in the equivalent rock on the granulite facies side (50 um c.f. 40 um).

Fabric plots and angular relationships between grains

Figures 3.6g, h and 3.3d.

3.2.7 Slaty Mylonite

Mesostructure

This rock is the central ultimate mylonite. It occurs between rocks 6A and 6B. The mylonitic schistosity S_M is extremely strong but the mylonitic lineation L_M is almost invisible.

Microstructure

S_M is defined by very strong preferred orientation of mica (001). A few ellipsoidal feldspar host grain remains are aligned parallel to S_M also. Quartz exhibits the following characteristics:

a) There are no discernable remains of quartz aggregates.

b) The rock is a homogeneous quartz-feldspar mica schist containing a few feldspar megacrysts.

c) The average grain size of quartz is 45 um.

d) Quartz grains are generally fairly equidimensional, any that are slightly elongate being aligned parallel to S_M (fig. 3.19b).

e) Quartz-quartz, quartz-feldspar and quartz-mica grain boundaries are all common. The former two are gently curved to rounded. Only some of the bigger grains show signs of strain shadowing. Grain boundary angles are variable.

Fabric plot

Figure 3.6c.

3.3 Discussion

3.3.1 Reliability and consistency of measurements

3.3.1.1 Fabrics

The fabric plots were all obtained from measurements on the N-section (i.e. the section normal to lineation and hence perpendicular to schistosity). The c-axis distribution in mylonitic rocks approaches a girdle normal to, or two crossed girdles at high angles to, the mylonitic lineation (Balk, 1952; Christie, 1963; Moore, 1970; Ross, 1973). Hence c-axes in the N-section lie at low angles to the plane of the section and are readily measured. Christie (1963) measured three sections cut at different angles to the lineation, and found the fabric plots from these were essentially similar to the fabric plots obtained from the N-sections. Similar tests were conducted by Balk (1952) with the same results. Hence it was considered unnecessary to test this again here especially when good girdle distributions were obtained.

Instead, other tests were made on the reliability of the fabric data (see section 3.1.2). It was found that the fabrics of new grains in which a single new grain was measured per host grain remain, are closely comparable with those in which three or more adjacent new grains were measured per host (compare fig. 3.5b and c; fig 3.5h and i). This shows that although new grains were measured in only a relatively small number of hosts whose fabric may not be truly representative (due to lack of statistics), the host control operative on new grain orientation (see section 3.3.3.1.2) did not significantly alter the new grain fabric from that when a larger sample of host grains was used.

The fabrics of new grains in rocks where very few host grain remains occured and hence many new grains per host were measured are very

similar to the fabrics of new grains measured from a large number of aggregates (compare figs. 3.4h and i; see also figs. 3.5e and f), on the amphibolite facies side. Hence once again, even though an even smaller and therefore perhaps even less representive number of host grains were measured, this in no way affected the new grain fabric. This of course is predictable since there is apparently very little host control on new grain orientation on the amphibolite facies side (see section 3.3.3.2.2).

3.3.1.2 Angular relationships between grains.

To obtain some idea of the reproducibility of the distributions obtained for angles between host and new grains and adjacent new grains, different total numbers of angles were first measured. These readings were then divided in two, plotted, and compared with each other and the graph for the total. It was found that the graphs with half the total angles, maintained the essential characters of the graph for the total, when one hundred angles were plotted in each. To ensure that the angular distributions were valid representations, over two hundred, and quite often three hundred angles were therefore measured and plotted.

A test graph was made by measuring every new grain and subgrain in an aggregate containing host grain remains within the coarse quartz feldspar mylonite on the granulite facies side. This was done to see whether the same host control was obtained as in the graphs where only three or so new grains were measured per host. It was found that the same host control was developed but to a greater degree (compare figs. 3.2a and h). This is discussed in section 3.3.3.1.2.

3.3.2 Pseudotachylite

Brittle deformation only occurs near and intensifies towards the

pseudotachylite. On the eastern side of the pseudotachylite zone, the mylonitic rocks show that the brittle fracturing and pseudotachylite production are later than the formation of S_M as both these features cross cut it (fig. 3.12b, 3.16c, d). Although this separation cannot be readily made west of the pseudotachylite zone (due to the non penetrative nature of S_M, fig. 3.11b), by analogy with the eastern side, and because the brittle deformation intensifies towards the pseudotachylite, it is considered to be later than the formation of S_M and associated with the pseudotachylite production.

Thin streams of pseudotachylite form in the centre of zones of intense strain which cross cut S_M at low angles (fig. 3.16c). The smaller subgrain and new grain size in the highly strained quartz and feldspar host grains in these zones relative to the unaffected mylonite around them, and the further decrease in size towards the streams of pseudotachylite suggest that the pseudotachylite is a product of increased strain rate (Holt, 1971; Staker and Holt, 1972; Korbel and Swiatkowski, 1972; Abson and Jonas, 1972). The pseudotachylite is thought to be a product of frictional fusion due to brittle failure as a result of the increased strain rate in these zones of intense deformation. The fusion origin is supported by the isotropic nature of the pseudotachylite, the presence of microlites within it and the occurence of pseudotachylite as discordant blind protuberances into undisturbed mylonite (fig. 3.16d). Similar suggestions that pseudotachylite is a product of frictional fusion associated with extreme mylonitization have been made by Hall and Molengraaff (1925); Scott and Drever (1953); Philpotts (1964) and McKenzie and Brune (1972). These authors believe however, that the mylonitization itself is a brittle process.

Much of the pseudotachylite contains a flow layering or weak schistosity which is approximately parallel to the trend of S_M. This could indicate that the pseudotachylite forms as a late stage event in the mylonitization due to an increase in the rate of deformation.

3.3.3 The stages in mylonitization until quartz is wholly recrystallized

3.3.3.1 Granulite facies side

3.3.3.1.1 Deformation and recovery of host (original) grains

Strain

The strain determined from the length to width ratios of host grains shows a gradual increase in the early stages of mylonitization. However, as mylonitization becomes more penetrative there is a rapid increase in strain from rock to rock towards the fine quartz-feldspar mylonite. The length to width ratios in rocks where the mylonitic schistosity is more penetrative are only minimum valves as many host remains neck and separate. This leads to a decrease in the size of host grain remains and a consequent decrease in the overall grain size. The strain is such that the host grains and quartz aggregates are flattened and strongly elongated in the plane of the mylonitic schistosity. The elongation helps define the mylonitic lineation, and the flattening helps define the mylonitic schistosity.

Deformation microstructures

The initial signs of mylonitization are narrow kink zones which often leave the host grain to either side undisturbed. In the slightly more mylonitic rocks strain shadows appear as well. In the first rocks mesoscopically identifiable as mylonites, the quartz host grains are strongly strain shadowed and deformation banded. The deformation bands

show a preferred orientation parallel to S_M. The degree of alignment increases with increasing strain. The grain shape also becomes progressively more ellipsoidal.

Subgrains

Subgrains form along deformation band boundaries and within the mass of the grain away from deformation bands. The latter are generally strongly polygonal with regular sides (fig. 3.13b). They are an excellent example of polygonization or recovery. They often increase in size towards the edge of the host grains where they sometimes merge into new grains. Elongation of subgrains sub parallel to S_M, and elongation and strain shadowing of new grains associated with them, indicate that the subgrains formed during deformation, that is, they are a product of dynamic recovery. The subgrains occuring directly adjacent to deformation band boundaries are smaller and more rounded. They are more easily visible once the deformation band boundary has begun to bulge around them (figs. 3.12c, 3.13a, 3.16b).

The subgrains decrease in size from the coarse to the fine quartz-feldspar mylonite. This suggests that the strain rate shows a general increase towards the centre of the mylonite zone (i.e. towards the slaty mylonite; Holt, 1971; Staker and Holt, 1972; Korbel and Swiatkowski, 1972; Abson and Jonas, 1972).

Fabric

The granulite facies acid gneiss fabric (fig. 3.4a) changes to a more mylonitic fabric with increasing strain by rotation of the c-axes towards the primitive circle. There is a tendency for the c-axes to rotate to positions either side (at about 40°) of S_M (fig. 3.5a). With increasing strain this tendency to develop maxima either side of S_M (fig.

3.5g - sometimes only one maximum develops) increases until the ultimate mylonite type distribution is attained for the host grain remains (fig. 3.5j). These fabrics are therefore a result of intra-granular ductile deformation.

3.3.3.1.2 Recrystallization - Nucleation

Nucleation Sites

New grains nucleate on host grain edges. They are intimately associated with adjacent subgrains within the host. There is a progressive increase in size and mismatch of subgrains from within the host to its edge, where the subgrains merge with new grains of a similar or larger size (see figs. 3.13b, 3.13c, 3.15b). New grains also form on deformation band boundaries. The boundary bulges where it is pinned by small subgrain boundaries which form along it. The degree of bulge increases with increasing size of the subgrains which often merge with new grains along the boundary before it disappears into a mass of new grains (see figs. 3.12c, 3.13a, 3.16b).

Angular relationships between host and new grains

There is a very strong host control on the orientation of new grains (figs. 3.2a, e, g). These graphs show that the c-axes of new grains are preferentially orientated at an angle of around twenty degrees to those of the host. A similar relationship was found for new grains measured from a single aggregate relative to the host (fig. 3.2h).

Angular relationships between adjacent new grains

These distributions contain a broad peak around twenty degrees and a drop off in frequency at high angles (figs. 3.3b, f). Since the new grains show a strong angular relationship to the host around twenty degrees, the maximum mismatch between c-axes of adjacent new grains

maintaining this would be 40-50°. The minimum would be seven degrees as mismatches less than this only occur between subgrains (definition). Hence a peak would be expected between seven and fifty degrees relative to the uniform distribution curve as was obtained.

Size of new grains and associated subgrains

The new grains measured for the above graphs were all directly adjacent to host grain remains. These new grains have a slightly larger size distribution than the adjacent subgrains, but those on the aggregate edge are considerably bigger. The degree of misorientation between adjacent new grains decreases from the aggregate edge towards the subgrains.

Fabric of new grains

The new grain fabrics (figs. 3.5b, c, h, i, k) are girdles normal to the mylonitic lineation. The maxima within them however are not symmetrically positioned either side of S_M. Nor do they coincide with host grain maxima (i.e. with maxima in figs. 3.5a, g, j) in the same rock. Instead the major new grain maxima tend to lie about twenty degrees from host grain maxima on the girdle normal to the mylonitic lineation.

Previous Work

Ransom (1971) obtained somewhat similar host-new grain angular relationships from single aggregates of quartz, but did not discuss the significance of the distributions in terms of nucleation and growth. Hobbs (1968), in syntectonic recrystallization experiments on single crystals of quartz, obtained new grains which in large areas of the specimen preserved the same shape and general size distribution that was present in adjacent areas of subgrains. The host-new grain angular

distributions he obtained were almost identical in one case only to those presented here (Hobbs, 1968, fig. 7I). The remainder contain higher frequencies of angles greater than forty degrees. Hobbs envisaged the process of nucleation of new grains as one which depends on deformation (in that adjacent subgrains increase their relative misorientations during deformation until an array of highly misoriented subgrains is developed) rather than growth to provide high angle boundaries for recrystallization. He considered that the new grains had not formed from sub microscopic subgrains because of the intimate and progressive relationship from subgrains through to new grains. If this is so growth control (such as a coincidence lattice control - see chapter 1) has had little or no effect on the results he obtained as the new grains are similar in size to the subgrains from which he suggests they form.

Conclusions

Critical strain for dynamic recrystallization: Dynamic recrystallization in metals only begins once the host material has reached a certain critical strain (Honeycombe and Pethen, 1972; McQueen and Bergerson, 1972; Glover and Sellars, 1973). Hence nucleation begins in the sites of highest strain, i.e. along deformation band boundaries and host grain edges (c.f., Cahn, 1966). If this applies to quartz, there would be a progressive dynamic recrystallization of the host as those portions of it adjacent to previously formed new grains reach the critical strain for nucleation. Hence new grains on the aggregate edge and closer to the aggregate edge have been growing longer and have been consequently more affected by the concurrent deformation than those closer to the host remains.

The relationship between subgrains and new grains: The intimate

association of sub and new grains on host grain edges and the progressive increase in size and degree of mismatch in subgrains towards the new grains would indicate that the new grains are forming by a process of subgrain growth and perhaps coalescence (chapter 1.3.3.1; Beck 1949; Cahn, 1950; Hu, 1963). The intimate association of subgrains, the bulge of deformation band boundaries where they are pinned by subgrain boundaries, and new grains would indicate that the latter are forming by a bulge nucleation mechanism (chapter 1.3.3.1; Bailey, 1960; Bailey and Hirsch, 1962). Since both of these are sites of high strain, they are also sites of relatively sharp local deviations in host orientation (especially the deformation band boundaries). This enables high angle boundaries to form quickly during and after the polygonization process. This could be further enhanced by the syntectonic nature of the recovery, the continued deformation helping to increase the relative mismatch of subgrains and thus provide more high angle boundaries. The intimate relationship between sub-grains and new grains and the progressive changes from one to the other would preclude the possibility that the new grains had grown from sub microscopic subgrains. This is supported by the fabric data (see later).

The angular relationship of new grains to the host: Since subgrains such as those within the host grain remains may have acted as nuclei for the new grains, it is probable that the latter are related in orientation to the host. This could account for the strong twenty degree angular relationship between them, especially since the new grains measured were those directly adjacent to host remains and therefore, probably not significantly rotated since nucleation, by the concurrent deformation (this is supported by lack of development of the mylonite type fabric

within them). These grains also, have not grown significantly since nucleation. Therefore they should be little affected by any host growth control (e.g. a coincidence lattice control, see chapter 1.3.3.2). This is supported by the angular distributions between adjacent new grains (see below).

Coincidence lattices have not been calculated for quartz. However the annealing recrystallization experiments of Hobbs(1968), (where growth control such as that exerted by a coincidence lattice is most likely to occur) gave strong angular relationships between host and new grains around 20 to 40°. Hence there could be a coincidence lattice in quartz around 30°. However if this is so, any contribution from this to the angular distribution is considered to be slight because:

a) The new grains adjacent to the host remains are only slightly larger than adjacent subgrains and therefore have not grown significantly.

b) The host-new grain angular relationship is relatively low, i.e. around 20°.

c) The distribution of angles between adjacent new grains (figs. 3.2b,f) shows a peak relative to the uniform distribution curve around 30° instead of a trough. The latter would be expected if significant growth had occured because adjacent grains at this angle would have the most mobile boundaries and hence one would consume the other rapidly, depleting their frequency.

New grain fabric: Since the new grains appear to be forming from subgrains from within the distorted host, they could be related in orientation to the path of distortion the host has undergone. In section 3.3.3.1.1 it was shown that the c-axes of host grains with increasing strain rotate to the girdle normal to L_M and then concentrate into tight maxima

within this girdle either side of S_M. The distortion of the host lattice during this latter rotation will tend to be in the girdle normal to L_M and new grains forming from subgrains in this distorted lattice will also tend to be oriented within that girdle. There is one maximum common to all these new grain fabrics and that is the one close to the plane of S_M (figs. 3.5b, c, h, i, k; it is the only maximum occuring in fig. 3.5k). With increasing strain of the host grains (and hence their increased preferred orientation) there is a greater tendency for only this maximum to develop. The significance of this is not known (it is not the product of interference by ascribing a 20^o small circle around each of the host grain maxima) and may be a result of some other factor in the nucleation process such as a thermodynamic control.

Comparison with other work: The actual detail of the mechanism for nucleation (on the host grain edges, and also adjacent to former deformation band boundary sites once they have become a line of new grains) differs slightly from that proposed by Hobbs, but they are compatible. In Hobbs' single quartz crystals, deformation rather than growth provided the high angle boundaries whereas in the rocks described here growth of subgrains is probably more important than the concurrent deformation in forming those new grains adjacent to the host remains. The increased importance of deformation in Hobbs' case, readily explains the greater frequency of higher misorientations of new grains with respect to the host remains, that he obtained.

3.3.3.1.3 Recrystallization - Growth

The grains on the aggregate edge are generally considerably bigger (often more than twice the size, see fig. 3.13b, c) than those close to the host remains and sometimes show slight strain shadowing. Elongate

grains are aligned sub-parallel to S_M. Hence they have undergone some strain since nucleation but growth appears to be dominant. In aggregates which have been almost entirely recrystallized, the new grains away from the host grain remains have gently curved to straight grain boundaries (c.f. the more rounded boundaries of the newly recrystallized grains adjacent to the host). This would indicate that the initial strong growth after nucleation is replaced by grain boundary adjustment once an aggregate of new grains has formed (Smith, 1964). However, since triple point boundaries at 120° are uncommon even in those aggregates wholly converted to new grains at the fine quartz-feldspar mylonite stage of mylonitization, grain growth and consequent grain boundary adjustment are still prevalent (Smith, 1964). The fabrics of the grains on the aggregate edges were not obtained on the granulite facies side so that deformation effects on preferred orientation and angles between grains are not known. However in the stages of mylonitization after there are no more quartz host remains, these effects were studied in detail.

3.3.3.2 Amphibolite facies side

3.3.3.2.1 Deformation and recovery of host grains

Strain

The strain determined from length to width ratios of host grains (and aggregates) shows an increase from the slightly affected country rock to the coarse quartz feldspar mylonite but the strain by this stage on the granulite facies side is over three times greater.

Deformation microstructures

The initial signs of mylonitization in quartz are strain shadows, diffusely bounded deformation bands and extensive new grain growth on the

host grain edges. The quartz aggregates and host grains however are rarely elongate parallel to S_M. Thus the mylonitization is initially quite penetrative. The slightly affected country rock contains the least signs of mylonitization of any rocks collected from the amphibolite facies acid gneiss. The country rock schistosity S_2 is the only schistosity readily visible in hand specimen. Although the host quartz grains are not ellipsoidal parallel to S_M, most are no longer ellipsoidal parallel to S_2 (a number of the feldspars are however, and these indicate its trend).

With increase in strain, that is in rocks closer to the slaty mylonite, the number and size of actual host grain remains decreases quite sharply so that by the coarse quartz-feldspar mylonite stage there are only a few small host remains left. This is due to the dominance of recrystallization (section 3.3.3.2.2). The aggregates however become more elliptical and aligned parallel to S_M indicating considerable ductile deformation.

Subgrains

There is an increase in the size and misorientation of subgrains towards the edge of the host grain where they merge with new grains (fig. 3.9a, b, d). The subgrains are generally strongly polygonal with regular sides. They are most probably a product of dynamic recovery because new grains apparently forming from them on the host edge (see section 3.3.3.2.2) are often strain shadowed. In some cases the subgrains themselves are slightly elongate parallel to S_M. The subgrains increase in size towards the coarse quartz-feldspar mylonite. This could be associated with the extra growth seen in these rocks or a lower strain rate (Holt, 1971; Staker and Holt, 1972; Korbel and Swiatkowski, 1972;

Abson and Jonas, 1972). Because of the dominance of growth in these rocks the former is more likely.

Fabric

The host grain fabric in the least mylonitized specimen of amphibolite facies gneiss (fig. 3.4c) may be sufficiently affected by the mylonitization that it retains little reflection of the original pre-mylonite fabric. This is possible because the mylonite fabric develops rapidly relative to strain on this side and hence the mylonitization may be sufficiently penetrative to have destroyed the original fabric. However, the fabric contains a number of maxima asymmetrically distributed about S_M some of which are most probably relicts of the original fabric.

The host grain fabric of the strongly affected country rock (fig. 3.4d) is strongly mylonitic in character and shows considerable development relative to the above fabric for a relatively small increase in strain. In fact although there is an increase in strain to the coarse quartz-feldspar mylonite there appears to be no significant increase in the degree of preferred orientation (although this is difficult to determine due to the small number of host grain remains and because they plot as a point maximum, fig. 3.5d). The occurrence of a point maximum instead of two maxima may by due to the location of this specimen with respect to a $BS_M^{S_M}$ fold. A number of point maximum distributions occur throughout the mylonite zone, in both senses relative to S_M. There is a possibility that the sign of the shear stresses set up in the limbs during the formation of such a fold, may favour the combination of slip and climb systems operating within the ductilely deforming quartz so as to produce only one of the maxima (Wonsiewicz and Chin, 1970). Hobbs (1966) showed that the sense of point maxima relative to the layering

anisotropy or the axial plane, can change around a fold hinge from limb to limb. The fabrics he obtained are very similar to those described here.

3.3.3.2.2 Recrystallization - Nucleation

Nucleation sites

New grains nucleate on host grain edges. They are intimately associated with adjacent subgrains within the host. There is a progressive increase in size and mismatch of subgrains from within the host towards its edge where they merge with new grains of a similar or larger size (figs. 3.9a, b, d, 3.10d). The new grains thus nucleate in sites of high strain (Cahn, 1966; they do not form along deformation band boundaries however).

Angular relationships between host and new grains

There is effectively no host control on the orientation of new grains directly adjacent to host grain remains except for a very slight increase at low angles and decrease at high angles relative to the uniform distribution curve (figs. 3.1a, b, 3.2c). Thus the angular distribution between host and new grains is almost uniform. Similar distributions were obtained for angles between host grains and new grains on the aggregate edge (fig. 3.1c, d).

Angular relationships between adjacent new grains

These also have a distribution with slightly increased frequencies at low angles and decreased frequencies at high angles relative to the uniform distribution curve (figs. 3.1e, f, g, h, 3.2d). There is a decrease in the peak between 10 and 20 degrees relative to the uniform distribution curve for both the slightly and strongly affected country rock from new grains adjacent to the host to those on the aggregate edge

(compare figs. 3.1e and g; f and h). This is not significant when the total angular distribution between 10 and 30 degrees relative to the uniform distribution curve is considered. However it may be a product of increased concurrent deformation of those grains of the aggregate edge relative to those adjacent to the host (see later).

The relative sizes of subgrains and new grains

The new grains adjacent to host grain remains have a slightly larger size distribution than the adjacent subgrains. However those new grains on the aggregate edge are often considerably larger than the subgrains within the host remains. However the change in misorientation between adjacent new grains, from adjacent to the host to the aggregate edge is slight (see above).

Fabric of new grains (c-axes)

The new grains adjacent to the host (fig. 3.4e,f) for the slightly and strongly affected country rock have patchy irregular fabrics (especially the former), which contain several maxima and are basically crossed girdle patterns at high angles to L_M. However the new grains on the aggregate edge have regular distributions very close to a girdle normal to L_M with one or both of the characteristic mylonite maxima developed either side of S_M (fig. 3.4g, h). However, between the grains on the aggregate edge and those adjacent to the host remains there are generally only one or two grains (due to the large new grain size on the amphibolite facies side).

Those new grains on the aggregate edge have been affected by the ductile deformation associated with the mylonitization to the extent where their fabrics are similar to the host grain fabrics. The fabrics of those new grains adjacent to the host remains however, show little

effect of this ductile deformation in the slightly affected country rock and only slightly greater effect in the strongly deformed country rock.

Conclusions.

Nucleation mechanisms: There are two possible nucleation mechanisms which could produce the observed host-new grain angular distributions.

a) The new grains grow from submicroscopic regions or subgrains, or at least subgrains far smaller than those now present, allowing sufficient syntectonic growth since nucleation to effectively destroy any host control that existed.

b) The new grains form by syntectonic rotation, growth and perhaps coalescence of subgrains such as those now adjacent to them. The new grains once formed must continue to rotate in the same manner as the subgrains. This mechanism is probably more dependent on migration of dislocations to subgrain and new grain boundaries than on ductile deformation or a combination of slip and climb systems.

The second alternative is favoured because:-

a) The subgrains and new grains are intimately related, and there is a progressive misorientation and size increase across the transition from one to the other.

b) There is a considerable difference in the fabric of new grains adjacent to the host grain remains and those on the aggregate edge (compare figs. 3.4e and g; 3.4f and h). The concurrent deformation has produced a mylonite type fabric in those grains on the aggregate edge. If those grains adjacent to the host grain remains have been growing for a long time, they should show it too, as they are only slightly smaller than the grains on the aggregate edge, and the development of a mylonite type of fabric is rapid relative to the

degree of strain.

The main objection in the second possibility, to simply ductile deformation and rotation causing progressive rotation of subgrains and new grains is the dissimilarity of fabrics of new grains adjacent to the host and on the aggregate edge, yet the strong similarity in their host-new grain angle distributions (approximately uniform). It is difficult to conceive how the new grains adjacent to the host have not developed a mylonite fabric, yet have been rotated sufficiently to produce a close to uniform angular distribution between them and the host grains, whereas those new grains on the aggregate edge, which in many cases are only one grain away, have developed the mylonite fabric. This is strongly supported by results of syntectonic recrystallization experiments on single crystals of quartz (Hobbs, 1968). The new grains produced in these experiments can be readily interpreted as a product of deformation progressively increasing the mismatch between adjacent subgrains and the adjacent new grains. Yet none of the host-new grain angular distributions approach the close to uniform distributions obtained for new grains adjacent to the host in this work.

The other phenomenon which causes rotation of subgrains and new grains during dynamic recovery and recrystallization is the migration of dislocations to their boundaries. The dislocations are generated by the concurrent deformation. McQueen and Bergerson (1972, p.28) made reference to such a mechanism as being involved in the dynamic recrystallization of copper during hot torsion. They state 'The observations that the nuclei are only slightly larger than the subgrains, and that fairly high misorientations are present within the more heavily worked grains, indicate that high-angle boundaries form from cell walls through the accumulation

of dislocations.' Bailey (1963) also discusses such a process during polygonization only and states that misorientations of approximately ten degrees are commonly produced. McQueen and Bergerson imply however that considerably higher misorientations than this are produced.

The combination of rotation due to dislocation migration to grain edges, ductile deformation on a combination of slip and climb systems, subgrain growth and perhaps coalescence, could probably produce a host-new grain distribution such as that obtained for new grains adjacent to the host and yet not cause the development of a mylonite fabric. Those grains on the aggregate edge however, which most probably nucleated first (see section 3.3.3.1.2 - Critical strain for dynamic recrystallization) would be more affected by the concurrent ductile deformation and therefore show better development of the mylonite fabric. This is supported by the drop off in frequency of angles between adjacent new grains around 10 to 20 degrees and consequent increase in frequencies at higher angles from new grains adjacent to the host to new grains on the aggregate edge.

3.3.3.2.3 Recrystallization - Growth

Strain and growth microstructures: The new grains on the aggregate edges often show signs of deformation (strain shadowing). In the more mylonitic rocks they often contain deformation bands at 45^{o} to the trend of S_M (fig. 3.14c) and some are elongate parallel to S_M. The new grains on the aggregate edges are generally bigger than those adjacent to the host grain remains. Hence they have grown significantly since nucleation. With increased degree of mylonitization the new grain size also increases.

Fabrics: With increasing degree of mylonitization, the new grain fabrics

show an increased development of the mylonite type fabric. There is also increased similarity in the fabrics of grains on the aggregate edge compared with those adjacent to the host (compare figs. 3.4e and g; f and h; fig. 3.5e and f: In fig. 3.5f the new grains were measured in aggregates containing no host grain remains).

Angular relationships between grains: Apart from the change in the peak between 10 and 20^{o} for angles between adjacent new grains from the host to the aggregate edge (section 3.3.3.2.2), the angular distributions are all very similar (even host-new cf new-new plots).

Conclusions: Thus from the host grain edge to the aggregate edge, and with increased degree of mylonitization, there is concurrently increased growth, deformation, development of preferred orientation (i.e. development of the mylonite type fabric) and convergence of host-new and new-new angular distributions. This would indicate that the new grains, once they have nucleated, grow syntectonically. They progressively develop the mylonite type fabric therefore, due to deformation and rotation.

3.3.3.3 Comparison of the granulite and amphibolite facies sides

The only difference between the granulite and amphibolite facies acid gneisses which is known to have a significant effect on ductile deformation and recrystallization of quartz and which could cause the observed differences, is the water content (fig. 2.10). A strain rate difference during the mylonitization might also produce the observed differences in ductile deformation and recrystallization. However this would most probably be a product of the difference in water content from side to side and therefore be an inherited feature.

3.3.3.3.1 The effects of water on dislocations, ductile deformation, recovery and recrystallization of quartz.

The water content is known to have considerable effects on ductile deformation (Griggs and Blacic, 1965; Griggs, 1967; Hobbs, 1968; Heard and Carter, 1968; Baeta and Ashbee, 1970; Hobbs, McLaren and Paterson, 1972), recovery (Hobbs, 1968; Green,Griggs and Christie, 1970; Hobbs et al (op cit)) and recrystallization (Hobbs, 1968; Green et al (op cit); Tullis, Christie and Griggs, 1973) of quartz. Griggs (1967) showed that quartz crystals weaken during experimental deformation at a critical temperature dependent on the water content. He proposed that Si-O-Si bonds are hydrolysed and dislocation motion can therefore occur by hydrogen bond exchange which requires less energy. Hobbs(1968) showed that natural dry single crystals of quartz fail to recrystallize in a dry environment yet recrystallize readily in a wet environment. He proposed that hydrolysation of Si-O-Si bonds by water enabled climb of dislocations and hence recovery to occur at lower activation energies, and rates controlled by the diffusion of (OH) through the quartz structure to dislocation sites. In 'dry' quartz, recovery is apparently a very slow process. In 'wet' quartz where recovery is more rapid, new grain growth occurs because the recovery provides sites for nucleation. This was subsequently supported by the work of Green et al (op cit) which showed that additional water promoted recovery and enhanced recrystallization rates.

The single crystal experiments of Griggs and Blacic, Griggs, Hobbs, and Hobbs et al (op cit), were performed on quartz crystals which contained up to .13 weight percent water. This amount is of the order of the total amount of water available in the rocks on the granulite

facies side (which however would be dominantly held within the accessory biotite and hornblende). The quartzites experimentally recrystallized by Tullis et al (op cit) contain similar amounts of water but the experiments were performed in the presence of additional, unspecified amounts of water.

Green et al (op cit) conducted their experiments on Novaculite (0.1 weight percent water) and Dover Flint (1.2 weight percent water). Thus the water content of the Novaculite is comparable with the total water content in the rocks on the granulite facies side, and that in the Dover Flint is of the order of that in the rocks on the amphibolite facies side (fig. 2.10). They recorded similar recrystallization differences to those that occur between the rocks on the granulite and amphibolite facies sides (see later). They were able to attribute all the differences they saw to the difference in water content. They also found that recovery rates were enhanced by the addition of water and they suggested that this was due to increased hydrolysis of Si-O-Si bonds.

Although the water content within the single quartz crystals experimentally deformed by Hobbs et al (op cit) was small compared with that of the rocks on the amphibolite facies side, the fact that it was held within the lattice of the quartz may have some significance. The lowest and highest water contents in the crystals they used were approximately 0.01 and 0.09 weight percent water. Hence the difference in water content between these two crystals is of the order of the difference between that of the granulite and amphibolite facies sides. The differences they recorded in the characteristics of the deformation bands in these two crystals, are very similar to those which occur

between the granulite and amphibolite facies sides (see section 3.3.3.3.2), even though the crystal with the highest water content does not contain as much water as the total available in even the rocks on the granulite facies side.

3.3.3.3.2 Deformation and recovery of host grains

Deformation bands

The deformation bands on the granulite facies side have sharp boundaries (fig. 3.19c). On the amphibolite facies side the deformation bands are quite broad and actually consist of a number of narrow diffuse deformation bands which progressively offset the lattice producing a broad zone of bending (fig.3.19d). Hobbs, McLaren and Paterson (1972; figs. 13 and 14) found a somewhat similar phenomenon occured in experimentally deformed single quartz crystals with different water contents (see section 3.3.3.3.1). These crystals were deformed in the same orientation and under similar conditions. Hence the difference would appear to be due to the difference in water content. By analogy, and since the water content is the most significant chemical difference between the two sides, and the only one known to effect deformation of quartz in such a way, it appears that the difference in deformation bands is a product of the different water contents. This difference in the character of the deformation bands is very important because new grains nucleate on their boundaries on the granulite facies side but not on the amphibolite facies side (see section 3.3.3.3.3).

The degree of fabric development relative to strain

There is a significant difference in the degree of fabric development relative to strain from side to side. A good mylonite fabric

(see chapter 1 for discussion of typical mylonite fabric) has developed at the strongly affected country rock stage of mylonitization on the amphibolite facies side (fig. 3.4d), where the length to width ratio of quartz aggregates is less than two. On the granulite facies side however, such a degree of fabric development is not attained until the medium quartz-feldspar mylonite stage (fig. 3.5g), where the length to width ratio of quartz aggregates is greater than nine. This difference may, to a certain extent, be dependent on the initial amphibolite facies country rock fabric which is not known. However, even if it was somewhat similar to that in the slightly affected country rock (fig. 3.4c), the large fabric difference between this and the strongly affected country rock (fig. 3.4d) relative to the slight strain difference, indicates that the difference in strain needed to produce the mylonite fabric on each side is still significant. This difference can only be due to a difference in the combination of slip and climb systems involved in the ductile deformation of quartz. Hobbs (1968; see section 3.3.3.3.1) proposed that the presence of small amounts of water caused hydrolysation of Si-O-Si bonds which allowed climb of dislocations and hence recovery to occur. Green et al (op cit; see also section 3.3.3.3.1) showed that the rate of recovery was greater in the fine grained quartz aggregates with the higher water content (the rocks with the lower water content contained a similar total amount of water to that in the single crystals used by Hobbs). They suggested that the increase in water content increased the hydrolysis of Si-O-Si bonds, which further reduced the barrier to climb and hence enhanced recovery rates. Thus it is quite possible that either 1) the rate of climb of individual dislocations increases, or 2) the number of dislocations able to climb increases, with increasing water

content. This would perhaps allow more climb systems to become available for ductile deformation (Groves and Kelly, 1969; see also chapter 1.3.1) and hence change the combination of slip and climb systems operating. This could then explain the difference in degree of fabric development relative to strain from the granulite to the amphibolite facies side. Hobbs et al (op cit) found that the rate of strain hardening was much higher in the lowest relative to the highest water content crystal. This indicates that the mechanisms of deformation in these crystals must differ considerably and they related this to water content. This is an identical conclusion to that drawn here. However they considered it in terms of Haasen's (1964) theory on dislocation dynamics, whereas here it is considered just in terms of climb.

Subgrain size

There is a considerable difference in the size of subgrains on either side, those on the granulite facies side being much smaller. This suggests that the strain rate is considerably less on the amphibolite facies side up to the stage of mylonitization before quartz wholly recrystallizes than on the granulite facies side (Holt, 1971; Staker and Holt, 1972; Korbel and Swiatkowski, 1972; Abson and Jonas, 1972). This is supported by the difference in length to width ratios relative to the degree of subgrain formation and recrystallization (see below and section 3.3.3.3.3).

Degree of subgrain formation relative to strain.

The degree of subgrain formation (and also recrystallization) in the slightly affected country rock on the amphibolite facies side where the strain is slight (section 3.2.1B) is equivalent to that in the coarse quartz-feldspar mylonite on the granulite facies side where the strain is

very great (section 3.2.3.1A). This would indicate that the strain rate to this stage of development was considerably greater on the granulite facies side than on the amphibolite facies side. It also indicates that the degree of recovery is far greater on the amphibolite facies side (relative to strain). This is considered to be due to the increased water content and hence increased hydrolysis of Si-O-Si bonds on the amphibolite facies side. This could promote climb and hence recovery (c.f. Green et al (op cit); section 3.3.3.3.1).

3.3.3.3.3 Recrystallization

Nucleation sites

On the granulite facies side new grains nucleate on deformation band boundaries and host grain edges. On the amphibolite facies side they nucleate only on the host grain edges. The deformation bands are fewer in number on the amphibolite facies side and their boundaries are broad and consist of a number of gentle kinks which progressively rotate the lattice rather than the sharp bending which occurs on the granulite facies side. This could be a result of the different combination of slip systems suggested above. The more gradual distortion of the lattice on the amphibolite facies side may mean the strain energy along these boundaries has not reached the critical limit for dynamic recrystallization to occur (Honeycombe and Pethen, 1972; McQueen and Bergerson, 1972; Glover and Sellars, 1973). Hobbs et al (op cit) do not appear to discuss the significance of the similar difference in the nature of the deformation bands that they attained in experiments on single crystals of quartz with different water contents.

New grain size and degree of recrystallization

The new grains are much larger and the host grains show considerably

more recrystallization relative to the degree of strain on the amphibolite facies side. Green et al (op cit) from their experiments on Dover Flint and Novaculite showed that the degree of recrystallization was greater, and the new grain size larger in the 'wetter rock' under the same experimental conditions. They attributed this to the increased water content enhancing recrystallization. The chemical analyses (fig. 2.10) strongly suggest that the difference in degree of recrystallization and size of new grains observed here can be attributed to a similar difference in water content. Because of the intimate association of new and subgrains on both sides it is likely that the difference in subgrain size is also controlled by the difference in water content. The manner in which water effects sub and new grain size and degree of recrystallization is probably that proposed by Green et al (op cit). That is, the increased water content increases the hydrolysis of Si-O-Si bonds allowing climb and recovery to occur more readily which in turn affects the subgrain and hence new grain size and the degree of recrystallization.

Angular relationships between grains

On the granulite facies side there is a strong host control on new grain orientation (figs. 3.2a, e, g, h) whereas on the amphibolite facies side the control is much weaker (figs. 3.1a, b, c, d and 3.2c). This is probably a result of their different water content (see below). The distribution of angles between adjacent new grains reflects the difference in host control on either side (figs. 3.1e, f, g, h and 3.2b, d, f).

Nucleation mechanisms

Nucleation occurs in two sites on the granulite facies side, i.e. grain margins and deformation band boundaries. Nucleation in the former sites initially involves dynamic recovery and the formation of subgrains.

These then syntectonically grow and perhaps coalesce to form new grains which are consequentially related in orientation to the host. Nucleation in the latter sites initially involves dynamic recovery along the deformation band boundary and formation of small subgrains. The deformation band boundary then bulges where it is pinned by subgrain walls and new grains form by syntectonic growth of these subgrains and are hence related in orientation to the host. Once an aggregate of new grains has formed along the deformation band boundary new grains will be effectively forming in the first discussed nucleation site and therefore form by the mechanism discussed there.

On the amphibolite facies side nucleation of new grains only occurs on host grain boundaries. It appears possible that 1) the rate of climb of individual dislocations, or 2) the number of dislocations able to climb is much greater on this side due to the difference in water content (see earlier discussion at the beginning of this section). This could explain why quite large rotations of subgrains relative to the host and each other occur during recovery and their subsequent syntectonic growth. The dislocations once produced can rapidly migrate to subgrain walls during dynamic recovery thus causing rotation. Once the subgrains have rotated sufficiently to be considered as new grains, the process continues due to the concurrent deformation producing more dislocations which migrate to new grain boundaries. Thus large misorientations of new grains with respect to the host and each other could occur. There could also be a difference in the rate of generation of dislocations from the granulite to the amphibolite facies side. The increased hydrolysation of Si-O-Si bonds may not only allow climb of dislocations to occur more easily, but also allow dislocations to form more readily. The increased

climb itself would promote dislocation generation considerably (Hull, 1965; Hirth and Lothe, 1968), and this would greatly enhance the degree of rotation of sub and new grains relative to the host and each other.

3.3.3.3.4 The lack of deformation lamellas

No deformation lamellas were observed in quartz host or new grains in any of the rocks studied. McLaren, Turner, Boland and Hobbs (1970) and Hobbs et al (op cit) showed that deformation lamellas in the quartz crystals they worked on consist of narrow slabs containing a high density of tangled dislocations. Hobbs et al found that as the temperature was increased, the prominence of deformation lamellas decreased, and the subgrain structure became more apparent optically. The reason for the lack of deformation lamellas in quartz in the rocks studied here is considered therefore to be a product of the degree of dynamic recovery and perhaps also the temperature of deformation (see chapter 6 for a discussion of the metamorphic grade of the mylonitization).

3.3.4 The stages in mylonitization once quartz is wholly recrystallized

3.3.4.1 Discussion and comparison of the granulite and amphibolite facies sides.

Strain of aggregates.

At the stage of mylonitization where the quartz has wholly recrystallized the aggregate size on the amphibolite facies side is considerably coarser than that on the granulite facies side. This is due to complete recrystallization of host grains on the amphibolite facies side before they have been strained sufficiently to neck and part. On the other side this ductile breaking up of host grains occurs prior to complete recrystallization.

The aggregates show greater increases in strain with increasing mylonitization (i.e. towards the central mylonite beyond the quartz wholly recrystallized stage) on the amphibolite facies side. However, the degree of strain does not equal that on the granulite facies side until the homogenization stage of mylonitization. This is therefore simply a product of the greater degree of recrystallization relative to strain on the amphibolite facies side discussed previously.

Strain of new grains

At the quartz wholly recrystallized stage of mylonitization strain shadowed new grains are rare on the granulite facies side but a few are slightly elongate parallel to S_M. On the amphibolite facies side however, grains within the aggregates are often strain shadowed and elongate parallel to S_M. With increased mylonitization, these grains continue to show more signs of strain on the amphibolite facies side. In fact the strain became so great that small strongly rounded new quartz grains nucleated on the boundaries of quartz grains within the aggregates at the homogenization stage of mylonitization. This apparently is a product of the greater strain of quartz aggregates once the quartz has wholly recrystallized, on the amphibolite facies side. The relatively slight signs of strain in new grains on the granulite facies side indicates that the aggregates did not undergo as much strain after complete recrystallization of the original host which supports the conclusion drawn above. They suffered enough however to develop a mylonite fabric (see below).

Fabric

The fabrics of new grains adjacent to host grains before complete recrystallization of the quartz on the granulite facies side, show little

effect of the mylonite deformation. However, those on the amphibolite facies side show increasing effects with increasing mylonitization. This is due to the proximity of these grains to the aggregate edge, those adjacent to the host remains in the coarse quartz-feldspar mylonite being often right on the aggregate edge (this occured because their coarse size meant there were considerably fewer new grains per aggregate than on the granulite facies side). Hence they were more strongly affected by the concurrent deformation. After complete recrystallization of the quartz however, the aggregate grains on the granulite facies side also attain the mylonite fabric (fig. 3.6a; see chapter one for discussion of typical mylonite fabric) in response to the continued ductile deformation. A single maximum is sometimes developed either side of S_M instead of the more common double maxima (a discussion of this phenomenon is given in section 3.3.3.2.1: Fabric).

Towards the slaty mylonite the typical mylonite fabric begins to break up and grains have a patchy distribution. This is considered to be due to the dominance of growth, the rate of strain relative to growth being insufficient to preserve the strain controlled preferred orientation. The mylonite fabric was shown to be a product of increasing strain (ductile deformation) of host grains (section 3.3.3.1.1 and 3.3.3.2.1). Similarly, with increasing strain, the new grains develop a more perfect mylonite type fabric (compare fig. 3.6a and c, b with d and e). Hence during the homogenization stage of mylonitization the deformation control on quartz orientation diminishes and a growth control ensues which does not produce a typical mylonite fabric.

Growth of quartz grains within quartz aggregates

There is a convergence in the size of aggregate grains towards the

central slaty mylonite. Those on the granulite facies side increase and those on the amphibolite facies side decrease. This is thought to be a product of the converging degree of strain discussed above. Since the quartz aggregates suffer less strain on the granulite facies side after complete recrystallization of the quartz, growth is of more consequence. However since the aggregates suffer considerable strain on the amphibolite facies side, the decrease in grain size could be partly due to an increased strain rate closer to the central mylonite (similar to that observed on the granulite facies side before complete recrystallization of the quartz), and partly to the nucleation of small new grains on the old new-grain edges.

The growth of quartz within other aggregates and foreign minerals within quartz aggregates.

In the stages of mylonitization where quartz has wholly recrystallized, there is increased nucleation and growth of quartz on grain boundaries in aggregates of feldspar and mica. This occured in the early stages of mylonitization (see chapters 4 and 5) but is more pronounced in the mica growth and homogenization stages. In the latter stage, the destruction of quartz aggregates due to growth of mica and feldspar within them, is also very strong (c.f. White, 1968; Flinn, 1969). Similar destruction of feldspar aggregates and any remains of mica aggregates also occurs. Thus at the slaty mylonite stage of mylonitization, the ultimate degree of mylonitization observed in this area, the rock is a very homogeneous schist with a strong preferred orientation of mica (001). A few feldspar hosts and aggregates are all that remain to disturb the homogeneity. Thus towards the central mylonite large scale diffusion becomes increasingly important.

Before considering this homogenisation any further, it is necessary to discuss the role of interfacial energy in some detail. Devore (1956, 1959) concluded that the interfacial or grain boundary free energy largely controls the sites of nucleation and crystal growth and that it could play a dominant role during nucleation, crystal growth, exsolution, replacement and diffusion transfer. The work of White (1968) and Flinn (1969) on phase distributions in ceramics and grain contacts in gneisses respectively, showed that unlike phase contacts are statistically more frequent than like phase contacts. Flinn attributed this to interfacial energies of contacts between like phases being greater than those between unlike phases. Byerly and Vogel (1973, p.187) attempted to refute this however, and claimed that 'from theoretical reasoning unlike phases should be higher energy because of the greater mismatch of lattices'. However Smith (1952) has actually measured the interface energy in metals. His data on solid-solid interphase interfaces and single-phase grain boundaries shows that 'the energy of the interface between crystals of different metallic phases in contact with each other is generally less than that of the interface between two differently oriented crystals of the same phase'. If this applies to silicates, Flinn's and White's data may be due to interfacial energy differences as Flinn suggested.

Thus it would appear that lower interfacial energy for unlike phases may favour the separation of grains of the same phase (in the solid state) rather than their aggregation. It is apparent from the mica growth and homogenization stages of mylonitization that monomineralic aggregates are being destroyed due to the nucleation of other minerals within them. This would indicate that diffusion is considerable and it could be due to a lower amount of energy being needed for nucleation on other phase

boundaries (as suggested by the above discussion) rather than those of the same mineralogical phase. Its increased importance in the mica growth and homogenization stages could be due to the increased degree of recrystallization of original large grains into aggregates of new grains, providing more high angle grain boundaries for diffusion. Increased chance of fluctuations in composition, sufficient in size to form a nucleus of a new mineral phase, would then follow.

Angular relationships between new grains

The distributions of angles between adjacent new grains show a convergence with increasing mylonitization such that at the mica growth stage they are quite similar from side to side (figs. 3.3b and c). This is thought to be a result of the strain the new grains have undergone since nucleation, that is, their rotation to the typical mylonite preferred orientation. Since this is similar from side to side, one would expect the distribution of angles between adjacent new grains to also be similar.

Summary

It thus appears that the increased water content on the amphibolite facies side increases either or both 1) the rate of climb of individual dislocations, or 2) the number of dislocations able to climb. This could explain:

1) The difference in degree of fabric development relative to strain.
2) The difference in subgrain and new grain size.
3) The difference in degree of recrystallization relative to strain.
4) The difference in host control on new grains and consequent difference in angular relationships between adjacent new grains.

CHAPTER 4

THE MICROSTRUCTURAL DEVELOPMENT OF MICA IN THE MYLONITES ASSOCIATED WITH THE WOODROFFE THRUST.

4.1 Introduction

The changes in mica microstructures during mylonitization are described from the sequence of rocks presented in chapter three (3.1.1) for the granulite and then the amphibolite facies side. The changes are delineated from country rock through to the central mylonite. The microstructures are then interpreted and discussed.

4.2 Microstructural description

4.2.1 Granulite facies side

4.2.1.1 Host Grains

Deformation of host grains

The mica (biotite) present in the slightly affected country rock is aligned parallel to the country rock schistosity S_2 (average mica length is 70 μm). The effects of the mylonite deformation on this mica during the early stages of mylonitization are strain shadowing, kinking and limited nucleation and growth of minute new mica (average diameter 3 μm) and quartz grains in the regions cut by the microstructures described for quartz (section 3.2.1A).

Within the more mylonitic rocks the host biotites have lost some of the distinctive red colouration characteristic of the granulite facies and are generally strain shadowed and kinked (fig. 4.1a). The kink boundaries are aligned sub-parallel to S_M. The edges of host grains are often highly strained by slip along (001) instead of kinking (fig. 4.1b). The kink boundaries are often serrate, especially at kink angles around forty five and seventy degrees (figs. 4.1c, 4.1d).

At the medium quartz-feldspar mylonite stage, host grain remains are small and rare. With increased mylonitization there is an increased degree of alignment of host mica (001) parallel to S_M. Kink remains are

rare due to strong growth of new grains along them.

No host grain remains were observed after the medium quartz-feldspar mylonite stage of mylonitization.

Subgrains

Bulging of kink band boundaries around microstructures which were interpreted as subgrains, occurs in intensely deformed host grain remains (fig. 4.2a, b) in a manner directly analogous to that seen in quartz (c.f. fig. 3.13a). The angles of rotation of the lattice across these kink band boundaries are around 150° and the kinks are asymmetric with one limb at a very low angle to the kink boundary ($5 - 10^{\circ}$). Subgrains also appear to occur on the edges of such host remains where there is no apparent kinking, together with some new grains (fig. 4.2c). Both these relationships were only discernable in one or two host grain remains. In most the angle of kinking was not sufficient, or the degree of recrystallization along the kink boundaries and on the host grain edges was too great.

4.2.1.2 New grains

Nucleation sites

Kinks: New mica grains nucleate along kinks in the host mica (figs. 4.2d, 4.3a). They vary from equidimensional with rounded boundaries to elongate, and have an average diameter of 3 μm. The average new grain size is slightly smaller in the fine quartz-feldspar mylonite (2 μm) but there are no host remains at this stage. (001) of the new grains tends to lie parallel to the kink band boundaries. Small (4 μm) strongly rounded grains of quartz and feldspar sometimes also nucleate along kinks in mica.

Host grain edges: New micas nucleate on and within the highly strained

edges of host grains (fig. 4.2c, 4.3a). These new grains (average diameter 3 μm) are often strongly rounded. If they are at all elongate they tend to align parallel to S_M. Small (4 μm) strongly rounded grains of quartz and feldspar sometimes nucleate on host mica edges.

Foreign mineral aggregates surrounding the mica host site: Mica also nucleates on grain boundaries in other mineral aggregates directly surrounding the host grain site. The spread of mica about the old host site increases with increasing degree of mylonitization. The micas if elongate, tend to be so parallel to (001) and aligned parallel to S_M (average grain size, 3 μm).

Unrecrystallized minerals: Small micas nucleate along certain crystallographic directions in feldspar (fig. 4.3b). Often minute (2 μm) rounded micas occur in feldspar in random positions. Biotite grows along the cleavage in orthopyroxene during the early stages of mylonitization.

Growth - Changes with increased mylonitization

Grain Size: After the host grain remains have entirely recrystallized, apart from the slight decrease in new grain size at the fine quartz-feldspar mylonite stage of mylonitization, there is a gradual increase in size with increasing mylonitization up to the mica growth stage (section 3.2.5A; average mica length 6 μm). With further increases in degree of mylonitization, there is a sharp increase in average mica length to 30 μm at the homogenization stage and then 50 μm at the slaty mylonite.

Mica aggregates: The aggregates of mica formed around original host grain sites in the earlier stages of mylonitization become strongly elongate and then increasingly diffuse with increased mylonitization. At the mica growth stage, mica occurs abundantly in many quartz and feldspar aggregates (fig. 4.3c) and at the homogenization stage it is homogeneously

distributed throughout the matrix and very few quartz and feldspar aggregates remain (fig. 4.3d).

Fabric: With increasing mylonitization the degree of alignment of mica (001) about S_M increases until at the homogenization stage and in the slaty mylonite there is an almost perfect alignment of (001) of individual micas.

4.2.2 Amphibolite facies side

4.2.2.1 Host grains

Deformation microstructures

In the slightly affected country rock, a few large micas have (001) aligned parallel to S_2. The early effects of mylonitization on these micas are strain shadowing and kinking (fig. 4.4a). Single kinks often vary in angle along their length. The kink boundaries begin to migrate (become serrated) as the kink angle approaches 70° (fig.4.4b). The axial planes of the kinks tend to align parallel to S_M.

With increasing mylonitization, the size of host grain remains decreases due to increased recrystallization. Host grains often strain on their edges by slip along (001) without kinking. Quartz and mica sometimes interfinger along (001) (fig. 4.4c) and mica hosts often contain thin quartz grains in their cleavage. Host grain remains have disappeared by the quartz wholly recrystallized stage of mylonitization. In this rock however, (this rock is very strongly weathered), there are a few randomly orientated phyllosilicates (biotite - vermiculite?) which occur in clusters and are sometimes radiating. They show no signs of strain. Figure 4.6d shows that they are an alteration product of biotite and that they can recrystallize at orientations other than that of the original grain.

With increasing mylonitization the number of kinks decreases. This is due to the increased recrystallization of new grains along them (see section 4.2.2.2).

Fabric

The host grains as stated above, initially tend to be aligned parallel to the country rock schistosity S_2. A number however are kinked and some are aligned parallel to the trend of S_M (the mylonitic schistosity). These often appear to have deformed by slip along (001) (fig. 4.4d). In the more mylonitic rocks, the degree of alignment of host mica (001) parallel to S_M increases.

4.2.2.2 New grains

Nucleation sites

Kinks: New mica grains nucleate along kink boundaries in the host mica (fig. 4.5a). The small micas, average length 10 um tend to have (001) parallel to the kink. The new grain size increases with increasing mylonitization. The degree of bending (w: Etheridge and Hobbs, 1973) due to kinking often increases along the length of the kink boundary. With increase in W, the kink boundary begins to migrate near sites of new grain growth (fig. 4.5b). Zones of new grain nucleation often occur along what appears to be quite low angle kinks (fig. 4.5c). These zones may originally have been narrow kink bands which left the host to either side undisturbed and which have entirely recrystallized. Quartz and/or feldspar are always present along these zones, whether or not new mica growth occurs. The new micas in the centre of these zones are rectangular and have (001) aligned parallel to the zone length, but on the edges they are equidimensional and (001) is not so strongly aligned. Quartz and feldspar nucleate in obvious kinks also, as highly rounded new grains

(fig. 4.5a).

Host grain edges: New grains nucleate on and within the highly strained edges of host grains (fig. 4.5d). They average 6 μm long and tend to align parallel to S_M.

Foreign mineral aggregates surrounding the mica host: Mica also nucleates on grain boundaries in other mineral aggregates directly surrounding the host grain site. The spread of mica about the old host site increases with increasing degree of mylonitization. These micas show strong alignment of (001) parallel to S_M trend.

Unrecrystallized minerals: Mica grows along certain crystallographic directions in many feldspars.

Growth - Changes with increased mylonitization

Grain size: After the mica host grains have entirely recrystallized (they have done so by the quartz wholly recrystallized stage of mylonitization), there is a gradual increase in size of new grains to the slaty mylonite.

Mica aggregates: The aggregates of mica formed around original host grain sites in the earlier stages of mylonitization become strongly elongate and then increasingly diffuse with increased mylonitization. At the mica growth stage mica is growing abundantly in quartz and feldspar aggregates (fig. 4.6a) and is unevenly spread over most of the rock.

At the homogenization stage the mica is nearly homogeneously distributed throughout the rock (fig. 4.6b). It is entirely homogeneous in the slaty mylonite (fig. 4.6c).

Fabric: With increasing mylonitization the degree of alignment of mica (001) parallel to S_M increases until the slaty mylonite, where there is almost a perfect alignment.

Muscovite: Muscovite forms in increasing amounts in the latter stages of mylonitization.

4.3 Interpretation and discussion of mica microstructures

The microstructural development of mica during mylonitization is similar on both sides of the central(ultimate) mylonite. Hence, in the following section the microstructural changes are discussed fully for one side only. Then the significance of the differences between the two sides is interpreted and discussed.

4.3.1 Amphibolite facies side

4.3.1.1 The stages of mylonitization until quartz is wholly recrystallized.

4.3.1.1.1 Deformation of original (host) grains

Prior to mylonitization the micas were aligned parallel to the country rock schistosity (S_2). The first signs in these micas of mylonitization are strain shadows and kinks, that is, signs of ductile deformation. The axial planes of the kinks tend to align parallel to the trend of S_M. No subgrains were observed either adjacent to the kinks or on the edges of the host grains. However, considerable migration of the kink boundaries has occured especially at misorientations around 45 and 70 degrees (fig. 4.5a, b). This phenomenon has been described by Etheridge and Hobbs (1973) in experimentally deformed micas for misorientations around seventy degrees. They suggest it could be due to the high degree of lattice coincidence which occurs at 45 and 73 degrees for a rotation about [010]. Coincidence or near coincidence lattice boundaries are known to be more mobile than other boundaries (Kronberg and Wilson, 1949; Aust and Rutter, 1959a, b, 1960a, b, 1962; Gordon and Vandermeer, 1966; Aust and Chalmers, 1970; Simpson and Aust, 1972; see discussion section 1.3.3.2). Hence kink band boundaries for misorientations close to coincidence lattice relationships, could be more mobile.

Changes with increased mylonitization - Fabric

With increased mylonitization the number and size of host grains decreases considerably. This is due to multiple kinking of host grains and subsequent recrystallization along the kinks and on the host grain edges, leaving only small isolated remnants of host grains in a matrix of new grains.

Extensive ductile rotation of mica by slip along (001) also occurs (fig. 4.4c, d). This together with bodily rotation, due to the strain in surrounding quartz and feldspar grains and aggregates, and kinking, produces increased alignment of host mica (001) parallel to S_M with increasing mylonitization. Hence, at the coarse quartz-feldspar mylonite stage most host mica remains are strongly aligned parallel to S_M. Very few contain any kinks. This is because the kinks formed initially have recrystallized and once (001) is aligned parallel to S_M it is perpendicular to the shortening direction (from the strain of quartz and feldspar aggregates) and it is therefore unlikely that kinks could form. The alignment of kink boundaries close to S_M in the early stages of mylonitization also indicates the strong flattening component normal to S_M in the strain (Etheridge, Hobbs and Paterson, 1973).

4.3.1.1.2 Recrystallization

Nucleation sites

Small mica grains nucleate along kinks (fig. 4.5a, b, c; together with quartz and feldspar), on host grain edges (fig. 4.5a, d) and on grain boundaries in aggregates of other minerals adjacent to the host mica site. These are all sites of high stored strain energy which can provide a driving force for the nucleation process. Micas also occur along various crystallographic orientations in feldspar. No subgrains

were observed in any of the host grain remains but submicroscopic subgrains may occur.

Nucleation mechanisms

Kinks: There are apparently two kinds of kinks. There are those still recognizable as kinks across which there is a lattice rotation (fig. 4.5b). Then there are zones of new grains, on either side of which the lattice is parallel or only slightly rotated (fig. 4.5c). These are thought to have been narrow kink bands which have entirely recrystallized (such kinks are common in feldspar; see chapter five). The former contain new grains of mica with or without quartz and feldspar whereas the latter contain quartz and feldspar with or without mica (and the mica is sometimes in contact with quartz or feldspar rather than host mica).

Since the new micas, in direct contact with host mica on either side, are aligned along the kink, they are in no way related in orientation to the intensely deformed region of host across the kink boundary. Hence it would appear that a subgrain growth and/or coalescence, or even a bulge nucleation mechanism is not involved. There is however, the possibility that the new grains are forming from submicroscopic subgrains which are rotating due to the syntectonic nature of the recrystallization. Etheridge and Hobbs (1973) suggested that this was unlikely because of the restricted dislocation structure (Amelynckx and Delavignette, 1961). They argued that the dominance of a single slip plane with only one or two slip directions, and the restriction of dislocation climb due to the tendency of dislocations in layer silicates to split into partials (Silk and Barnes, 1960), did not favour the formation of subgrains. However, in the coarse quartz-feldspar mylonite on the granulite facies side, some microstructures were observed in mica

which were interpreted as subgrains (fig. 4.2a, c). No such microstructures were seen in micas on the amphibolite facies side but the possibility that they occured cannot be precluded. However the subgrains seen on the granulite facies side were only observed in a few very intensely deformed micas. They might therefore be a peculiar product of the unusual intensity of deformation that these host micas have suffered (see section 4.3.2).

Hence if subgrains do not generally form, it would appear that some other nucleation mechanism may occur. Quartz and feldspar also nucleate along these kinks (figs. 4.5b, c), which suggests they are zones of high diffusion of material. It is thus possible that diffusive processes are important in the nucleation mechanism. There are two nucleation mechanisms that could account for the lack of host control and which in the solid state are greatly affected by diffusive processes. These are:

a) Nucleation in the clasical sense.

b) Spinodal decomposition.

The latter is less likely where quartz and feldspar also occur, as these minerals appear to nucleate simultaneously with or even preceding the mica. This may prevent spinodal decomposition. However, in the obvious kinks where the kink boundary shows increasing migration and then merges into new mica grains (fig. 4.5b), spinodal decomposition is a distinct possibility. However, since the quartz and feldspar cannot be nucleating by spinodal decomposition, and since some mica nucleates in contact with quartz and feldspar rather than the host material, classical nucleation is the most likely of the two mechanisms.

The classical nucleation mechanism requires a compositional fluctuation of sufficient size to form a nucleus which exceeds a critical

size above which the surface free energy is less than the volume free energy and where molecules tend to stay combined rather than disperse (c.f. section 1.3.3.1). Hence, in the case of the quartz and feldspar nucleating in a mica host, it requires sufficient diffusion of their molecular components into the mica kink boundary that such a compositional fluctuation could occur. The constituents of mica though are readily available, and in the case where mica is recrystallizing in contact with host mica it is possibly a thermal rather than a compositional fluctuation that is required. Etheridge (1971) and Etheridge and Hobbs (1973) have shown that the critical size of a mica nucleus forming by heterogeneous classical nucleation without any contribution from energy due to a chemical change is too large and therefore the activation energy required too high for such nucleation to take place. They used a flat rectangular solid (sides 10:10:1) for a nucleus shape. However, the smallest newly recrystallized mica grains in these rocks are equidimensional (fig. 4.5b). Hence it is possible that the nucleus is spherical and that mica grains only achieve their normal rectangular habit after some growth. Using a spherical nucleus instead of a rectangular nucleus reduces the surface area and hence the inhibiting surface free energy term by over one half, but the nucleus is apparently still too big. There may however be some chemical change of the newly recrystallized micas relative to the host (they do not have the red colouration of the host on the granulite facies side) such as that found by Etheridge and Hobbs (1973), which could provide additional energy for the nucleation process (see section 1.3.3.1).

In the case of quartz and feldspar nucleating within the mica kinks, the interfacial energy difference, between quartz-mica and feldspar-mica compared with mica-mica interfaces, may favour the nucleation of

quartz and feldspar over mica and be sufficient to promote nucleation in the classical sense in such sites. Smith (1952) has shown that unlike phases generally have lower interfacial energies than like phases, and Devore (1956, 1959) has discussed the importance of interfacial energy on nucleation and nucleation sites (see section 3.3.4.1).

Host grain edges: Those micas growing within the host grain edges are generally aligned parallel to S_M and often cross cut the host (001) without there being any visible kink (fig. 4.5d). These micas most probably are forming by a similar mechanism to that described above, using the stored strain energy of the strained host grain edges. Their preferred orientation parallel S_M is discussed below.

Foreign mineral aggregates: The micas nucleating on grain boundaries in other mineral aggregates are most probably nucleating in a similar manner to that described for quartz and feldspar within host mica above. Again the possible decrease in interfacial energy due to unlike phases being in contact probably favours their nucleation in such sites, besides the supply of stored strain energy along the grain boundary. Their strong preferred orientation parallel to S_M is discussed below.

Changes with increasing mylonitization

With increasing mylonitization the degree of recrystallization increases (until no host grains remain). The spread of new mica grains around the host site, the new grain size and the degree of preferred orientation parallel to S_M, also increases.

The increased recrystallization of host grains until none remain may be a product of the increased strain in the more mylonitic rocks. That is, as the strain increased more mica reached the critical strain for dynamic recrystallization (Honeycombe and Pethen, 1972; McQueen and Bergerson,

1972; Glover and Sellars, 1973). This means that the micas in rocks closer to the slaty (central) mylonite have been growing for a longer time and therefore are bigger. This however is also a product of the increased diffusion which is evident towards the slaty mylonite (section 3.3.4.1). That is, with increased recrystallization, more original grains were converted to aggregates of small new grains and hence there were more grain boundaries for diffusion.

The increased tendency for mica to spread out around the host is thought to be a consequence of the increased diffusion and the concurrent deformation allowing interfacial energy to play a more important role in nucleation. White (1968) and Flinn (1969) recorded the tendency for unlike phase boundaries to be in contact after annealing recrystallization rather than like phase boundaries. When diffusion is great, the choice of nucleation sites could depend very strongly on interfacial energy considerations (Devore, 1956, 1959) even though the crystallization is syntectonic. The drop in interfacial energy due to nucleation in contact with an unlike phase may allow nucleation to occur that much more readily.

Fabric

The mica grains show a strong tendency to align parallel to S_M soon after nucleation. For those grains growing along kinks and grain boundaries this may be partly a result of control on the direction of diffusion of material exerted by the surroundings such as suggested by Etheridge, Paterson and Hobbs. However, for those new grains nucleating within the edges of host micas and growing across the host (001) with no visible signs of prior kinking (fig. 4.5d), such factors as mentioned above don't enter into consideration (there may be dislocations present however, which could exert some directional control on diffusion), yet

these new grains still show strong alignment parallel to S_M. There must therefore be some other control acting on the new grain orientation such as the thermodynamic control postulated by Kamb (1959 - see section 1.3.3.2).

The increase in degree of preferred orientation of mica (001) parallel to S_M with increase in the degree of mylonitization is probably due to two factors:

a) The increased number of micas due to breakdown of the feldspar (see chapter 2.3.1.2).

b) The increased microstructural anistropy parallel to the trend of S_M. The latter is due to the increased degree of ductile deformation with increased mylonitization. This causes a greater degree of alignment of deformation bands, kinks, (001) of host micas, and elongate aggregates of new grains. This would mean that diffusion could most readily occur parallel to S_M and hence effect an anisotropic growth control as proposed by Etheridge, Paterson and Hobbs (1973). Diffusion may also be influenced by some sort of stress gradient related to the fabric.

The randomly oriented, sometimes radiating phyllosilicates which show no signs of strain and occur as clusters in the quartz wholly recrystallized stage of mylonitization are an alteration product of biotite (fig. 4.6d). They can recrystallize in orientations other than that of the original grain. Since they are randomly oriented and show no signs of strain, they cannot be host grain remains. They may however be recrystallizing from host grain remains. Their random orientation also indicates that they are not associated with the mylonite deformation. Since this rock is highly weathered they may be a weathering product of the biotite, that is vermiculite (whether they are biotite or vermiculite

was not definite). However, they could also be a product of post deformation annealing recrystallization. There is however no other evidence in the rock for such an event, that is the microstructures in the quartz and feldspar, and the quartz fabrics are not indicative of such an event.

4.3.1.2 The ultimate stages of mylonitization

In the rocks where there are no host mica remains, the dispersion of mica is very evident, especially at the mica growth and homogenization stages of mylonitization. The sharp increase in the breakdown of feldspar to mica during these stages (see chapter 2.3.1.2) emphasizes this. Muscovite is a prominent feldspar breakdown product in the later stages.

The effects of increased diffusion due to recrystallization of large original grains into aggregates of small new grains, were discussed in section 4.3.1.1.2 and will not be repeated in detail here. However, it is this and the increased relative importance of interfacial energy in controlling nucleation and nucleation sites that are thought to be the dominant processes operating during the mica growth and especially the homogenization stages of mylonitization. The tendency for nucleation to produce unlike phases in contact is extremely pronounced. It is this which causes break up of the originally monomineralic aggregates thus homogenizing the rock (c.f. White, 1968; Flinn, 1969).

Fabric - Growth

There is a strong increase in the size of new grains passing from the mica growth to the slaty mylonite stage of mylonitization. There is also a strong increase in the degree of preferred orientation of mica (001) such that at the slaty mylonite stage it is near perfect (fig.4.6c)

It is thought this increase in length of new mica grains and degree of preferred orientation is due to a compounding of the anisotropic growth effects discussed at the end of the last section. That is with increasing alignment of mica (001), diffusion of material is further restricted to the plane of S_M and this continues until a near perfect preferred orientation of mica (001) is attained.

The increased breakdown of feldspar to mica during the latter stages of mylonitization possibly contributes to the increased size and degree of preferred orientation of mica grains by providing a ready supply of the molecular constituents of mica.

4.3.2 The differences between the granulite and amphibolite facies sides and their significance.

4.3.2.1 The differences.

4.3.2.1.1 Kinking.

The host grain remains on the granulite facies side show a very much greater degree of kinking than those on the amphibolite facies side. That is, host grain remains on the granulite facies side often contain multiple high angle kink bands with lattice rotations across the kink band boundaries of 150°. These kinks are also often strongly asymmetric such that one limb is at only $5 - 10^{\circ}$ to the kink band boundary (fig. 4.2a, b, d). On the amphibolite facies side however the kinking is less intense with generally fewer kink bands per host, lower degrees of lattice rotation across kink band boundaries, and less asymmetry (figs. 4.4a, b; 4.5a, b).

4.3.2.1.2 Subgrains.

On the granulite facies side microstructures which are interpreted as subgrains (average diameter 2 - 3 μm) occured in one or two intensely

deformed host grain remains. These subgrains occured adjacent to kinks (fig. 4.1d), in kink bands (fig. 4.2a, b) and on the edge of the host grain (fig. 4.2c). The kink and kink band boundaries bulge around the subgrains (fig. 4.1d, 4.2a, b) in a manner very similar to that seen in quartz (c.f. fig. 3.13a) on the granulite facies side. On the host grain edge the subgrains merge with new mica grains within an apparently unkinked region of the host (fig. 4.2c). No subgrains were seen on the amphibolite facies side, however.

4.3.2.1.3 Degree of recrystallization relative to strain.

The degree of recrystallization relative to strain is far greater on the amphibolite facies side than on the granulite facies side (c.f. quartz, chapter 3). Thus the mica has almost wholly recrystallized on the amphibolite facies side at less than half the strain (from length to width ratios of quartz aggregates) for an equivalent degree of recrystallization on the granulite facies side.

4.3.2.1.4 New grain size.

There is a very large difference in new grain size on either side at all stages of mylonitization. Those on the granulite facies side are far smaller than those on the amphibolite facies side.

4.3.2.2 The significance of these differences.

The occurence of subgrains within heavily deformed host grain remains on the granulite facies side reasserts the possibility of subgrain mechanisms being involved in nucleation during the recrystallization of mica. The bulge of kink and kink band boundaries around the subgrains would especially indicate bulge nucleation (Bailey, 1960; Bailey and Hirsch, 1962) as a feasible nucleation mechanism. In fact in figures 4.1d and 4.2a, the degree of bulge about one particular subgrain in each

photo is so great that the subgrain in each case is sitting within host remains on the other side of the kink and kink band boundary respectively. Since three quarters of the boundary for each subgrain is therefore high angle, they are effectively new grains. However such occurrences are rare and most new grains along kink and kink band boundaries appear to be in no way related to the host on either side or in the kink hinge (i.e. they generally occur with (001) parallel to the kink boundary). There is a strong possibility that subgrain rotation due to the syntectonic nature of the recrystallization occurs though. This possibility is supported by the intermingling of subgrains and new grains on the host grain edge where no kinks are apparent (fig. 4.2c). This figure shows that subgrains and new grains are of a similar size and that there is a progressive increase in the number of new grains relative to subgrains from the bottom to the top of the photo (i.e. closer to the aggregate edge). Hence the new grains could be forming by progressive rotation of subgrains due to the syntectonic nature of the recrystallization, that is, in a similar manner to that suggested by Hobbs (1968) for quartz in his syntectonic recrystallization experiments.

This means that much of the recrystallization of mica within mica hosts on the granulite facies side could be by subgrain mechanisms rather than by classical nucleation mechanisms as was suggested for the amphibolite facies side. It also reopens the possibility that nucleation can occur in a similar manner on the amphibolite facies side, even though no subgrains were observed in host mica remains there.

The presence of subgrains on the granulite facies side could be due to the intense degree of kinking of host grain remains relative to that on the amphibolite facies side. That is, the multiple high angle

kink bands with strong asymmetry may mean that dislocations are generated within these host grains of sufficiently diverse orientation to allow recovery and the formation of subgrains. This follows from the need for dislocations of a number of orientations for the complete enclosure of small subgrains (Jaoul, Bricot and Lacombe, 1957). On the amphibolite facies side however, the far less intense kinking, lower angle kinks and lower degree of asymmetry, may mean that dislocations of sufficient diversity for recovery and subgrain formation are not produced.

The increased degree of recrystallization and size of new grains on the amphibolite facies side could be a direct consequence of this.

The cause of these differences.

There are three factors which may differ from the granulite to the amphibolite facies side and which could account for the differences observed:

a) The original host micas on the granulite and amphibolite facies sides are different in composition.

b) The strain rate could be different from side to side because of the effect of water on the ductile deformation of quartz and feldspar.

c) The water content difference.

In the following sections these differences are considered in terms of recrystallization of new mica grains within a mica host involving:

1. Subgrain mechanism on both sides.
2. Subgrain mechanism on granulite facies side but not on the amphibolite facies side.
3. Classical nucleation mechanism on both sides.

Difference in host mica composition: The exact compositions of the original biotites in the country rock on either side are unknown but

they are obviously different because of the difference in colour. Those in the granulite facies acid gneiss are reddish whereas those in the amphibolite facies acid gneiss are brown.

1. The slight chemical differences may have little effect on dislocation generation and hence subgrain mechanisms.
2. The chemical difference between host and new grains on the amphibolite facies side relative to the granulite facies side may energetically favour classical nucleation before sufficient kinking and hence sufficient dislocation production for the formation of subgrains, can occur.
3. A more favourable energy change from host to new on the amphibolite facies side could greatly enhance degree of recrystallization relative to strain and hence new grain size and degree of kinking before complete recrystallization. However the effects of the initial composition are unknown at this stage.

Strain rate: Quartz and feldspar make up the bulk of the rock on either side. Hence differences in their ductile deformation from side to side, due to the effect of the increased water content on the amphibolite facies side, could have considerable effects on the rate of deformation of the mica. This could greatly effect the amount of kinking sustained before recrystallization, the angle of lattice rotation and the asymmetry of the kink itself. Stoffler (1972, p.85) from the thesis work of Schneider (1971) showed that the asymmetry of kink bands increases with increasing shock pressure as does the intensity of kinking whereas the kink band width decreases. If increase in shock pressure can be correlated with increase in strain rate then these changes are similar to those observed in host biotites between the amphibolite and granulite facies

sides (see discussion on strain rates from quartz subgrain size and aggregate elongation, chapter 3). However, Etheridge, Hobbs and Paterson (1973) have shown in mica deformed experimentally at relatively low strain rates, there is a crystallographic control on slip directions in (001) whereas in shock experiments there is apparently no such control (Horz and Ahrens, 1969). This may weaken the correlation made above as it may indicate that deformation of mica in shock experiments is entirely different from that at lower strain rates.

1. The strain rate has a considerable effect on the size of subgrains in metals (Holt, 1971; Staker and Holt, 1972; Korbel and Swiatkowski, 1972; Abson and Jonas, 1972). At lower strain rates the subgrains are larger. Hence they should be more readily observable on the amphibolite facies side. However none were seen.
2. If increased strain rate can be correlated with increased shock pressure and is the cause of the greater intensity of kinking, and kink asymmetry this could readily explain the production of subgrains on the granulite facies side and not on the amphibolite facies side as discussed earlier and hence the recrystallization differences observed.
3. How strain rate affects nucleation in the classical sense is not known. Hence if recrystallization involves this mechanism for mica within mica on both sides, the reason for degree of recrystallization and new grain size differences is not known.

Water content difference: Because water has such strong effects on the ductile deformation, recrystallization and hence new grain size of quartz, it could effect mica in a similar way. However what the effect is at this stage (if any) remains unknown. It could be that increased hydrolysis

of Si-O-Si and Si-O-M bonds occurs allowing dislocation climb to occur more readily, a process which is apparently very difficult in layer silicates (Etheridge and Hobbs, 1973).

1. The increased water content on the amphibolite facies side could increase the rate of recrystallization to such a degree that the moment subgrains form they rotate and become new grains (due to the rate of dislocation movement to subgrain walls). Subgrains were therefore preserved on the granulite facies side due to lower rates of dislocation movement. This could explain the increased recrystallization, new grain size and less intense kinking.
2. The increased water content on the amphibolite facies side could effect the style of kinking in a manner similar to that seen in quartz (Hobbs, McLaren and Paterson, 1972), whereby the kink bands are less intense broader, lower angle and possibly less asymmetric. Hence the necessary diversity of dislocation orientation for subgrain formation is not produced and hence subgrains do not form. On the granulite facies side however they do.
3. Increased hydrolysis may mean increased climb and hence increased diffusion of the amphibolite facies side. This may have some bearing on degree of recrystallization and new grain size.

Conclusion

The factors which could affect kinking, subgrain formation, the degree of recrystallization and new grain size of mica are known. However, if and how they affect them is not known for certain, and until more experimental data is available on the deformation and recrystallization of mica, this will probably remain unresolved.

So far, the difference in size of new mica grains nucleating in

foreign mineral aggregates surrounding the host mica site, and the size of quartz and feldspar grains nucleating in host micas has not been discussed. The formation of these grains may involve classical nucleation mechanisms on both sides of the slaty mylonite and their change in size matches that seen in new mica grains nucleating within mica hosts from side to side. It is therefore apparent that new grain size could be affected by the above discussed differences from side to side for a classical nucleation mechanism. However, the possibility that subgrains form in host mica on the granulite facies side but not on the amphibolite facies side (2 above) is favoured for the nucleation of new mica within host mica. Hence the nucleation mechanisms are different from side to side. At this stage it is the only possibility that can be explained by each of the known differences (water content and strain rate and the possible differences due to the change in chemistry of the host mica), and which readily fits the observations.

CHAPTER FIVE

THE MICROSTRUCTURAL DEVELOPMENT OF FELDSPAR IN THE MYLONITES ASSOCIATED WITH THE WOODROFFE THRUST.

5.1 Introduction.

This chapter deals with the microstructural changes in feldspar for the sequence of rocks described in chapter three. The microstructures are firstly described and then discussed and interpreted. To avoid repetition, the microstructures are described for the amphibolite facies side with grain sizes and any other differences that occur on the granulite facies side placed in square brackets.

5.2 Microstructure description.

5.2.1 Pseudotachylite

The brittle fracture associated with the pseudotachylite which occurs on the granulite facies side of the mylonite zone (see map) was described and discussed in chapter three. The only brittle fracture seen in feldspar occurs directly adjacent to this zone. It intensifies towards the zone from either side, and as discussed in chapter three, can be attributed to the pseudotachylite production and is later than the main mylonitization. Actual fractures associated with the microshears are few in number and are infilled with opaque. This is only evident at high magnifications as at low magnifications the very heterogeneous plastic deformation gives the feldspars a fractured appearance (i.e. the local intense kinking). The remainder of this section therefore considers only the ductile aspects of deformation in the region west of the pseudotachylite, i.e. in the slightly and strongly affected country rock on the granulite facies side.

5.2.2 The amphibolite facies side.

Differences which occur on the granulite facies side are recorded in square brackets.

5.2.2.1 Host Grains.

Deformation Microstructures.

A few large ellipsoidal feldspars are aligned parallel to the country rock schistosity (S_2) in the slightly affected country rock. The feldspar is mainly orthoclase and microcline with some plagioclase. The initial effects of mylonitization on these feldspars are strain shadowing, deformation twinning and kinking (fig. 5.1a [5.1b]). In many cases the kinks are just local thin lines of birefringence variation. Under high magnification these are seen to be either, kinks where the lattice on either side is parallel but which in the near vicinity of the kink, bends into the kink from either or both sides (fig. 5.1c), or narrow kink bands within which the lattice shows strong birefringence variation but to either side of which it is undisturbed.

In the more mylonitic rocks the host grains are more strongly strain shadowed, kinked and deformation twinned (fig. 5.1d [5.2a]). However, after the quartz wholly recrystallized stage of mylonitization the number of kinks in host grain remains decreases until at the homogenization stage there are very few kinks at all. At this stage there are less deformation twins also [this is not so apparent on the granulite facies side]. The alignment of deformation twin sets relative to S_M is variable. At the homogenization and slaty mylonite stages of mylonitization there is a weak tendency, if two sets of deformation twins occur, for them to be aligned symmetrically either side of S_M (fig. 5.2b).

With increasing degree of mylonitization the feldspar host grains become ellipsoidal in shape parallel to S_M (at the coarse quartz-feldspar mylonite stage) and decrease in length from initially 900 μm [500 μm] to 600 μm [200 μm] by the time quartz has wholly recrystallized. With further increases in the degree of mylonitization they continue to

decrease in size until they are 200 μm [150 μm] at the homogenization stage [the feldspar host grains show a more gradual decrease in size after the quartz wholly recrystallized stage of mylonitization on the granulite facies side]. Not only does the size of host remains decrease, but also the number of host grains decreases with increasing degree of mylonitization. However, the average length to width ratio of the ellipsoidal host remains stays constant at approximately 1½. There are a few host grain remains even in the slaty mylonite.

Both orthoclase and microcline microperthite appear in the early stages of mylonitization. The microperthite is generally rod like (Spry, 1969) and aligned parallel to deformation twins or strain shadows (fig. 5.1a [5.1b]). The amount of microperthite decreases in the more mylonitic rocks and is a rarity after the mica growth stage.

Subgrains.

Very small (3 μm) subgrains occur along kink boundaries [on the granulite facies side the subgrains are even smaller; approx. 1½ μm]. The boundary often bulges around them (fig. 5.1c). The edges of host grains generally have a narrow rim which shows strong birefringence variation. Small subgrains (5 μm [3½ μm]) occur within this thin rim of host (fig. 5.2c [5.3d]) and these often merge with new grains on the extreme edge. Such subgrains also occur within narrow kink bands. Adjacent original feldspars sometimes exhibit grain boundary bulge where the boundary is pinned by subgrain walls (fig. 5.2d).

With increase in the degree of mylonitization the average size of subgrains on the host grain edges decreases to 2 - 3 μm at the mica growth stage of mylonitization [on the granulite facies side, the average subgrain size decreases from 3.5 μm in the coarse quartz-feldspar

mylonite to around 2 - 3 μm in the fine quartz-feldspar mylonite. It remains around 2 - 3 μm in the more mylonitic rocks].

5.2.2.2 New grains.

Nucleation sites and growth.

Kinks: New feldspar grains nucleate along kinks (fig. 5.3a [5.3b]) and in the intensely deformed regions within narrow kink bands (fig. 5.3c). The new grains forming along single kinks can sometimes be seen to form adjacent to serrate portions of the kink boundary where it is bulging around subgrains (fig. 5.1c). Those forming within kink bands often occur adjacent to slightly smaller subgrains (fig. 5.3c).

The average size of new grains forming along kinks is 5 μm [2 μm] in the early stages of mylonitization. In the more mylonitic rocks the average size of new grains forming along kinks increases as the number of new grains along and adjacent to the kink increases. However in those kinks with only a few new grains along them the size remains small.

Host grain edges: New grains of feldspar often nucleate on host grain edges within the thin rim of highly strained host material. They form adjacent to and are intimately associated with subgrains of a slightly smaller size (fig. 5.2c [5.3d]). The average size of new grains in these sites is 7 μm [new grains do not form in such sites during the very early stages of mylonitization on the granulite facies side]. With increasing mylonitization the size of new grains directly adjacent to the host grain remains decrease slightly [on the granulite facies side after the medium quartz-feldspar mylonite stage, the new grains directly adjacent to host grain remains average 3 μm in diameter. They are slightly bigger in the coarse quartz-feldspar mylonite]. However the new grain size increases rapidly away from the edge of the host grain

remains (fig. 5.4a [5.4b]). Hence there is an increase in the average new grain size to 20 μm [4 μm] in the coarse quartz-feldspar mylonite and hence a gradual increase to 50 μm in the slaty mylonite [on the granulite facies side the average new grain size is only 6 μm at the mica growth stage. It increases sharply to 30 μm and then 50 μm at the homogenization and slaty mylonite stages respectively].

Deformation twins: New grains sometimes nucleate along deformation twins (fig. 5.4c).

Grain boundaries.

The boundaries of new grains forming along kinks and on the edges of host grains are rounded. In new grain aggregates of feldspar which contain no host remains (these become obvious at the quartz wholly recrystallized stage but do occur in the coarse quartz-feldspar mylonite) grain boundaries are rounded to gently curved (fig. 5.4d [5.5a]). In the more mylonitic rocks still (i.e. the mica growth and homogenization stages of mylonitization) the grain boundaries within feldspar aggregates vary from gently curved to straight (fig. 5.5b [5.5c]).

Elongation of feldspar aggregates.

With increasing mylonitization (after some feldspar host grains have been fully converted to aggregates of new grains) feldspar aggregates become increasingly ellipsoidal parallel to S_M.

Homogenization.

During the mica growth stage of mylonitization micas nucleate and grow on grain boundaries in many of the aggregates of new feldspar grains (fig. 5.5b [5.5c]). This is very pronounced during the homogenization stage where the nucleation and growth of quartz and mica in feldspar aggregates has changed many of them to effectively matrix material. Hence

in the slaty mylonite there are relatively few monomineralic feldspar aggregates remaining as such and homogenization has been so complete that the rock is a very homogeneous quartz-feldspar-mica schist containing a few ellipsoidal feldspar host grain remains (fig. 5.5d). Feldspar grains in the matrix change from 30 μm to 40 μm from the homogenization stage to the slaty mylonite. These grains are generally fairly equidimensional but if elongate they tend to align parallel to trend of S_M. [There are more feldspar aggregate remains in the homogenization stage on the amphibolite facies side than on the granulite facies side as there homogenization is more advanced].

5.3 Interpretation and discussion of the feldspar microstructures.

Since the microstructural development of feldspar during mylonitization is similar from the amphibolite to the granulite facies side of the slaty mylonite, it is discussed fully for one side only. Then the significance of the differences between the two sides is interpreted and discussed.

5.3.1 Amphibolite facies side.

5.3.1.1 Deformation and recovery of original (host) grains.

Deformation microstructures.

Prior to mylonitization the feldspars were ellipsoidal and aligned parallel to the country rock schistosity (S_2). The first signs of mylonitization in these feldspars are strain shadows, deformation twins and kinks, all of which are signs of ductile deformation. With increasing degree of mylonitization the above phenomena intensify but then the number of kinks decreases. This is due to the increased degree of recrystallization along them (see below). Apparently the original feldspars are deformed initially by kinking to a certain strain. When recrystallization is sufficient, further deformation tends to be accomodated by strain of surrounding grains and movement on grain boundaries rather than by further kinking of the host remains. Hence the kinks are gradually replaced by new grains reducing the size of host remains and the number of kinks. This would explain why the length to width ratios of feldspar host grain remains does not increase.

Subgrains

Small rounded subgrains form along the kinks which leave the lattice away from the kink to either side unrotated (fig. 5.1c). They form in the regions of local intense bending of the feldspar lattice on

either side, but directly adjacent to the kink. They appear to be a product of recovery of this portion of the host. The kink bulges where it is pinned by their walls (fig. 5.1c).

Subgrains also form in the deformed region of host within kink bands (fig. 5.3c) and on host grain edges (fig. 5.2c). Grain boundary bulge sometimes occurs between adjacent feldspars where the grain boundary is pinned by subgrain walls (fig. 5.2d).

The subgrain size in the feldspar host grain remains decreases with increase in the degree of mylonitization (i.e. towards the slaty mylonite) from 5 μm to 2 - 3 μm. The work done in metals on subgrain size and strain rate (Holt, 1971; Staker and Holt, 1972; Abson and Jonas, 1972) would indicate that this means there was an increase in strain rate towards the slaty mylonite during mylonitization.

5.3.1.2 Recrystallization.

Nucleation sites.

New grains nucleate along kink boundaries (fig. 5.3a). They often occur along the kink adjacent to where it is bulging around subgrains (fig. 5.1c). New grains also nucleate within narrow kink bands adjacent to slightly smaller subgrains (fig. 5.3c). They also form on host grain edges where they are intimately associated with subgrains of a slightly smaller size (fig. 5.2c). Figure 5.2d shows new grains associated with the bulge of a grain boundary (between adjacent feldspars) around subgrains, that is, where it is pinned by their walls. New grains sometimes also nucleate along deformation twins (fig. 5.4c).

Nucleation mechanisms.

Thus the new grains are forming in sites of high strain within the host grains (c.f. Cahn, 1966). The intimate association of sub and new

grains along the kinks and also along the boundaries between adjacent feldspars (figs. 5.1c and 5.2d), and the progressive increase in bulge and degree of mismatch in those subgrains closer to the new grains indicates that the latter are forming by a bulge nucleation mechanism (chapter 1.3.3.1; Bailey, 1960; Bailey and Hirsch, 1962).

Similarly the intimate association of new grains and subgrains on host edges and between closely spaced kinks, would indicate that the new grains are forming by subgrain growth and perhaps coalescence aided by rotation of subgrains due to the concurrent deformation, rather than growth of submicroscopic regions (chapter 1.3.3.1; Beck, 1949; Cahn, 1950; Hu, 1963). These sites are those of sharp variation in the host lattice orientation and hence high angle boundaries can form readily and thus allow recrystallization to proceed rapidly.

That the recrystallization is syntectonic is apparent from the strain shadowing and deformation twinning in new grains.

Changes with increasing degree of mylonitization.

With increasing myloniitzation the average size of new grains increases. However, those new grains directly adjacent to host grain remains, remain approximately constant in size. There is however, a rapid increase in new grain size away from the host edge towards the edge of the feldspar aggregate (fig. 5.4a). This is a product of the progressive recrystallization of the host grains. When the edge of the host grain reaches the critical strain for dynamic recrystallization (Honeycombe and Pethen; McQueen and Bergerson, 1972; Glover and Sellars, 1973), new grains nucleate. The process is then repeated if deformation continues, causing a progressive recrystallization of the host. Hence those grains on the aggregate edge have been growing for a longer time than those adjacent to

the host grain remains and are therefore bigger. The increase in average new grain size towards the slaty mylonite is also a product of this. The strain increases towards the slaty mylonite (from length to width ratios of quartz aggregates, chapter three). Hence those host grains in rocks closer to the slaty mylonite reached the critical strain for dynamic recrystallization before those further away. Hence the new grains within them have been growing for a longer time and are therefore bigger.

During the mica growth and homogenization stages break up of the monomineralic feldspar aggregates occurs due to nucleation and growth of mica and quartz within them. This occurs to such an extent that within the slaty mylonite there are only a few feldspar host and aggregate remains (fig. 5.5d). The rock is thus an extremely homogeneous quartz-feldspar-mica schist (apart from the feldspar host remains). The nucleation and growth of mica within feldspar aggregates and feldspar, and in mica and quartz aggregates, was discussed at some length in chapters three and four. In summary, it is considered that the increasing degree of recrystallization and hence reduction of large original grains to aggregates of small grains, with increasing degree of mylonitization, allows increased diffusion. The numerous grain boundaries act as paths for diffusion enabling nucleation of new grains to be controlled by such considerations as interfacial energy (Devore 1956, 1959). Hence monomineralic aggregates tend to break up due to the nucleation of unlike mineral phases within them, which is generally a lower energy situation (Smith, 1952) and has been recorded in ceramics (White, 1968) and rocks (Flinn, 1969).

5.3.2 The differences between the amphibolite and granulite facies sides and their significance.

Host grain size.

The decrease in the size of host grain remains is much greater relative to the degree of recrystallization on the granulite facies side than the amphibolite facies side up to and including the stage of mylonitization where quartz has wholly recrystallized. However, with further increases in the degree of mylonitization the decrease in size of host grain remains on the amphibolite facies side is very rapid whereas on the granulite facies side it is quite gradual. The size of the host grain remains thus converges towards the slaty mylonite.

Subgrain size.

During the stages of mylonitization before quartz is wholly recrystallized the subgrain size is larger on the amphibolite facies side than on the granulite facies side (i.e. 5 μm c.f. 2 - 3.5 μm: On the granulite facies side the subgrain size drops from 3.5 μm in the coarse quartz-feldspar mylonite to 2 - 3 μm in the fine quartz-feldspar mylonite). After the quartz wholly recrystallized stage of mylonitization the subgrain size on the amphibolite facies side decreases to 2 - 3 μm whereas that on the granulite facies side remains approximately constant.

Degree of recrystallization relative to strain.

The degree of recrystallization relative to strain is initially far greater on the amphibolite facies side than on the granulite facies side. New grain growth is very strong even in the slightly and strongly affected country rock on the amphibolite facies side (fig. 5.1a, d). Such a degree of recrystallization is not attained until the medium quartz-feldspar mylonite on the granulite facies side. However after quartz has wholly recrystallized, the degree of recrystallization on either side is more similar.

New grains.

The average size of new grains on the granulite facies side is much smaller than that on the amphibolite facies side along kinks and on host grain edges at all stages until homogenization.

The significance of these differences.

Subgrain size: By analogy with the effect of strain rate on subgrain size seen in experimental deformation of metals (Holt, 1971; Staker and Holt, 1972; Korbel and Swiatkowski, 1972; Abson and Jonas, 1972), the strain rate was higher on the granulite facies side than on the amphibolite facies side in the rocks up to where the quartz has wholly recrystallized. In fact the strain rate increased from the coarse quartz-feldspar mylonite to the fine quartz-feldspar mylonite on the granulite facies side.

After the quartz wholly recrystallized stage of mylonitization, the strain rate closer to the slaty mylonite on the amphibolite facies side increased, but that on the granulite facies side remained approximately constant such that by the homogenization stage, the strain rate was similar from side to side (subgrain size on both sides at this stage is 2 - 3 μm). This is supported by the length to width ratios of quartz aggregates.

Subgrain size combined with the other differences: The suggested differences in strain rate (from change in subgrain size), the difference in reduction in the size of host grain remains relative to the degree of recrystallization, the difference in degree of recrystallization and the difference in new grain size may be a product on the initial difference in water content between the granulite and amphibolite facies sides (c.f. degree of recrystallization of quartz, chapter 3). Griggs (1967) stated that hydrolytic weakening had been observed in a number of other silicates apart from quartz, including plagioclase feldspar. In fact all

the silicates that had been tested at that stage exhibited hydrolytic weakening and it has since been clearly documented in olivine (Blacic, 1972). Hence it is reasonable to assume that it also occurs in orthoclase and microcline. Thus the increased water content on the amphibolite facies side may cause similar effects in feldspar to those seen in quartz (chapter three). Certainly the increased degree of recrystallization, subgrain and new grain size on the amphibolite facies side relative to the granulite facies side up to the stage where quartz is wholly recrystallized, reflect the differences seen in quartz from side to side.

Thus increased hydrolysis of Si-O-Si bonds may cause increased climb, recovery and hence recrystallization (in the early stages of mylonitization) on the amphibolite facies side. The possible manner in which this affects the size of host grain remains before and after the quartz wholly recrystallized stage of mylonitization, and the subgrain and new grain size is discussed below.

Since considerably more strain is needed on the granulite facies side to produce similar degrees of recrystallization to that on the amphibolite facies side, the host grains are consequently more deformed and kinked. Hence at the quartz wholly recrystallized stage of mylonitization, where there has been sufficient recrystallization along many of the kinks to separate original single host grains into smaller host remnants, the host remnants on the granulite facies side show a greater reduction in size. The strain in rocks on the granulite facies side levels off at the quartz wholly recrystallized - mica growth stages. Hence the feldspar host remnants kink no further from the mica growth stage and do not decrease in size from then on. On the amphibolite facies side however, the strain increases markedly after the quartz has

wholly recrystallized (since quartz recrystallizes so early with respect to degree of strain and since the strain at the homogenization stage from side to side is similar). Hence the feldspar hosts undergo considerable deformation after the quartz has wholly recrystallized and probably therefore kink sufficiently for syntectonic recrystallization to reduce host remnants sharply in size before homogenization begins in earnest so that at the homogenization stage they are similar in size to those on the granulite facies side.

The subgrain and hence new grain size is therefore coarser in the early stages of mylonit ization due to the lower strain rates up to the mica growth stage on the amphibolite facies side.

6.1 Relationship between petrology, geochemistry and fabric.

Throughout the previous three chapters, the amphibolite and granulite facies sides of the mylonite zone have been separated on microstructural grounds by the slaty mylonite. This is supported by the following petrographical and geochemical evidence that the rocks to one side of the slaty mylonite were originally granulite facies acid gneisses while those to the other were originally amphibolite facies acid gneisses:

a. Augite: Augite remains occur in the mylonites on the granulite facies side up to and including the mylonite at the homogenization stage. Clinopyroxene has only been observed in granulite facies or retrograded (transitional) granulite facies acid gneisses in the Amata region (this thesis; Collerson, 1972; Collerson, Oliver and Rutland, 1972).

b. Rb/Sr: The Rb/Sr ratio is low on the granulite facies side and high on the amphibolite facies side of the slaty mylonite (fig. 2.10). The Rb/Sr ratio is generally low in granulite facies acid gneisses and higher in amphibolite facies acid gneisses in the Musgrave Ranges (c.f. Collerson, 1972, table 4.2; Lambert and Heier, 1968, table 11).

c. Water: The water content is low on the granulite facies side and high on the amphibolite facies side of the slaty mylonite (fig. 2.10). Collerson (1972, table 4.2) found that the average water content (using weight loss on ignition as an approximation) was less in the granulite than in the amphibolite acid gneisses just to the south of the area mapped.

It is thus concluded that the differences in microstructural development are closely tied to the differences between the granulite and amphibolite facies country rock. However, these differences for the

minerals studied microstructurally in detail are only slight, apart from the initial mica content and composition difference. Geochemically the differences are also very slight, apart from the water content and the Rb/Sr ratio. Hence the differences in microstructural development can be dominantly attributed to the initial water content difference.

It is concluded that the slaty mylonite occurs near the contact between two tectonic units (see below) and in fact that this contact lies between the slaty mylonite and the homogenization stage mylonite on the granulite facies side (since the slaty mylonite exhibits amphibolite facies side characters in terms of Rb/Sr ratio and water content).

6.2 Microstructural development.

The conclusions of general significance due to this study of the microstructural development of mylonites and mylonitic rocks associated with the Woodroffe Thrust are:

1. Natural mylonites can develop entirely by ductile deformation and recrystallization phenomena.
2. Field support for the Frank-Griggs hypothesis of hydrolytic weakening in silicates, and the radical effect of water content on the recrystallization of quartz observed experimentally (and to a certain extent on feldspar), and also the effect of water on the combination of slip and climb systems operating during ductile deformation of quartz.
3. There is a close similarity between recent microstructural observations on dynamic recrystallization in metals with those seen here. The nucleation mechanisms also appear to be similar. The subgrain size variation in quartz and feldspar across the mylonite zone gives an indication of the strain rate variation relative to distance from the

slaty mylonite. The strain rate increases rapidly on the granulite facies side moving into the mylonite zone (there is a sharp increase near the pseudotachylite belt), and then levels off closer to the slaty mylonite. On the amphibolite facies side it increases slowly at first and then more sharply closer to the slaty mylonite.

4. Quartz, feldspar and mica each behave in a slightly different manner during mylonitization. However, the microstructures observed in each mineral support the indications with regards to deformation, strain rate and mode of recrystallization of the others on the same side of the slaty mylonite and in similar positions with respect to it.
5. There is no support for coincidence lattice control on growth of new quartz grains within a quartz host during dynamic recrystallization.
6. This study contains strong evidence that subgrains can form in mica and that mica can perhaps recrystallize by subgrain mechanisms.
7. Diffusional processes on the scale of at least several grains are very important during dynamic recrystallization once sufficient grain boundaries have been formed by nucleation of new grains. The main control on nucleation sites in rocks near the slaty mylonite appears to be interfacial energy and nucleation tends to be such that unlike phases are in contact which causes a general homogenization of the rock.
8. The pseudotachylite is a product of fusion after a transition from ductile to brittle behaviour due to an increase in the strain rate of deformation (from decrease in subgrain size) either as a late stage in the mylonite deformation event or entirely afterwards.

6.3 Mesoscopic structures and deformation style.

6.3.1 The mylonites.

The mylonitization was an extremely intense, ductile but heterogeneous deformation. For example, folds of country rock schistosity with mylonitic schistosity axial plane ($BS_2^{S_M}$) occur adjacent to folds of mylonitic schistosity with another weak mylonitic schistosity developing as axial plane ($BS_M^{S_M}$), such that the axial planes of both are parallel. Due to the heterogeneity of the deformation they can apparently be forming concurrently.

The mylonitization is most intense at the central slaty mylonite and the intensity decreases towards the country rock on either side. The deformation possibly began in weaker zones within the country rock. Hence in the early stages of the deformation these would be more mylonitized and as mylonitization proceeded rocks adjacent to those in the weaker zone would be mylonitized and so on. Hence $BS_2^{S_M}$ folds could form in the latter rocks while $BS_M^{S_M}$ folds were forming in the adjacent more mylonitic rocks essentially contemporaneously. This is apparently occuring over very small distances. For example, figure 2.4a shows the mylonitic lineation on the upper schistosity surface is bent while that on the lower is straight and coincides with the direction of movement needed to bend the lineation above (both schistosity surfaces are planar and parallel). This means that the schistosity surface with the bent lineation must have been formed and deforming while the schistosity surface with the straight lineation was forming. This is feasible because of the heterogeneity of the deformation. Blocks of altered but still relatively unmylonitized country rock occur sporadically within the mylonites. Mylonitic schistosity forming on their edges is developing

slightly later during the deformation than that in the more mylonitic parts. Hence the above relationship could develop.

Not only does L_M bend in the plane of the mylonitic schistosity. The $BS_2^{S_M}$ and $BS_M^{S_M}$ fold axes also bend through angles of more than 90^o in S_M. L_M and these fold axes can only bend if the direction and/or local magnitude of strain changes during the deformation process. The $BS_M^{S_M}$ folds which are local and intrafacial possibly form because the mylonitic schistosity is pinned by obstructions such as the relatively unmylonitized country rock remains or because these blocks cause a local change in the orientation of the plane of strain.

6.3.2 Mylonitic lineation and the direction of movement.

The mylonitic lineation L_M is an elongation direction within the mylonites. It need have no relationship to the relative displacement of the country rock on either side and hence cannot be used to define their relative movements. "Geologists have often misunderstood the significance of this maximum elongation in the material describing it as the 'flow direction', and often falsely assuming that it represents the actual displacement direction in the rock" (Ramsay, 1969, p.54).

6.3.3 $BS_2^{S_M}$ on the granulite facies side of the slaty mylonite.

The $BS_2^{S_M}$ folds west of the central mylonite are actually $BS_1^{S_M}$ folds if this was originally granulite facies acid gneiss as is strongly suggested by the data summarized in section 6.1. However, this is dependant on the degree of displacement across the pseudotachylite zone. If this is large, the rocks east of the pseudotachylite although very likely originally granulite facies acid gneisses, may not have suffered a deformation history similar to those on the west side prior to mylonitization and hence the folded schistosity may not be S_1. However

these granulite facies acid gneisses remain structurally similar over large areas (compare this area with that of Collerson et. al.,op cit) and hence the latter possibility is unlikely.

6.3.4 Rotation of blocks of country rock.

Just as L_M, $BS_2^{S_M}$ and $BS_M^{S_M}$ fold axes deform through large angles in the plane of S_M, so apparently can large blocks of amphibolite facies country rock (several kilometres long), separated by mylonites, ductiley rotate through large angles (90^o) on the plane of S_M. This is feasible since L_M bends on a macroscopic as well as a mesoscopic scale. Thus the mylonitization in sub area two (fig. 2.1a) was a ductile deformation which has caused a ductile relative rotation of the blocks of country rock to either side (sub areas 1 and 3, fig. 2.1a) of approximately 90^o. This means that the penetrative nature of the mylonitization within the amphibolite facies country rock could have widespread effects on amphibolite facies country rock orientations.

6.3.5 Penetration of mylonitization into the amphibolite but not the granulite facies country rocks.

The mylonites penetrate into the amphibolite facies country rock as far as the outcrop of amphibolite facies country rock can be traced. This may not be a significant distance normal to the mylonitic schistosity due to its shallow dip. However no mylonites associated with those along the Woodroffe Thrust penetrate the granulite facies rocks beyond their main contact with them. This difference could be a response of the mylonite deformation to the greater water content on the amphibolite facies side and hence greater ease of deformation due to increased ductility. It may also mean that the amphibolite facies acid gneisses were originally a zone of weakness compared with the strong granulite

facies acid gneisses.

6.3.6 Deformations in the country rock.

Prior to mylonitization the amphibolite facies country rock had suffered three deformations while that on the granulite facies side apparently only one.

6.3.7 The strain associated with mylonitization.

These mylonitic rocks are strongly flattened normal to S_M (c.f. Johnson,1967; McLeish,1971; Ross,1973; see section 1.1.2). This is apparent from the deformation of quartz host grains and aggregrates. They are not forming in simple shear zones as described by Ramsay and Graham (1970) as the mylonitic schistosity forms axial plane to folds in the country rock. However this does not preclude a simple shear component to the deformation. They may therefore be a result of simple shear combined with strong flattening. Such a deformation could possibly produce orthorhombic quartz fabrics.

6.4 Tectonic Implications.

6.4.1 Geochronology.

The isotope dating done so far suggests that the amphibolite facies country rock is older than the granulite facies country rock. Arriens and Lambert (1969) dated amphibolite facies acid gneisses east of Ernabella and granulite facies acid gneisses near Ernabella at 1400-1600 m.y. and 1380 ± 120 my respectively (cessation of metamorphism in the latter case) by Rb/Sr methods. Amphibolite facies gneisses even further east have been dated at 1300-2400 m.y. (personal communication by Arriens to Major, 1968). The increased number of deformations in the amphibolite facies country rock may indicate that it is an older basement but this is not necessarily so.

6.4.2 Statistical parallelism of S_1 and S_M.

The country rock schistosity (S_1) in the granulite facies acid gneisses is statistically parallel to the mylonitic schistosity (compare fig. 2.7, $5S_1$ with fig. 2.5, $4S_M$). However on the local scale, that is across the contact of the mylonites with the granulite facies country rock, they are discordant in strike. This statistical parallelism may have some significance as it was also found to occur in the area described by Collerson et al (op cit) to the south. S_M is definitely later than S_1 and S_M definitely cross cuts S_1. Hence the statistical parallelism could be due to:

1) Coincidence.
2) The high strain on the mylonite zone which rotated S_1 into near parallelism with the zone, whereas S_2 on the amphibolite facies side deformed more homogeneously (certainly the amphibolite facies country rocks have taken up a considerable amount of the strain).
3) The initial relationship between granulite and amphibolite facies country rocks before mylonitization. This may have been a fault in which case S_1 could have been close to the orientation of the zone of weakness along which mylonitization occured. Or also it may have been the initial tectonic environment. For example, if the granulite facies gneisses were originally sediments they may have been laid down in a trough abutting a deformed amphibolite facies basement. After burial and metamorphism the contact between them and the abutting amphibolite facies block may have been a zone of considerable crustal weakness.

REFERENCES

ABSON, D.J. & JONAS, J.J., 1972: Substructure strengthening in zirconium and zirconium-tin alloys. J. Nucl. Mat., 42, 73-85.

AMELYNCX, S. & DELAVIGNETTE, P., 1962: Dislocations in layer structures. Proc. Tech. Conf. on Direct observations of imperfections in crystals, Missouri, 295-356.

ARRIENS, P.A. & LAMBERT, I.B., 1969: On the age and strontium isotopic geochemistry of granulite-facies rocks from the Fraser Range, Western Australia, and the Musgrave Ranges, central Australia. Spec. Publs. geol. Soc. Aust., 2, 377-388.

AUST, K.T., 1969: Interface migration. In, Interfaces, ed. R.C. Gifkins, Aust. Inst. Metals Conf. Butterworths, Australia, 307-334.

AUST, K.T. & CHALMERS, B., 1970: Structure of grain boundaries. Metall. Trans., 1, 1095-1104.

AUST, K.T. & RUTTER, J.W., 1959a: Grain boundary migration in high purity lead and dilute lead-tin alloys. Trans. A.I.M.E., 215, 119-127.

AUST, K.T. & RUTTER, J.W., 1959b: Temperature dependance of grain migration in high purity lead containing small additions of tin. Trans. A.I.M.E., 215, 820-831.

AUST, K.T. & RUTTER, J.W., 1960a: Effect of solute impurities on preferred orientation in annealed high-purity lead. Trans. A.I.M.E., 218, 50-54.

AUST, K.T. & RUTTER, J.W., 1960b: Trans. A.I.M.E., 218, 1023.

AUST, K.T. & RUTTER, J.W., 1962: Effect of grain-boundary mobility and energy on preferred orientation in annealed and high purity lead. Trans. A.I.M.E., 224, 111-115.

BAËTA, R.D. & ASHBEE, K.H.G., 1970a: Mechanical deformation of quartz I. Constant strain-rate compression experiments. Phil. Mag., 22, 601-623.

BAËTA, R.D. & ASHBEE, K.H.G., 1970b: Mechanical deformation of quartz II. Stress relaxation and thermal activation parameters. Phil. Mag., 22, 625-635.

BAILEY, J.E., 1960: Electron microscope observations on the annealing processes occurring in cold worked silver. Phil. Mag., 5, 833-842.

BAILEY, J.E., 1963: Electron microscopy and strength of crystals. p.535, New York and London (Interscience).

BAILEY, J.E. & HIRSCH, P.B., 1962: The recrystallization process in some polycrystalline metals. Proc. Roy. Soc., Ser. A., 267, 11-30.

BALK, R., 1952: Fabric of quartzite near Thrust Faults. J. Geol., 60, 415-435.

BECK, P.A., 1949: The formation of recrystallization nuclei. J. Appl. Phys., 20, 633-634.

BECK, P.A., 1954: Annealing of cold worked metals. Adv. Phys., 3, 245-324.

BECK, P.A. & HU, H., 1966: The origin of recrystallization textures. In. Recrystallization, grain growth and textures. Ed. H. Margolin, Am. Soc. Metals, 393-433.

BECKER, R., 1938: Die keimbildung bei der ausscheidung in metallischem mischkristallen. Ann. Physik., 32, 128-140.

BECKER, R. & DORING, W., 1935: Kinetische behundlung der keimbildung in übersattigten dömpfen. Ann. Phys., 24, 719-752.

BISHOP, J.F.W., & HILL, R., 1951a: A theory of the plastic distortion of a polycrystalline aggregate under combined stresses. Phil. Mag., 42, 414-427.

BISHOP, J.F.W. & HILL, R., 1951b: A theoretical derivation of the plastic properties of a polycrystalline face-centred metal. Phil. Mag., 42, 1298-1307.

BLACIC, J.D., 1972: Effect of water on the experimental deformation of olivine. In: Flow and fracture of rocks. Geophys. Mon. Ser., No. 16, 109-115.

BRANDON, D.C., RALPH, B., RANGANOTHAN, S. & WALD, M.S., 1964: A field ion microscope study of atomic configuration at grain boundaries. Acta Met., 12, 813-821.

BURKE, J., 1965: The kinetics of phase transformations in metals. Pergammon Press, Oxford, 226 pp.

BURKE, J.E. & TURNBULL, D., 1952: Recrystallization and grain growth. Prog. Met. Phys., 3, 220-292.

BYERLY, G.R. & VOGEL, T.A., 1973: Grain boundary processes and development of metamorphic plagioclase. Lithos, 6, 183-202.

CAHN, J.W., 1956: The kinetics of grain boundary nucleated reactions. Acta Metall., 4, 449-459.

CAHN, J.W., 1957: Nucleation on dislocations. Acta Metall., 5, 168-172.

CAHN, J.W., 1962a: On spinodal decomposition in cubic crystals. Acta Metall., 10, 179-185.

CAHN, J.W., 1962b: Coherent fluctuations and nucleation in isotropic solids. Acta Metall., 10, 907-913.

CAHN, J.W., 1966: The later stages of spinodal decomposition and the beginnings of particle coarsening. Acta Metall., 14, 1685-1692.

CAHN, J.W. & HILLIARD, J.E., 1958: Free energy of a non uniform system I. Interfacial free energy. J. Chem. Phys., 28, 258-267.

CAHN, J.W. & HILLIARD, J.E., 1959: Free energy of a non uniform system. III. Nucleation in a two component incompressible fluid. J. Chem. Phys., 31, 688-699.

CAHN, R.W., 1950: A new theory of recrystallization nuclei. Proc. Phys. Soc. Lond., 63A, 323-336.

CAHN, R.W., 1966: Recrystallization mechanisms. In: Recrystallization grain growth and textures. Ed. H. Margolin. Am. Soc. Metals, 99-127.

CALNAN, B.A. & CLEWS, C.J.B., 1950: Deformation textures in face centred cubic metals. Phil. Mag., 41, 1085-1100.

CARTER, N.L., CHRISTIE, J.M. & GRIGGS, D.T., 1964: Experimental deformation and recrystallization of quartz. J. Geol., 72, 687-733.

CHIN, G.Y. & MAMMEL, W.L., 1967: Computer solution to the Taylor analysis for axisymmetric flow. Trans. Met. Soc. A.I.M.E., 239, 1400-1405.

CHIN, G.Y. & MAMMEL, W.L., 1969: Generalization and equivalence of the minimum work (Taylor) and maximum work (Bishop-Hill) principles for crystal plasticity. Trans. Met. Soc. A.I.M.E., 245, 1211-1214.

CHIN, G.Y., MAMMEL, W.L. & DOLAN, M.T., 1967: Taylors theory of texture for axisymmetric flow in body centred cubic minerals. Trans. Met. Soc. A.I.M.E., 239, 1854-1855.

CHIN, G.Y., MAMMEL, W.L. & DOLAN, M.T., 1969: Taylor analysis for {111}<112> twinning and {111}<110> slip under conditions of axisymmetric flow. Trans. Met. Soc. A.I.M.E., 245, 383-388.

CHRISTIE, J.M., 1960: Mylonitic rocks of the Moine thrust zone in the Assynt region, northwest Scotland. Edinburgh Geol. Soc. Trans., 18, 79-93.

CHRISTIE, J.M., 1963: The Moine thrust zone in the Assynt region, northwest Scotland. California Univ. Pubs. Geol. Sci., 40, 345-419.

COLLERSON, K.D., 1972: High grade metamorphic and structural relationships near Amata, Musgrave Ranges, central Australia. Unpub. Ph.D. thesis, University of Adelaide.

COLLERSON, K.D., OLIVER, R.L. & RUTLAND, R.W.R., 1972: An example of structural and metamorphic relationships in the Musgrave Orogenic Belt, central Australia. J. geol. Soc. Aust., 18, 379-393.

CRAWFORD, A.R. & OLIVER, R.L., 1968: The Precambrian geochronology of Ceylon. Geol. Soc. Aust., Spec. Publ. No.2, 283-306.

DEVORE, G.W., 1956: Surface chemistry as a chemical control on mineral associations. J. Geol., 64, 31-56.

DEVORE, G.W., 1959: Role of minimum interfacial free energy in determining the macroscopic features of mineral assemblages. I. The model. J. Geol., 67, 211-226.

ETHERIDGE, M.A., 1971: Experimental observations of mica preferred orientation. Unpublished Ph.D. thesis, Australian National University.

ETHERIDGE, M.A. & HOBBS, B.E., 1973: Chemical and deformational controls on recrystallization of mica. Submitted to Contrib. Mineral. Petrol.

ETHERIDGE, M.A., HOBBS, B.E. & PATERSON, M.S., 1973: Experimental deformation of single crystals of biotite. Contr. Mineral. Petrol., 38, 21-36.

ETHERIDGE, M.A., PATERSON, M.S. & HOBBS, B.E., 1973: Experimentally produced preferred orientation in synthetic mica aggregates. In press.

FELTHAM, P., 1953: The plastic flow of iron and plain carbon steels above the A_3-point. Proc. Phys. Soc. Lond., 66B, 865-883.

FLINN, D., 1969: Grain contacts in crystalline rocks. Lithos, 3, 361-370.

GIBBS, J.W., 1948: J.W. Gibbs, Collected Works. Yale University Press, New Haven, Connecticut. 1, 105-115, 252-258.

GIBBS, J.W., 1961: The scientific papers of J. Willard Gibbs. I. Dover Publications, New York, N.Y., 434 pp.

GIFKINS, R.C., 1958-59: Recrystallization of lead during creep. J. Inst. Met., 87, 255-261.

GLOVER, G. & SELLARS, C.M., 1973: Recovery and recrystallization during high temperature deformation of α-iron. Metal. Trans., 4, 765-775.

GORDON, P. & VANDEMEER, R.A., 1966: Grain boundary migration. In: Recrystallization, grain growth and textures. Ed., H. Margolin. Am. Soc. Metals, 205-266.

GRAHAM, C.D.Jr. & CAHN, R.W., 1956: Trans. A.I.M.E., 200, 517.

GREEN, H.W., GRIGGS, D.T. & CHRISTIE, J.M., 1970: Syntectonic and annealing recrystallization of fine-grained quartz aggregates. In: Experimental and natural rock deformation. Ed., P. Paulitsch. Springer-Verlag, Berlin, 272-335.

GREEN, H.W. & RADCLIFFE, S.V., 1972: Deformation processes in the upper mantle. In: Flow and fracture of rocks. Am. Geophys. Union, Geophys. Mon. Ser., No.16, 139-156.

GREENWOOD, J.H. & WORNER, H.K., 1939: Types of creep curve obtained with lead and its dilute alloys. J. Inst. Met., 64, 135-158.

GRIGGS, D.T., 1967: Hydrolytic weakening of quartz and other silicates. Geophys. J. Roy. Astron. Soc., 14, 19-31.

GRIGGS, D.T. & BLACIC, J.D., 1965: Quartz: anomalous weakening of synthetic crystals. Science, 147, 292-295.

GROVES, G. & KELLY, A., 1963: Independant slip systems in crystals. Phil. Mag., 8, 877-887.

GROVES, G. & KELLY, A., 1969: Change of shape due to dislocation climb. Phil. Mag., 19, 977-986.

HALL, A.L. & MOLENGRAAFF, G.A.F., 1925: The Vredefont mountain land in the southern Transvaal and northern Orange Free State: Verh, Koninkl. Nederlandse Akad. Wetersch., Shaler Memorial ser., 24, no. 3, 183 pp.

HARDWICK, D. & TEGART, W.J.McG., 1961: Structural changes during the deformation of copper, aluminium, and nickel at high temperatures and high strain rates. Jour. Inst. Metals, 90, 17-21.

HARDWICK, D., SELLARS, C.M. & TEGART, W.J.McG., 1961-62: The occurrence of recrystallization during high temperature creep. Jour. Inst. Met., 90, 21-22.

HEARD, H.C. & CARTER, N.L., 1968: Experimentally induced 'natural' intragranular flow in quartz and quartzite. Am. J. Sci., 266, 1-42.

HEIER, K.S., 1961: The amphibolite-granulite facies transition reflected in the mineralogy of potassium feldspars. Curs. Y Conf., J.8, 131-137.

HIGGINS, M.W., 1971: Cataclastic rocks. Geol. Surv. Prof. Pap., 687, 1-97.

HOBBS, B.E., 1966: Microfabric of tectonites from the Wyangala Dam area, New South Wales, Australia. B.G.S.A., 77, 685-706.

HOBBS, B.E., 1968: Recrystallization of single crystals of quartz. Tectonophysics, 6, 353-401.

HOBBS, B.E., McLAREN, A.C. & PATERSON, M.S., 1972: Plasticity of single crystals of synthetic quartz. Geophys. Monograph Ser., 16, 29-53. Flow and Fracture of Rocks. A.G.U.

HOLT, D.L., 1971: A modified analysis of dislocation cell formation in metals. Proc. Second Int. Conf. on Strength of Metals and Alloys, Asilomar 1970, p.477.

HONEYCOMBE, R.W.K. & PETHEN, R.W., 1972: Dynamic recrystallization. J. Less Common Met., 28, 201-212.

HOSFORD, W.F.Jr. & BACKOFEN, W.A., 1964: Fundamentals of deformation processing. W.A. Bockofen et al., eds., 259-298. Syracuse University Press, New York.

HREN, J., 1965: An analysis of the atomic configuration of an incoherent twin boundary with the field ion microscope. Acta Metal., 13, 479-485.

HSÜ, K.J., 1955: Granulites and mylonites of the region about Cucamonga and San Antonio Canyons, San Gabriel Mountains, California. California Univ. Pubs. Geol. Sci., 30, 223-352.

HU, H., 1963: Annealing of silicon-iron single crystals. In: Recovery and Recrystallization of Metals. Ed., L. Himmel, Interscience Pub., New York, p.311-362.

JAOUL, B., BRICOT, I. & LACOMBE, P., 1957: Deformation bands and kinks in Al crystals. Revue Metall., 54, 756.

JOHNSON, M.R.W., 1967: Mylonite Zones and Mylonite Bonding. Nature, 213, No.5073, 246-247.

JONAS, J.J., McQUEEN, H.J. & WONG, W.A., 1968: Dynamic recovery during the extrusion of aluminium. Iron & Steel Instit., Pub. 108, 49-59.

JONAS, J.J., SELLARS, C.M. & TEGART, W.J.McG., 1969: Strength and structure under hot working conditions. Met. Review, 14, 1-24.

KAMB, B., 1961: The thermodynamic theory of non hydrostatically stressed solids. J. Geophys. Res., 66, 259-271.

KAMB, B., 1972: Experimental recrystallization of ice under stress. In: Flow and fracture of rocks. Geophys. Mon. Ser., no.16, 211-241.

KAMB, W.B., 1959: Theory of preferred crystal orientation developed by recrystallization under stress. Jour. Geol., 67, 153-170.

KORBEL, A. & SWIATKOWSKI, K., 1972: The role of strain in the formation of dislocation structure and its influence on the mechanical properties of aluminium. Met. Sci. J., 6, 60-63.

KRONBERG, M.L. & WILSON, F.H., 1949: Secondary recrystallization in copper. Trans. A.I.M.E., 185, 501-514.

LAPWORTH, C., 1885: The highland controversy in British geology; its causes, course and consequences. Nature, 32, 558-559.

LEWIS, H.C., 1885: Some examples of pressure-fluxion in Pennsylvania. Nature, 32, 559-560.

LI, J.C.M., 1961: High angle tilt boundary - a dislocation core model. J. Appl. Phys., 32, 525-541.

LI, J.C.M., 1962: Possibility of subgrain rotation during recrystallization. J. Appl. Phys., 33, 2958-2965.

LI, J.C.M., 1963: Discussion of paper by K.J. Aust and J.W. Rutter in Recovery and recrystallization of metals. Ed., L. Himmel, 1963. N.Y., Gordon & Breach, p.160.

LÜCKE, K. & IBE, G., 1964: Technical report to ARO(D) from Institute für Allgemeine Metallphisik der Technischen Hochschulen, Aachen, Sept. 1964.

LUTON, M.J. & SELLARS, C.M., 1969: Dynamic recrystallization in nickel and nickel-iron alloys during high temperature deformation. Acta Metal., 17, 1033-1043.

MacDONALD, G.J.F., 1960: Orientation of anisotropic minerals in a stress field. Geol. Soc. Am. Mem., 79, 1-8.

MAJOR, R.B., 1973: Explanatory notes for the Woodroffe 1:250,000 Geological Map. Dept. Mines, Geol. Surv. South Aust.

MAJOR, R.B., JOHNSON, J.E., LAESON, B. & MIRAMS, R.C., 1967: Woodroffe 1:250,000 Geological Map. Mines Dept., Geol. Surv. South Aust.

McKENZIE, D. & BRUNE, J.N., 1972: Melting on fault planes during large earthquakes. Geophys. J. Roy. ast. Soc., 29, 65-78.

McLAREN, A.C. & HOBBS, B.E., 1972: Transmission electron microscope investigation of some naturally deformed quartzites. Geophysical Monograph Ser., 16, 55-66. Flow and fracture of rocks. A.G.U.

McLEISH, A.J., 1971: Strain analysis of deformed Pipe Rock in the Moine Thrust zone, northwest Scotland. Tectonophysics, 12, 469-504.

McQUEEN, H.J. & BERGERSON, S., 1972: Dynamic recrystallization of copper during hot torsion. Met. Sci. J., 6, 25-29.

MOORE, A.C., 1970: Descriptive terminology for the textures of rocks in granulite facies terrains. Lithos, 3, 123-127.

OROWAN, E., 1954: Dislocations in metals. A.I.M.E., New York, N.Y., 183 pp.

PARLANGE, J.-Y., 1968: Orientation of nuclei produced under non hydrostatic stress. Science, 162, 358-359.

PATERSON, M.S., 1973: Non hydrostatic thermodynamics and its geological applications. Preprint.

PHILPOTTS, A.R., 1964: Origin of pseudotachylites. Am. J. Sci., 262, 1008-1035.

RAMSAY, J.G., 1969: Measurement of strain and displacement in orogenic belts. In: Kent, P.E. et al (Eds.): Time and place in orogeny. London (Geological Society), 43-79.

RAMSAY, J.G. & GRAHAM, R.H., 1970: Strain variation in shear belts. Can. J. Earth Sci., 7, 786-813.

RANSOM, D.M., 1971: Host control of recrystallized quartz grains. Mineralog. Mag., 38, 83-88.

ROSS, J.V., 1973: Mylonitic rocks and flattened garnets in the southern Okanagan of British Columbia. Can. J. Earth Sci., 10, 1-17.

RICHARDSON, G.J., SCHNABLE, E. & STÜWE, H.P., 1969: Das periodische kriechen von kupfer. Acta Metall., 23, 1139-1143.

RICHARDSON, G.J., SELLERS, C.M., McTEGART, W.J., 1966: Recrystallization during creep of nickel. Acta Metall., 14, 1225-1236.

ROSSARD, C. & BLAIN, P., 1959: Mem. Sci. Rev. Met., 56, 286.

ROSSARD, C. & BLAIN, P., 1960: Rev. Met., 57, 173.

SCHMID, E., 1925: Zn-Normal stress law. Proc. Int. Congr. Appl. Mech. Delft 1924, p.342.

SCOTT, J.S. & DREVER, H.I., 1953: Frictional fusion along a Himalayan thrust. Roy. Soc. Edinburgh Proc., sec.B, 65, pt.2, 121-140.

SEEGER, A., 1957: Dislocations and mechanical properties of crystals. Wiley, New York, 243-329.

SHELLEY, D., 1971: Hypothesis to explain the preferred orientations of quartz and calcite produced during syntectonic recrystallization. Bull. geol. Soc. Am., 82, 1943-1954.

SHOECK, G., 1961: Mechanical behaviour of materials at elevated temperatures. Ed., J.E. Dorn, p.79-107.

SILK, E.C.H. & BARNES, R.S., 1960: The observation of dislocations in mica. AERE-R3333.

SIMPSON, C.J. & AUST, K.T., 1972: Grain boundary migration. Surface Science, 31, 479-497. Conf. on grain boundaries and interfaces.

SMITH, C.S., 1952: Interphase interfaces. In: Imperfections in nearly perfect crystals. Ed., W. Shockley. Wiley, N.Y., 377-401

SMITH, C.S., 1964: Some elementary principles of polycrystalline microstructures. Met. Rev., 9, 1-48.

STAKER, M.R. & HOLT, D.L., 1972: The dislocation cell size and dislocation density in copper deformed at temperatures between 25 and 700°C. Acta Metall., 20, 569-579.

STÖFFLER, D., 1972: Deformation and transformation of rock-forming minerals by natural and experimental shock processes. I. Behaviour of minerals under shock compression. Fortschr. Miner., 49, 50-113.

TAYLOR, G.I., 1938: Plastic strain in metals. J. Inst. Metals, 62, 307-324.

TEALL, J.J.H., 1918: Dynamic Metamorphism. Proc. Geol. Assoc., 29, 1-15.

TULLIS, J., CHRISTIE, J.M. & GRIGGS, D.T., 1973: Microstructures and preferred orientations of experimentally deformed quartzites. Bull.

geol. Soc. Am., 84, 297-314.

UHLMANN, D.R. & CHALMERS, B., 1965: The energetics of nucleation. Ind. Engin. Chem., 57, No.9, 19-43.

VOLMER, M. & WEBER, A., 1926: Keimbildung in übersättigten Gebilden, Ztschr. phys. Chem., 119, 277-301.

VON-MISES, R., 1928: Mechanik der plastichen forman derung von kristallen. Z. agnew. Math. u. Mech., 8, 161-185.

WATERS, A.C. & CAMPBELL, C.D., 1935: Mylonites from the San Andreas fault zone. Am. Jour. Sci., 5th ser., 29, 473-503.

WHITE, J., 1968: Phase distribution in ceramics. In: Fulrath, R.M. & Pask, J.A., Eds., Ceramic microstructures. John Wiley & Sons, New York, 728-762.

WILLIAMS, R.O., 1962: Shear textures in copper, brass, aluminium, iron and zirconium. Trans. Met. Soc. A.I.M.E., 224, 129-140.

WINKLER, H.G.F., 1965: Petrogenesis of metamorphic rocks. Springer-Verlag, Berlin. 220 pp.

WONG, W.A., McQUEEN, H.J. & JONAS, J.J., 1967: Recovery and recrystallization of aluminium during extrusion. J. Inst. Met., 95, 129-134.

WONSICWICZ, B.C. & CHIN, G.Y., 1970: Inhomogeneity of plastic flow in constrained deformation. Metall. Trans., 1, 57-61.

YUND, R.A. & McCALLISTER, R.H., 1970: Kinetics and mechanisms of exsolution. Chem. Geol., 6, 5-30.

MYLONITE DEVELOPMENT IN THE WOODROFFE THRUST, NORTH OF AMATA, MUSGRAVE RANGES, CENTRAL AUSTRALIA

VOLUME 2

by

Timothy Hampton Bell,
B.Sc.(Hons), Adelaide

Department of Geology and Mineralogy
University of Adelaide

June, 1973

THE MAP

The map is placed as a fold out in the back of this volume.

FIGURE 2.1

(a) Sketch map showing structural sub areas and broad geological relationships.

(b) $B_S^{S_1}$ fold from granulite facies acid gneiss in sub area 7. The layering S is intrafolially folded with schistosity S_1 as axial plane.

(c) A block of gneissic rock contained within granulite facies acid gneiss in sub area 7. The locality is marked on the map. The schistosity is at a low angle to the plane of the diagram and hence appears to bend around the block more than it actually does. The gneissic layering and cross cutting schistosity (other than S_1) in the block have been deformed during the production of S_1.

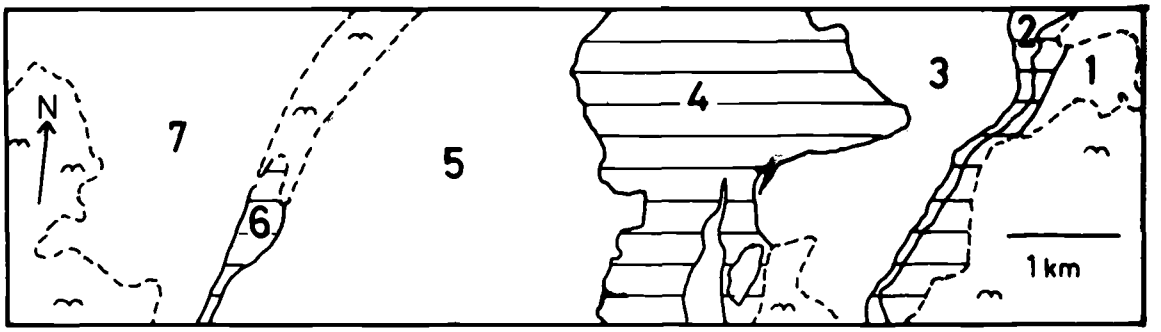

Sub-areas 1 and 3 - Amphibolite Facies Country Rock
Sub-areas 5 and 7 - Granulite Facies Country Rock
Sub-areas 2,4 and 6 - Mylonitic Rock Types

a

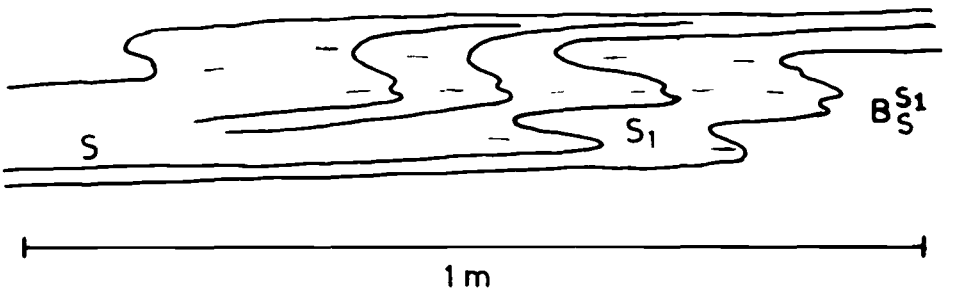

b

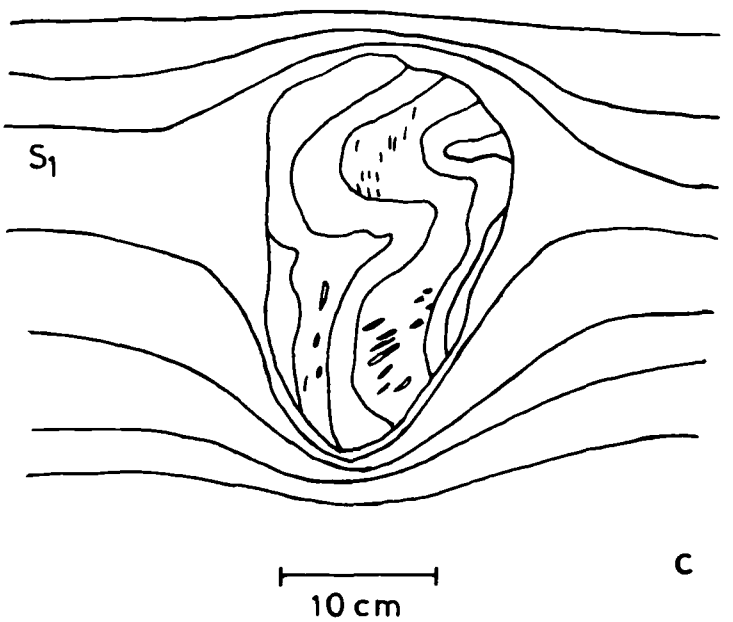

c

FIGURE 2.2

(a) This figure shows a number of $B^{S_2}_{S}$ ($B^{S_2}_{S_1}$) folds of layering (S) and schistosity (S_1: observable in the fold hinges) which have a schistosity S_2 formed parallel to the axial plane. S_2 has been folded by a large fold (B_{S_2}) which has no axial plane structure, and by a local $B^{S_3}_{S_2}$ fold (S_3 is the axial plane schistosity to this fold).

(b) This figure shows a $B^{S_M}_{S_2}$ fold, i.e. a fold of country rock schistosity S_2 with an axial plane mylonitic schistosity.

(c) This figure shows a $B^{S_M}_{S_M}$ fold, i.e. S_M has been deformed. The fold has a weak mylonitic schistosity developed as axial plane (observable only in thin section) and refolds a $B^{S_M}_{S_2}$ fold.

(d) This figure shows a $B^{S_3}_{S_M}$ fold. These are local intrafolial folds with an axial plane schistosity (S_3).

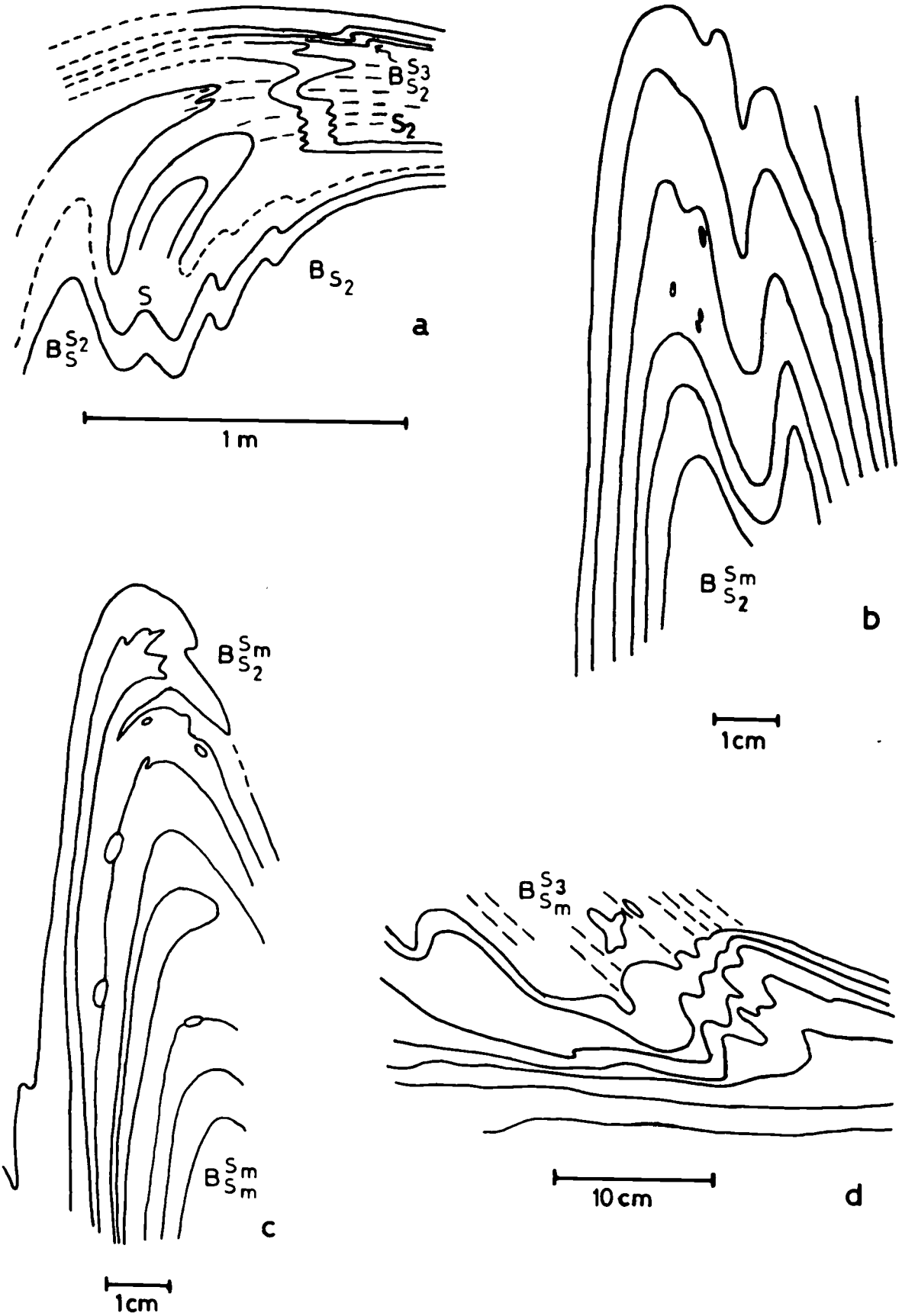
$B^{S_3}_{S_2}$
S_2
B_{S_2}
S
$B^{S_2}_{S}$
a
1 m
$B^{Sm}_{S_2}$
b
1cm
$B^{Sm}_{S_2}$
B^{Sm}_{Sm}
c
1cm
$B^{S_3}_{Sm}$
10 cm
d

FIGURE 2.3

(a) This photo shows a $B^{S_M}_{S_2}$ fold, i.e. a fold of country rock schistosity S_2 with an axial plane mylonitic schistosity.

(b) This photo shows a $B^{S_M}_{S_M}$ fold, i.e. S_M has been deformed. The fold has a weak mylonitic schistosity developed as axial plane (observable only in thin section) and refolds a $B^{S_M}_{S_2}$ fold.

(c) This photo shows folded country rock schistosity (S_2) with mylonitic schistosity as axial plane (i.e. $B^{S_M}_{S_2}$ folds). The mylonitic schistosity intensifies towards the top of the photo.

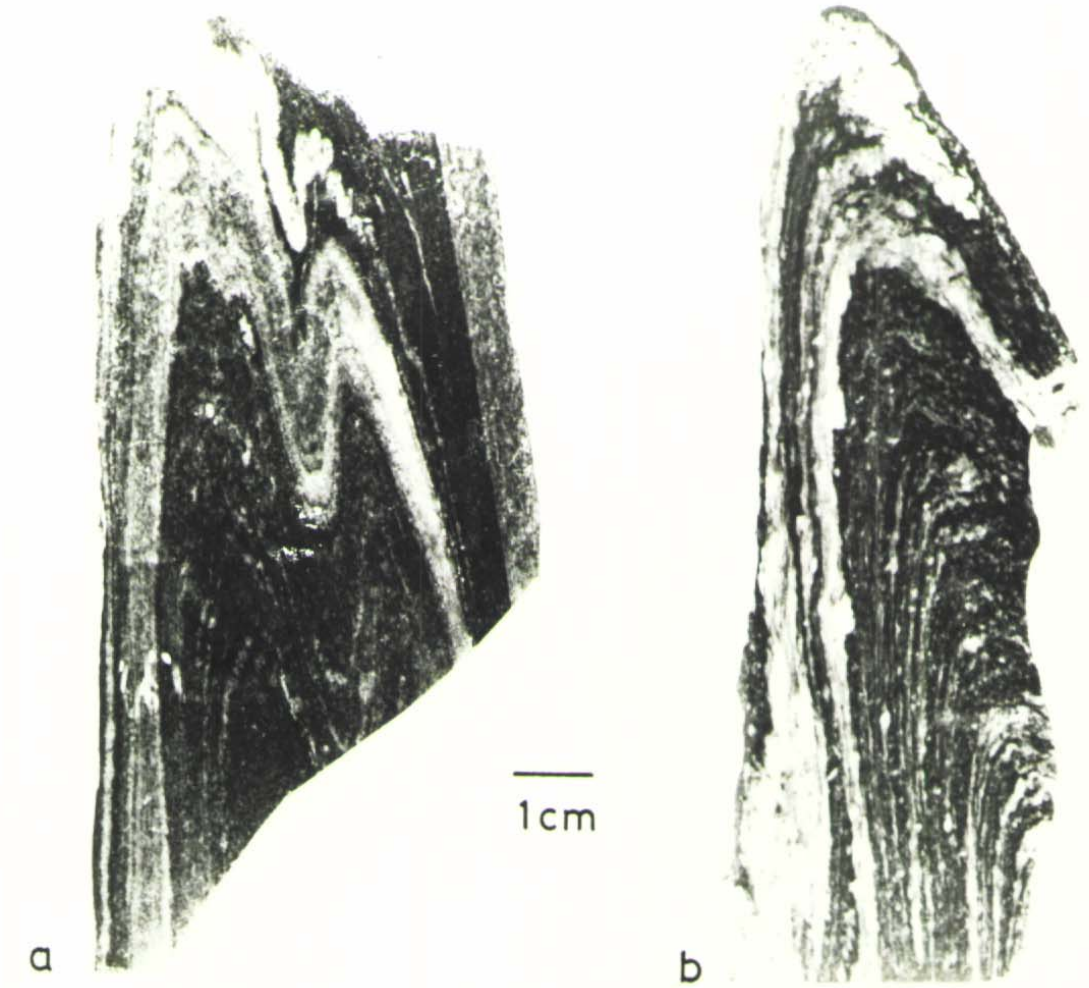

c

FIGURE 2.4

(a) This photo shows deformed mylonitic lineation (L_M) on an upper schistosity surface and undeformed mylonitic lineation on a lower schistosity surface which trends in the direction about which the former is bent. The lineation is deformed within the plane of S_M.

(b) This photo shows the block of gneissic rock sitting within granulite facies acid gneiss that is sketched in fig. 2.1c.

(c) $1\beta_{S_2}$ and $3\beta_{S_2}$ (the statistical B_{S_2} fold axes in sub areas 1 and 3) lie on the 86° small circle about the pole to $S_M(\pi S_M)$ 94° apart. This diagram shows the procedure used to rotate the $1S_2$, 4% contour extremities by the above amount.

πS_M was rotated to the primitive circle on the 90° small circle (dotted line) about a horizontal axis. $1\beta_{S_2}$, $3\beta_{S_2}$ and 3 points (circles) defining the extremities of the $1S_2$, 4% contour were also rotated in a similar way about the same axis (dotted lines). $1\beta_{S_2}$ was then rotated on the 86° small circle about πS_M to coincide with $3\beta_{S_2}$ (dashed line, arrow shows sense). The three points were similarly rotated (on their appropriate small circles). Then they were rotated back the amount needed to return πS_M to its original position (dash-dot lines). Their distribution after this (triangles) coincides with the $3S_2$,3% contour.

a

b

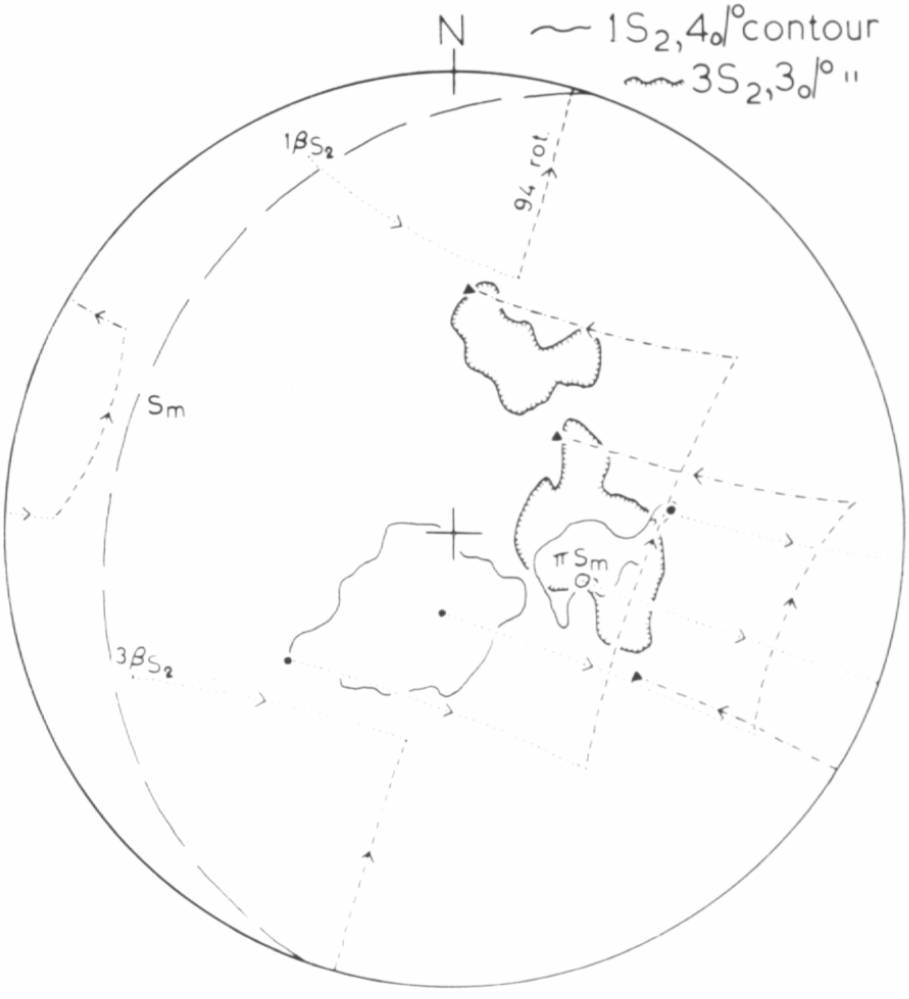

c

FIGURE 2.5

Equal area stereographic projections of field data contoured by the Schmidt method. Contour intervals are in percent per one percent area. The mylonitic schistosity (S_M), mylonitic lineation (L_M), and fold axes ($B^{S_M}_{S_2}$) prefixes indicate the sub area (fig. 2.1a). For example, $1S_M$ is the mylonitic schistosity in sub area one.

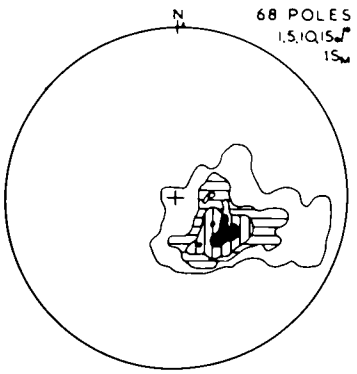
N
68 POLES
1,5,10,15σ%
1S_M

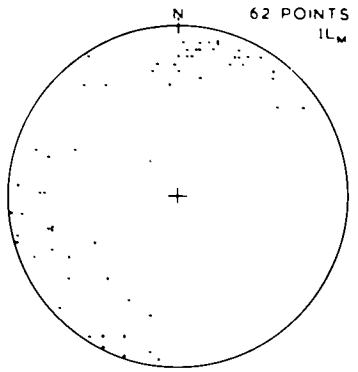
N
62 POINTS
1L_M

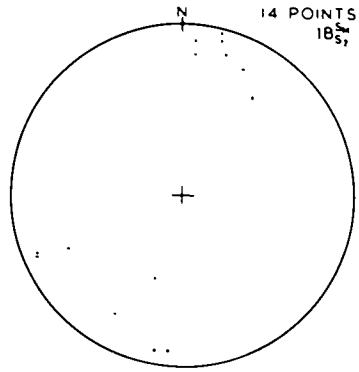
N
14 POINTS
1B S_M / S_1

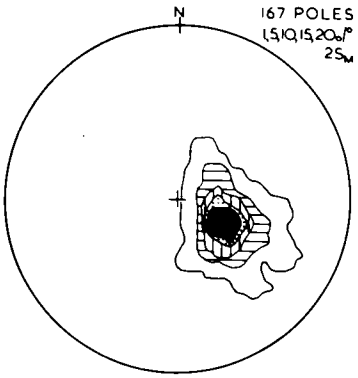
N
167 POLES
1,5,10,15,20σ%
2S_M

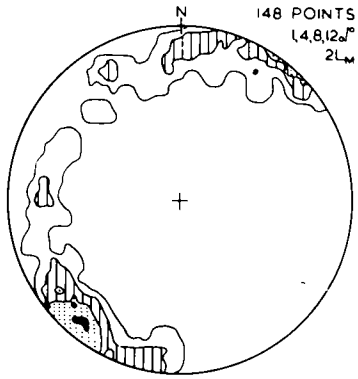
N
148 POINTS
1,4,8,12σ%
2L_M

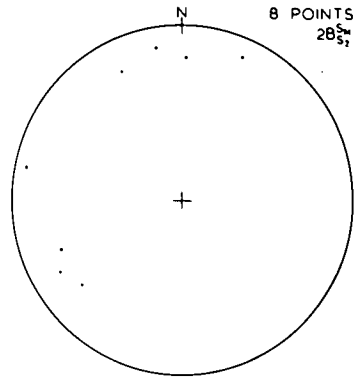
N
8 POINTS
2B S_M / S_1

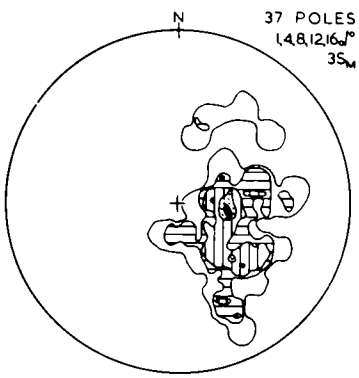
N
37 POLES
1,4,8,12,16σ%
3S_M

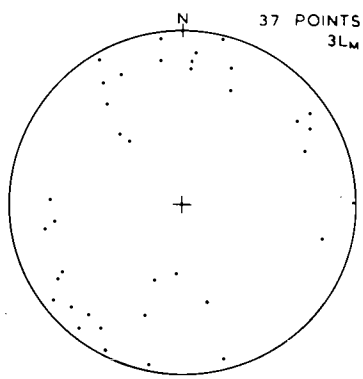
N
37 POINTS
3L_M

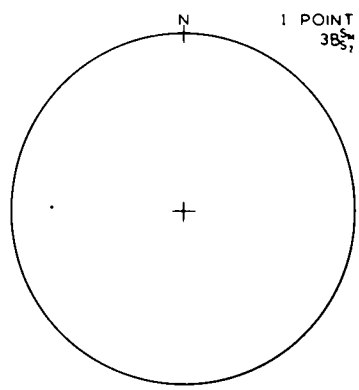
N
1 POINT
3B S_M / S_1

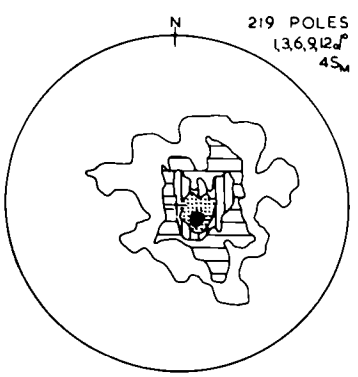
N
219 POLES
1,3,6,9,12σ%
4S_M

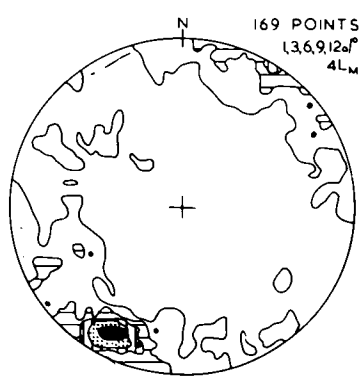
N
169 POINTS
1,3,6,9,12σ%
4L_M

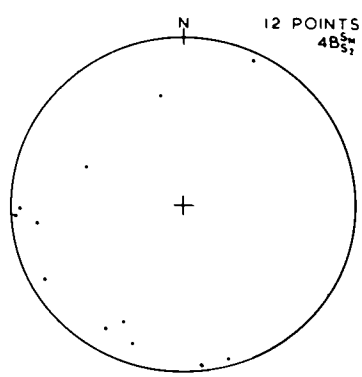
N
12 POINTS
4B S_M / S_1

FIGURE 2.6

Equal area stereographic projections of field data contoured by the Schmidt method. Contour intervals are in percent per one percent area. The country rock schistosity (S_2), lineation (L_2) and fold axes prefixes indicate the sub area (fig. 2.1a). For example, $1S_2$ is the country rock schistosity in sub area one.

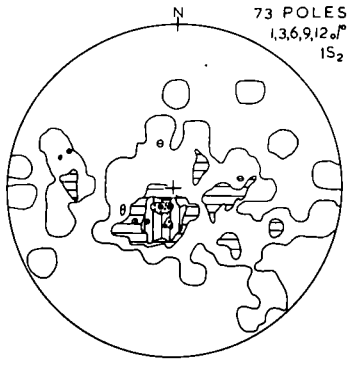
N
73 POLES
1,3,6,9,12 σ%
1S2

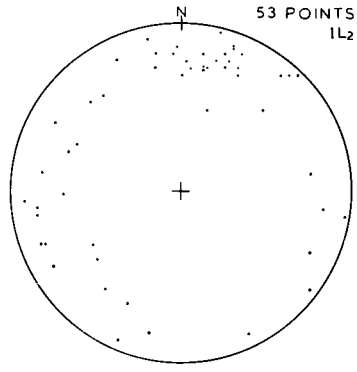
N
53 POINTS
1L2

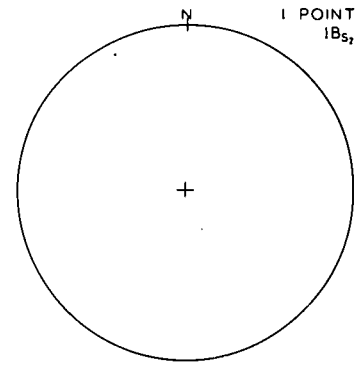
N
1 POINT
1BS1

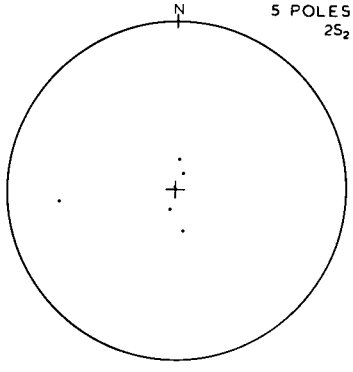
N
5 POLES
2S2

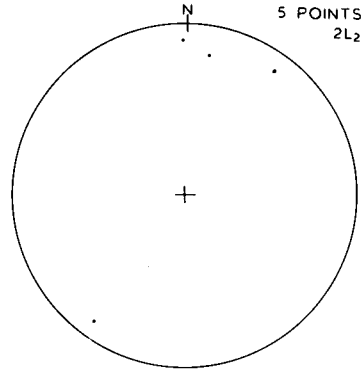
N
5 POINTS
2L2

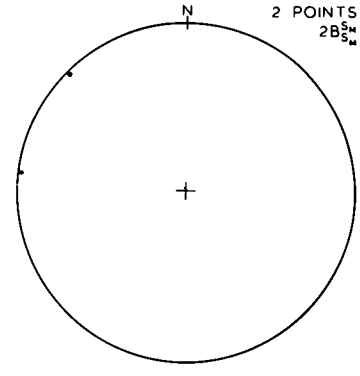
N
2 POINTS
2BSM SM

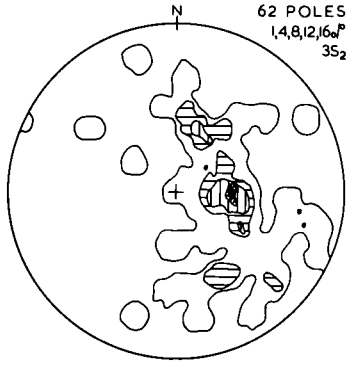
N
62 POLES
1,4,8,12,16 σ%
3S2

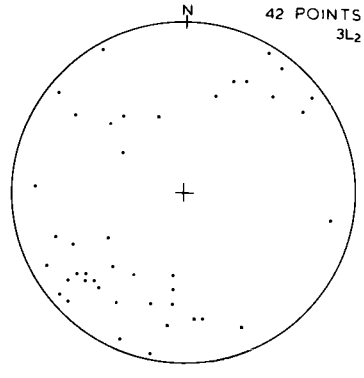
N
42 POINTS
3L2

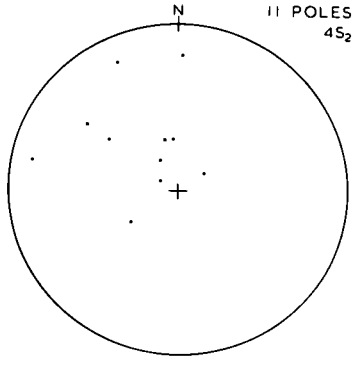
N
11 POLES
4S2

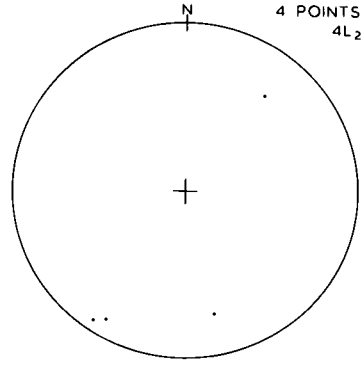
N
4 POINTS
4L2

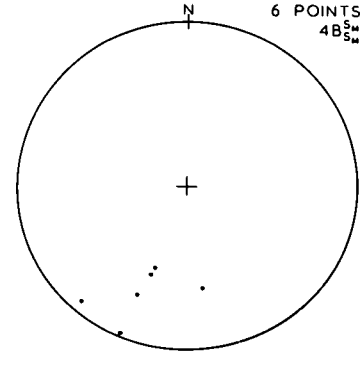
N
6 POINTS
4BSM SM

FIGURE 2.7

Equal area stereographic projections of field data contoured by the Schmidt method. Contour intervals are in percent per one percent area. The country rock schistosity (S_1) and lineation (L_1), mylonitic schistosity (S_M) and mylonitic lineation (L_M) prefixes indicate the sub area (fig. 2.1a). For example, $5S_1$ is the country rock schistosity in sub area five.

The equal area stereographic projections of the schistosity (S_3) and the fold axes ($B^{S_3}_{S_2}$, $B^{S_3}_{S_M}$) are projections of total data obtained from sub areas 1, 2, 3 and 4.

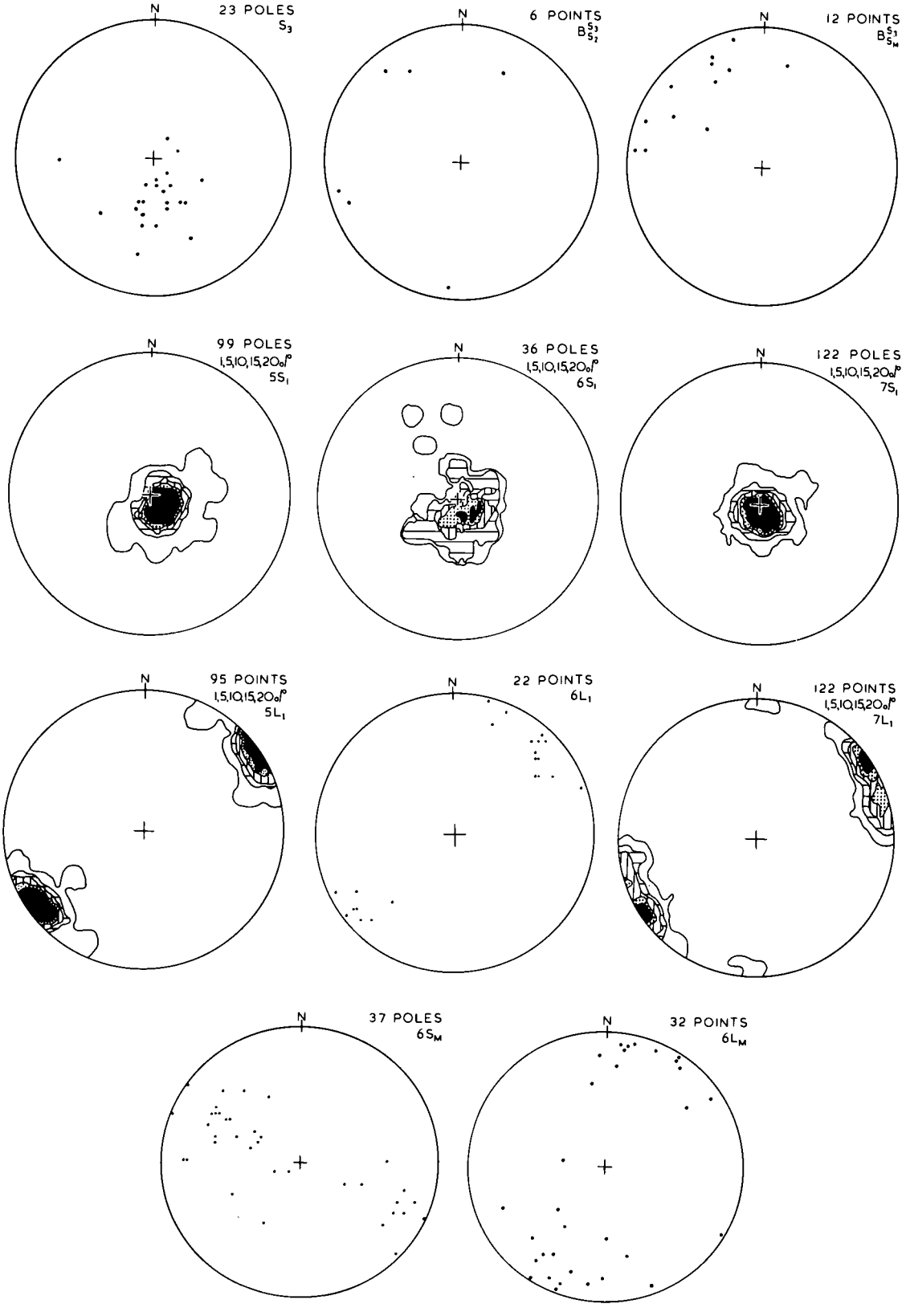
N
23 POLES
S_3
N
6 POINTS
$B^{S_3}_{S_2}$
N
12 POINTS
$B^{S_1}_{S_M}$
N
99 POLES
1,5,10,15,20₀/°
$5S_1$
N
36 POLES
1,5,10,15,20₀/°
$6S_1$
N
122 POLES
1,5,10,15,20₀/°
$7S_1$
N
95 POINTS
1,5,10,15,20₀/°
$5L_1$
N
22 POINTS
$6L_1$
N
122 POINTS
1,5,10,15,20₀/°
$7L_1$
N
37 POLES
$6S_M$
N
32 POINTS
$6L_M$

Figure 2.8

Structural symbols used in chronological order East of the Woodroffe Thrust.

S - layering. Always parallel S_1 or S_2.

S_1 - schistosity seen rarely in hinges of $B_S^{S_2}$ folds.

S_2 - dominant schistosity.

L_2 - mineral elongation and streaking lineation in S_2. Forms parallel to hinges of $BS_1^{S_2}$ ($B_S^{S_2}$) folds.

S_M - mylonitic schistosity.

L_M - mylonitic lineation in S_M.

S_3 - axial plane schistosity to $BS_M^{S_3}$ and $BS_2^{S_3}$ folds.

West of the Woodroffe Thrust.

S - layering.

S_1 - dominant schistosity.

L_1 - mineral elongation in S_1.

S_M - mylonitic schistosity (sub area 6).

L_M - mylonitic lineation in S_M (sub area 6).

FIGURE 2.9

(a) S_M vertical. Well developed in top right hand corner of photo. Defined by elongate quartz and feldspar grains and a few aligned mica (001).

S_3 diagonal. Well developed in lower half of photo. Defined by aligned mica (001), small elongate quartz grains and deformation bands in the larger quartz grains elongate parallel to S_M.

A360-98-821B

Crossed polars. Width of field: 570μm

(b) S_M diagonal. Defined by aligned mica (001). A few quartz and feldspar grains are elongate parallel to S_M but most are elongate parallel to S_3, which is vertical.

A360-98-821B

Crossed polars. Width of field: 570μm

(c) S_M vertical. Defined by aligned mica (001) and mica trains. S_3 diagonal. Defined by a few aligned mica (001).

A360-98-821B

Plane polarized light. Width of field: 1.4 mm

a

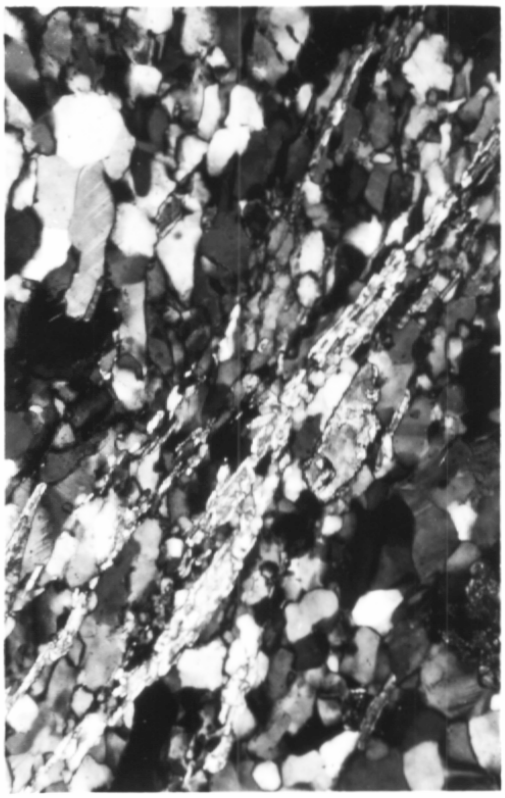

b

c

FIGURE 2.10

Whole rock analyses.

Whole Rock Analyses

No.	SiO_2	Al_2O_3	Fe_2O_3	MgO	CaO	Na_2O	K_2O	TiO_2	MnO	P_2O_5	H_2O	TOTAL	Rb/Sr
1A	63.65	14.66	8.18	1.30	4.66	2.80	3.14	1.33	0.19	0.48	0.16	100.55	0.33
2.1A	59.96	15.00	10.61	2.00	5.73	2.60	2.57	1.70	0.23	0.56	0.05	101.01	0.15
2.2A	56.12	16.37	9.05	3.60	6.16	2.80	3.55	1.40	0.19	0.62	0.30	100.15	0.18
3.1A	63.69	14.72	7.04	1.40	3.35	2.70	5.03	1.27	0.17	0.65	0.20	100.20	0.92
3.2A	63.35	14.76	7.06	1.50	3.24	2.70	5.04	1.10	0.16	0.46	0.38	99.74	0.91
3.3A	64.04	14.70	7.17	1.50	3.12	2.30	5.00	1.13	0.18	0.60	0.27	100.00	0.97
4A	69.11	14.19	4.76	1.00	2.37	2.60	5.03	0.71	0.17	0.18	0.41	100.51	1.36
61A	68.71	13.51	5.48	1.00	2.64	2.40	3.83	0.77	0.13	0.21	0.40	99.08	0.73
61B	73.27	13.02	2.45	0.40	1.55	2.60	5.52	0.37	0.10	0.10	0.17	99.54	1.70
62	69.85	13.43	5.65	0.70	2.58	2.20	4.13	0.72	0.16	0.17	0.24	99.83	1.17
64	71.65	14.05	3.80	0.90	2.82	2.60	3.44	0.60	0.12	0.13	0.34	100.45	1.30
65	69.52	14.84	4.00	1.20	2.62	2.30	3.98	0.46	0.12	0.06	0.30	99.40	0.40
5A	67.65	13.59	4.41	1.80	2.70	2.20	5.13	0.64	0.14	0.26	0.58	99.11	1.00
66B	68.21	13.89	6.44	1.60	2.71	2.40	3.96	0.86	0.20	0.22	0.42	100.90	0.72
67	68.41	15.37	4.85	1.40	2.42	3.00	3.64	0.62	0.14	0.06	0.49	100.40	0.53
7	67.57	14.40	4.68	1.10	1.63	1.90	5.93	0.76	0.13	0.32	0.94	99.35	2.14
791A	66.25	15.05	5.84	1.10	2.25	2.40	5.54	0.89	0.15	0.46	0.71	100.65	1.65
791B	65.34	14.88	5.94	1.20	2.71	2.70	5.34	0.89	0.16	0.45	0.34	99.95	1.42
6B	68.38	13.86	4.65	1.20	2.27	1.90	5.00	0.70	0.12	0.23	0.90	99.20	1.89
5B	65.65	14.25	6.03	1.70	2.94	2.30	4.61	0.80	0.17	0.28	0.92	99.66	1.97
4B	65.59	14.98	5.97	1.10	2.10	2.40	5.49	0.91	0.15	0.46	1.23	100.38	1.38
2B	68.96	13.22	3.99	0.80	2.03	2.40	4.84	0.56	0.17	0.11	0.95	98.28	1.89
1B	68.78	13.91	4.91	1.00	1.83	1.90	4.90	0.79	0.16	0.42	0.85	99.46	2.09

* Total Fe as Fe_2O_3

FIGURE 3.1

The sine curve on each graph delineates a uniform angular distribution. F% is frequency percent. θ is the angle between graphs.

(a) Angular distribution between host and directly adjacent new grains (Chapter 3.2.1B).

(b) Angular distribution between host and directly adjacent new grains. (Chapter 3.2.2B).

(c) Angular distribution between host and new grains on aggregate edge (Chapter 3.2.1B).

(d) Angular distribution between host and new grains on aggregate edge (Chapter 3.2.2B).

(e) Angular distribution between new grains adjacent to the host (Chapter 3.2.1B)

(f) Angular distribution between new grains adjacent to the host (Chapter 3.2.2B).

(g) Angular distribution between new grains on the aggregate edge (Chapter 3.2.1B).

(h) Angular distribution between new grains on the aggregate edge (Chapter 3.2.2B).

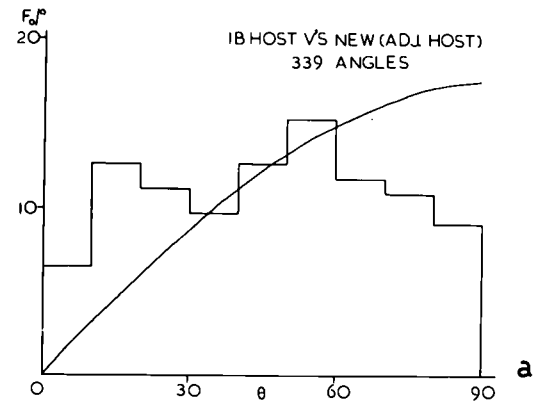
1B HOST V'S NEW (ADJ. HOST)
339 ANGLES
$F_o/^o$
20
10
0
30
θ
60
90

a

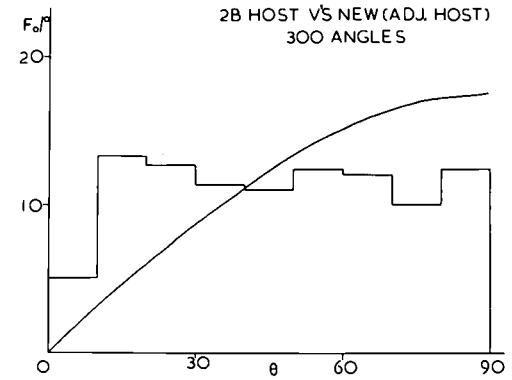
2B HOST V'S NEW (ADJ. HOST)
300 ANGLES
$F_o/^o$
20
10
0
30
θ
60
90

b

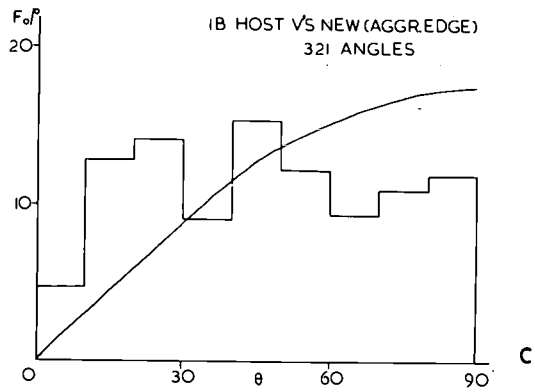
1B HOST V'S NEW (AGGR. EDGE)
321 ANGLES
$F_o/^o$
20
10
0
30
θ
60
90

c

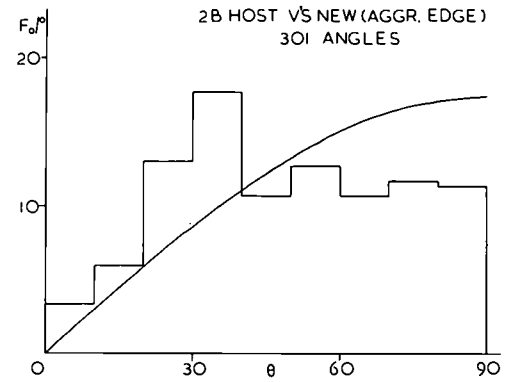
2B HOST V'S NEW (AGGR. EDGE)
301 ANGLES
$F_o/^o$
20
10
0
30
θ
60
90

d

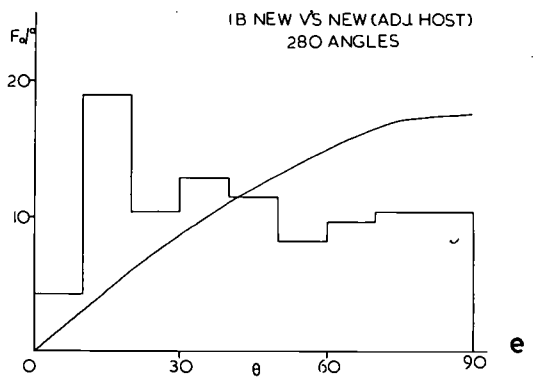
1B NEW V'S NEW (ADJ. HOST)
280 ANGLES
$F_o/^o$
20
10
0
30
θ
60
90

e

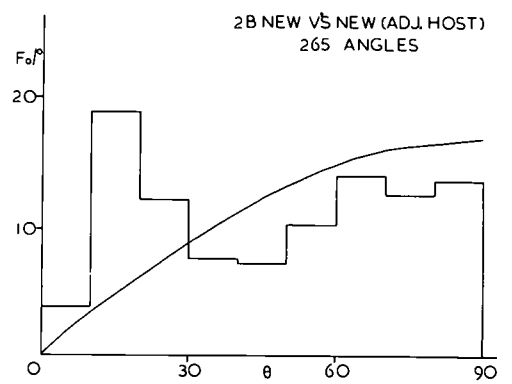
2B NEW V'S NEW (ADJ. HOST)
265 ANGLES
$F_o/^o$
20
10
0
30
θ
60
90

f

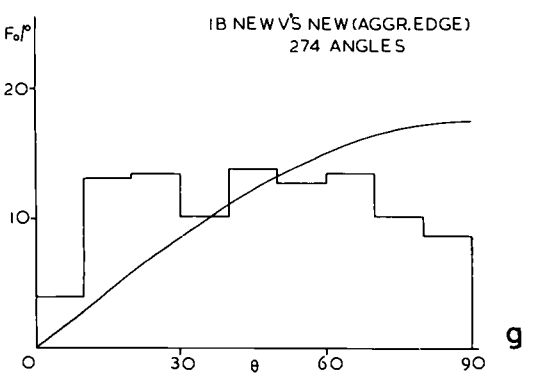
1B NEW V'S NEW (AGGR. EDGE)
274 ANGLES
$F_o/^o$
20
10
0
30
θ
60
90

g

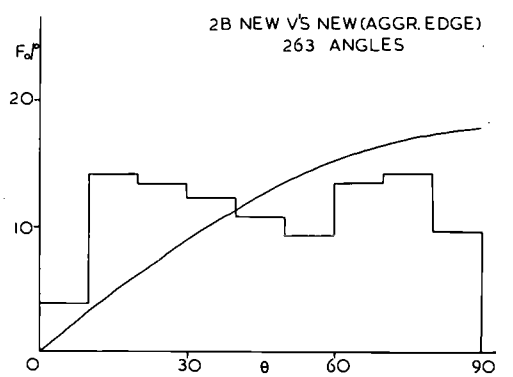
2B NEW V'S NEW (AGGR. EDGE)
263 ANGLES
$F_o/^o$
20
10
0
30
θ
60
90

h

FIGURE 3.2

The sine curve on each graph delineates a uniform angular distribution. F% is frequency percent. θ is angle between graphs.

(a) Angular distribution between host and directly adjacent new grains (Chapter 3.2.3.1A).

(b) Angular distribution between new grains adjacent to the host (Chapter 3.2.3.1A).

(c) Angular distribution between host and directly adjacent new grains (Chapter 3.2.3B).

(d) Angular distribution between new grains adjacent to the host (Chapter 3.2.3B).

(e) Angular distribution between host and directly adjacent new grains (Chapter 3.2.3.2A).

(f) Angular distribution between new grains adjacent to the host (Chapter 3.2.3.2A).

(g) Angular distribution between host and new grains (Chapter 3.2.3.3A).

(h) Angular distribution between host and new grains for a single aggregate (Chapter 3.2.3.1A).

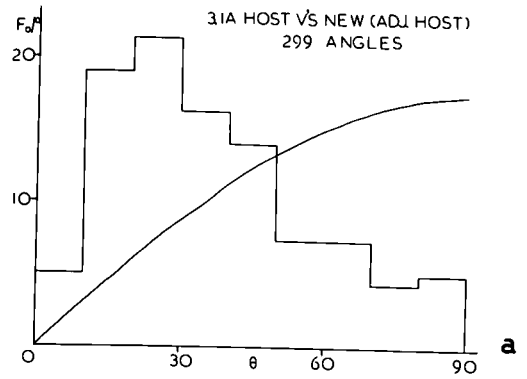
3.1A HOST V'S NEW (ADJ. HOST)
299 ANGLES
F_o/P
20
10
0
30
θ
60
90

a

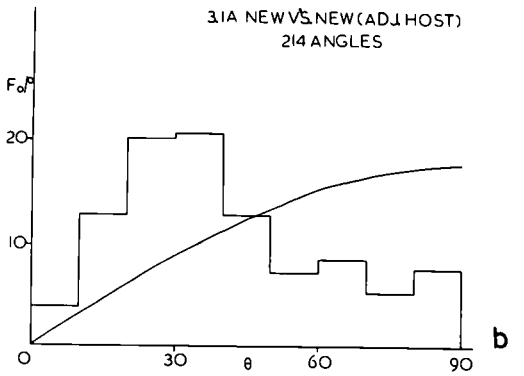
3.1A NEW V'S NEW (ADJ. HOST)
214 ANGLES
F_o/P
20
10
0
30
θ
60
90

b

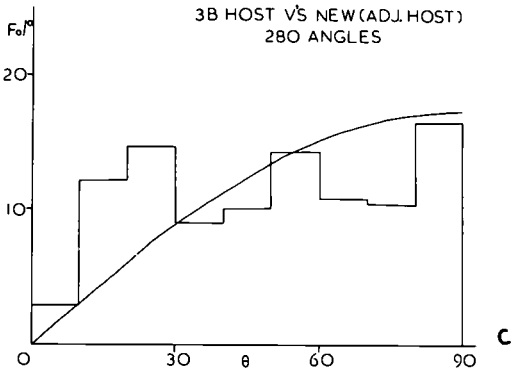
3B HOST V'S NEW (ADJ. HOST)
280 ANGLES
F_o/P
20
10
0
30
θ
60
90

c

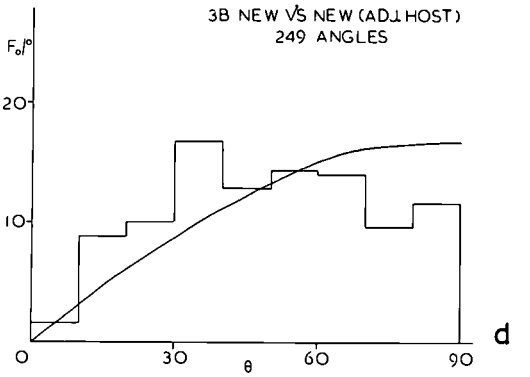
3B NEW V'S NEW (ADJ. HOST)
249 ANGLES
F_o/P
20
10
0
30
θ
60
90

d

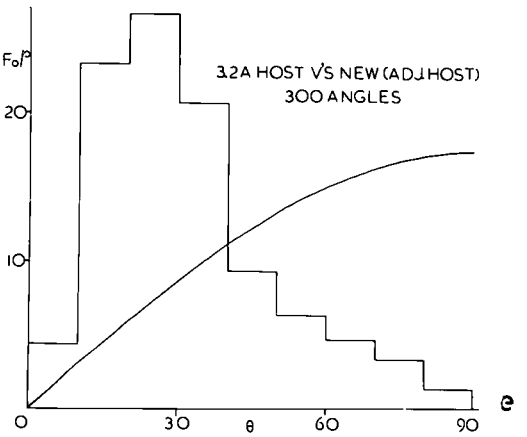
3.2A HOST V'S NEW (ADJ. HOST)
300 ANGLES
F_o/P
20
10
0
30
θ
60
90

e

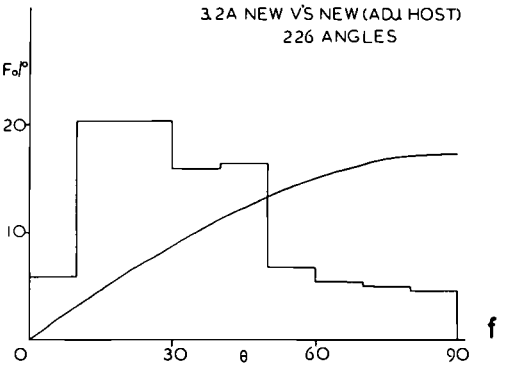
3.2A NEW V'S NEW (ADJ. HOST)
226 ANGLES
F_o/P
20
10
0
30
θ
60
90

f

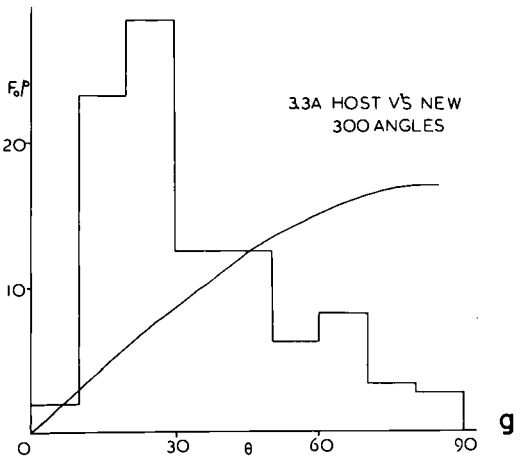
3.3A HOST V'S NEW
300 ANGLES
F_o/P
20
10
0
30
θ
60
90

g

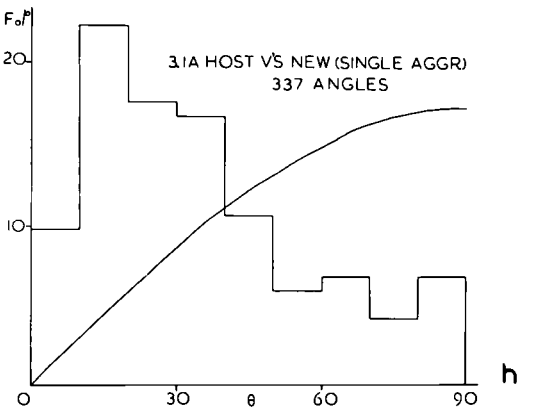
3.1A HOST V'S NEW (SINGLE AGGR)
337 ANGLES
F_o/P
20
10
0
30
θ
60
90

h

FIGURE 3.3

The sine curve on each group delineates a uniform angular distribution. F% is frequency percent. θ is angle between graphs.

(a) Angular distribution between new grains
(Chapter 3.2.4B)

(b) Angular distribution between new grains
(Chapter 3.2.5A)

(c) Angular distribution between new grains
(Chapter 3.2.5B)

(d) Angular distribution between new grains in quartz aggregate remains
(Chapter 3.2.6B)

(e) Angular distribution between new grains
(Chapter 3.2.2B)

(f) Cluster analysis of the whole rock chemical analysis data (fig. 2.10) and rubidium-strontium ratios.

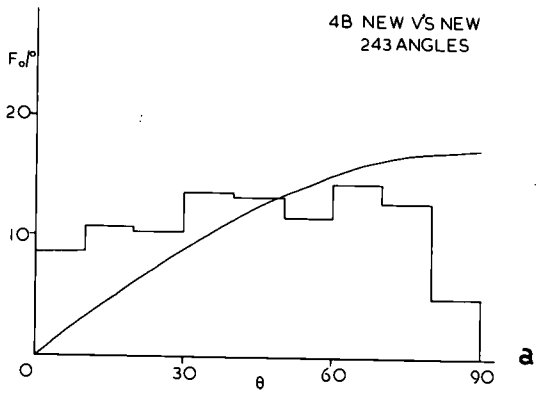
4B NEW V'S NEW
243 ANGLES
F₀/°
20
10
0
30
θ
60
90

a

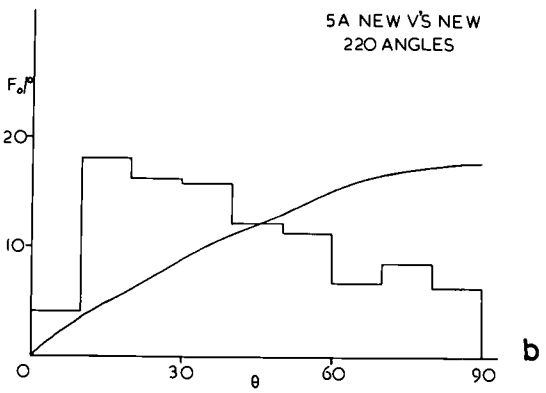
5A NEW V'S NEW
220 ANGLES
F₀/°
20
10
0
30
θ
60
90

b

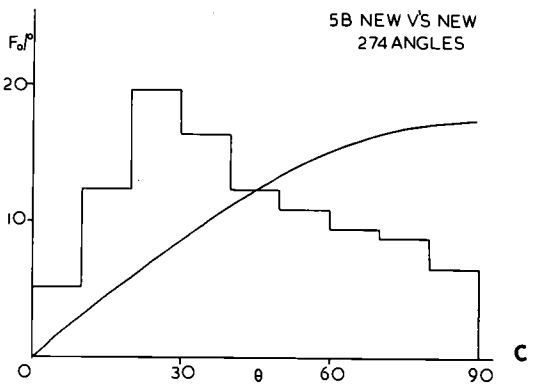
5B NEW V'S NEW
274 ANGLES
F₀/°
20
10
0
30
θ
60
90

c

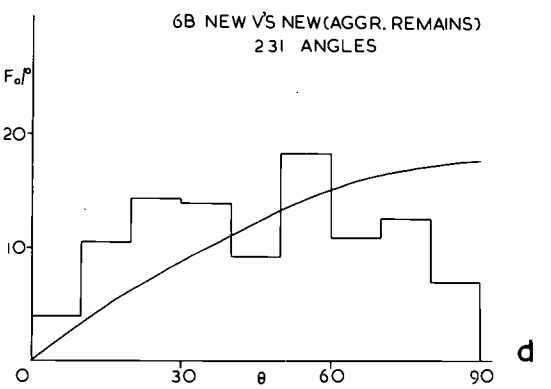
6B NEW V'S NEW(AGGR. REMAINS)
231 ANGLES
F₀/°
20
10
0
30
θ
60
90

d

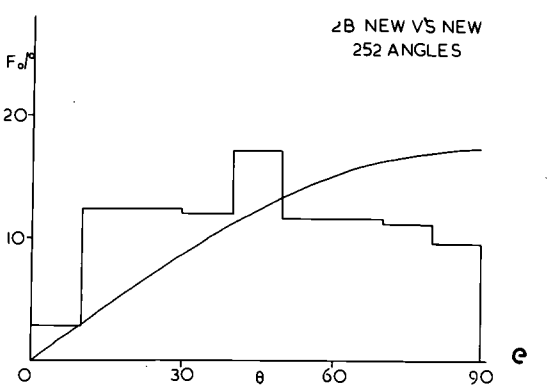
2B NEW V'S NEW
252 ANGLES
F₀/°
20
10
0
30
θ
60
90

e

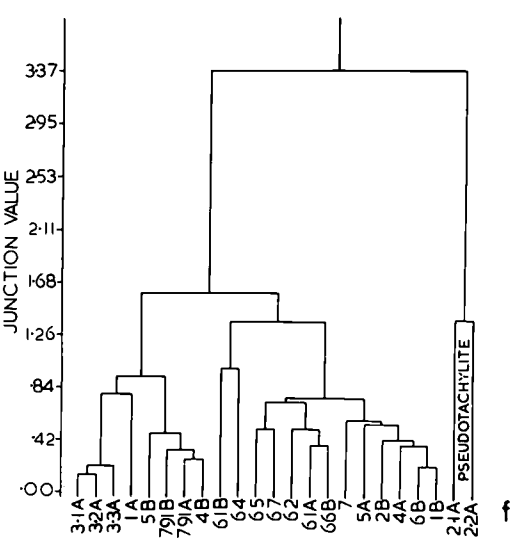
JUNCTION VALUE
3·37
2·95
2·53
2·11
1·68
1·26
·84
·42
·00
3·1A
3·2A
3·3A
1A
5B
7·9B
7·9A
4B
6·1B
6·4
6·5
6·7
6·2
6·1A
6·6B
7
5A
2B
4A
6B
1B
2·1A
2·2A
PSEUDOTACHYLITE

f

FIGURE 3.4

Quartz fabrics. All are contoured by the Kamb (1963) method.

(a) A = 0.029, E = 8.7, σ = 2.9, max = 6.9σ

Contour Intervals 2, 3, 4, 5, 6 σ

(b) A = 0.032, E = 8.7, σ = 2.9, max = 7.9σ

Contour Intervals 2, 3, 4, 5, 6 σ

(c) A = 0.043, E = 8.0, σ = 2.9, max = 10.4σ

Contour Intervals 2, 4, 6, 8, 10 σ

(d) A = 0.129, E = 7.8, σ = 2.6, max = 8.4σ

Contour Intervals 2, 3½, 5, 6½, 8 σ

(e) A = 0.029, E = 8.7, σ = 2.9, max = 10.0σ

Contour Intervals 2, 3½, 5, 6½, 8 σ

(f) A = 0.029, E = 8.7, σ = 2.9, max = 9.6σ

Contour Intervals 2, 3½, 5, 6½, 8 σ

(g) A = 0.029, E = 8.7, σ = 2.9, max = 10.0σ

Contour Intervals 2, 3½, 5, 6½, 8 σ

(h) A = 0.029, E = 8.7, σ = 2.9, max = 11.0σ

Contour Intervals 2, 4, 6, 8, 10 σ

(i) A = 0.029, E = 8.7, σ = 2.9, max = 9.3σ

Contour Intervals 2, 3½, 5, 6½, 8 σ

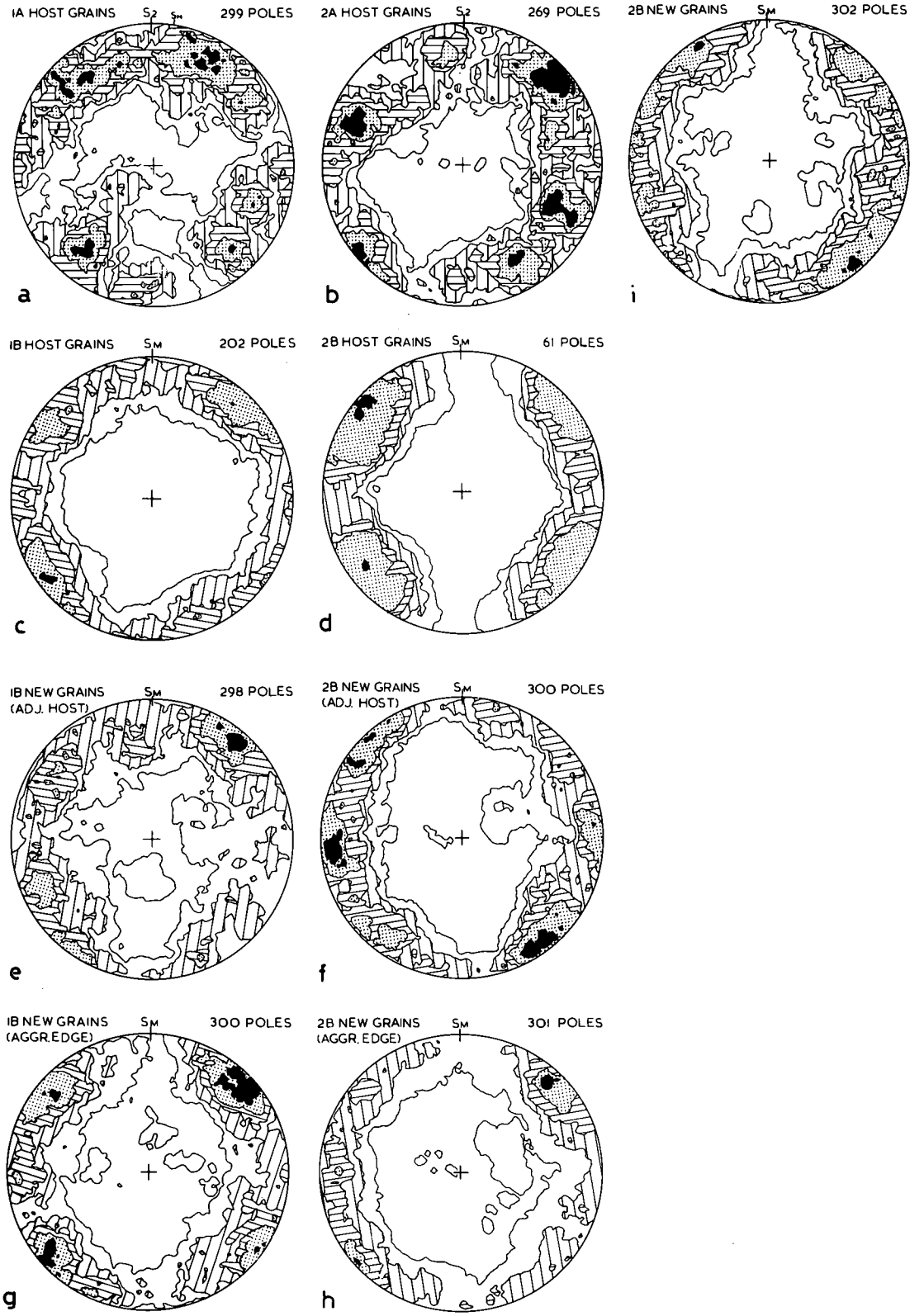
1A HOST GRAINS
S2
SM
299 POLES
a
2A HOST GRAINS
S2
269 POLES
b
2B NEW GRAINS
SM
302 POLES
i
1B HOST GRAINS
SM
202 POLES
c
2B HOST GRAINS
SM
61 POLES
d
1B NEW GRAINS
(ADJ. HOST)
SM
298 POLES
e
2B NEW GRAINS
(ADJ. HOST)
SM
300 POLES
f
1B NEW GRAINS
(AGGR. EDGE)
SM
300 POLES
g
2B NEW GRAINS
(AGGR. EDGE)
SM
301 POLES
h

FIGURE 3.5

Erratum: N in diagrams a, b, and c should read S_M.

Quartz fabrics. All are contoured by the Kamb method.

(a) A = 0.029, E = 8.7, σ = 2.9, max = 11.0σ

Contour Intervals 2, 4, 6, 8, 10 σ

(b) A = 0.029, E = 8.7, σ = 2.9, max = 9.3σ

Contour Intervals 2, 3½, 5, 6½, 8 σ

(c) A = 0.029, E = 8.7, σ = 2.9, max = 10.6σ

Contour Intervals 2, 4, 6, 8, 10 σ

(d) A = 0.170, E = 7.5, σ = 2.5, max = 10.4σ

Contour Intervals 2, 4, 6, 8, 10 σ

(e) A = 0.031, E = 8.7, σ = 2.9, max = 11.0σ

Contour Intervals 2, 4, 6, 8, 10 σ

(f) A = 0.029, E = 8.7, σ = 2.9, max = 11.0σ

Contour Intervals 2, 4, 6, 8, 10 σ

(g) A = 0.033, E = 8.7, σ = 2.9, max = 14.1σ

Contour Intervals 2, 5, 8, 11, 14 σ

(h) A = 0.029, E = 8.7, σ = 2.9, max = 16.5σ

Contour Intervals 2, 5½, 9, 12½, 16 σ

FIGURE 3.5 (continued)

(i) A = 0.026, E = 8.8, σ = 2.9, max = 12.7σ

Contour Intervals 2, 4½, 7, 9½, 12 σ

(j) A = 0.029, E = 8.7, σ = 2.9, max = 23.0σ

Contour Intervals 2, 7, 12, 17, 22 σ

(k) A = 0.029, E = 8.7, σ = 2.9, max = 16.8σ

Contour Intervals 2, 5½, 9, 12½, 16 σ

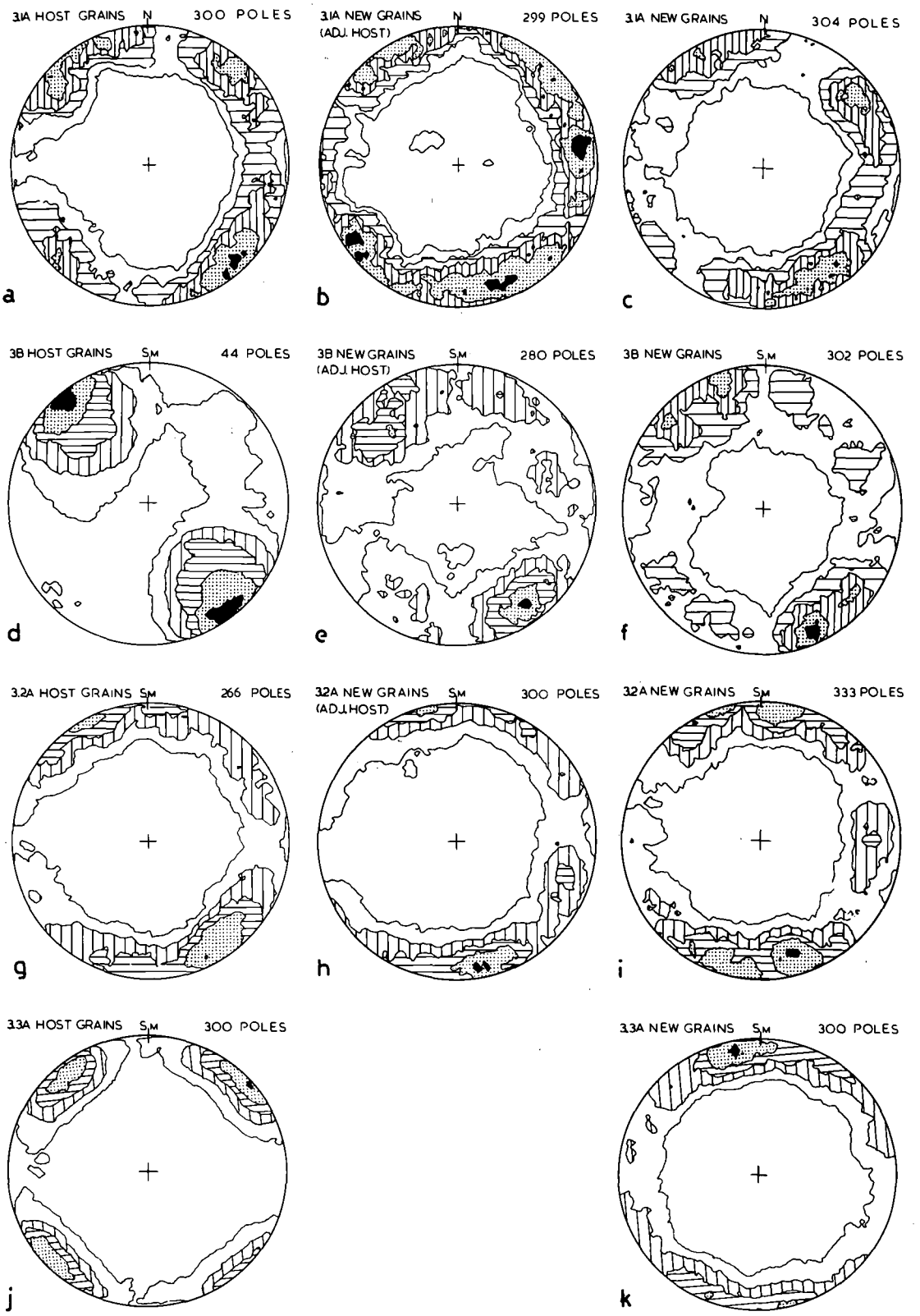
3.1A HOST GRAINS N 300 POLES
a
3.1A NEW GRAINS (ADJ. HOST) N 299 POLES
b
3.1A NEW GRAINS N 304 POLES
c
3B HOST GRAINS SM 44 POLES
d
3B NEW GRAINS (ADJ. HOST) SM 280 POLES
e
3B NEW GRAINS SM 302 POLES
f
3.2A HOST GRAINS SM 266 POLES
g
3.2A NEW GRAINS (ADJ. HOST) SM 300 POLES
h
3.2A NEW GRAINS SM 333 POLES
i
3.3A HOST GRAINS SM 300 POLES
j
3.3A NEW GRAINS SM 300 POLES
k

FIGURE 3.6

Quartz fabrics. All are contoured by the Kamb method.

(a) A = 0.029, E = 8.7, σ = 2.9, max = 19.9σ

Contour Intervals 2, 6, 10, 14, 18 σ

(b) A = 0.029, E = 8.7, σ = 2.9, max = 11.7σ

Contour Intervals 2, 4, 6, 8, 10 σ

(c) A = 0.029, E = 8.7, σ = 2.9, max = 18.2σ

Contour Intervals 2, 6, 10, 14, 18 σ

(d) A = 0.029, E = 8.7, σ = 2.9, max = 25.4σ

Contour Intervals 2, 7½, 13, 18½, 24 σ

(e) A = 0.092, E = 8.2, σ = 2.7, max = 29.0σ

Contour Intervals 2, 8½, 15, 21½, 28 σ

(f) A = 0.029, E = 8.7, σ = 2.9, max = 9.6σ

Contour Intervals 2, 3½, 5, 6½, 8 σ

(g) A = 0.043, E = 8.6, σ = 2.9, max = 11.8σ

Contour Intervals 2, 4, 6, 8, 10 σ

(h) A = 0.029, E = 8.7, σ = 2.9, max = 10.6σ

Contour Intervals 2, 4, 6, 8, 10 σ

(i) A = 0.029, E = 8.7, σ = 2.9, max = 10.3σ

Contour Intervals 2, 4, 6, 8, 10 σ

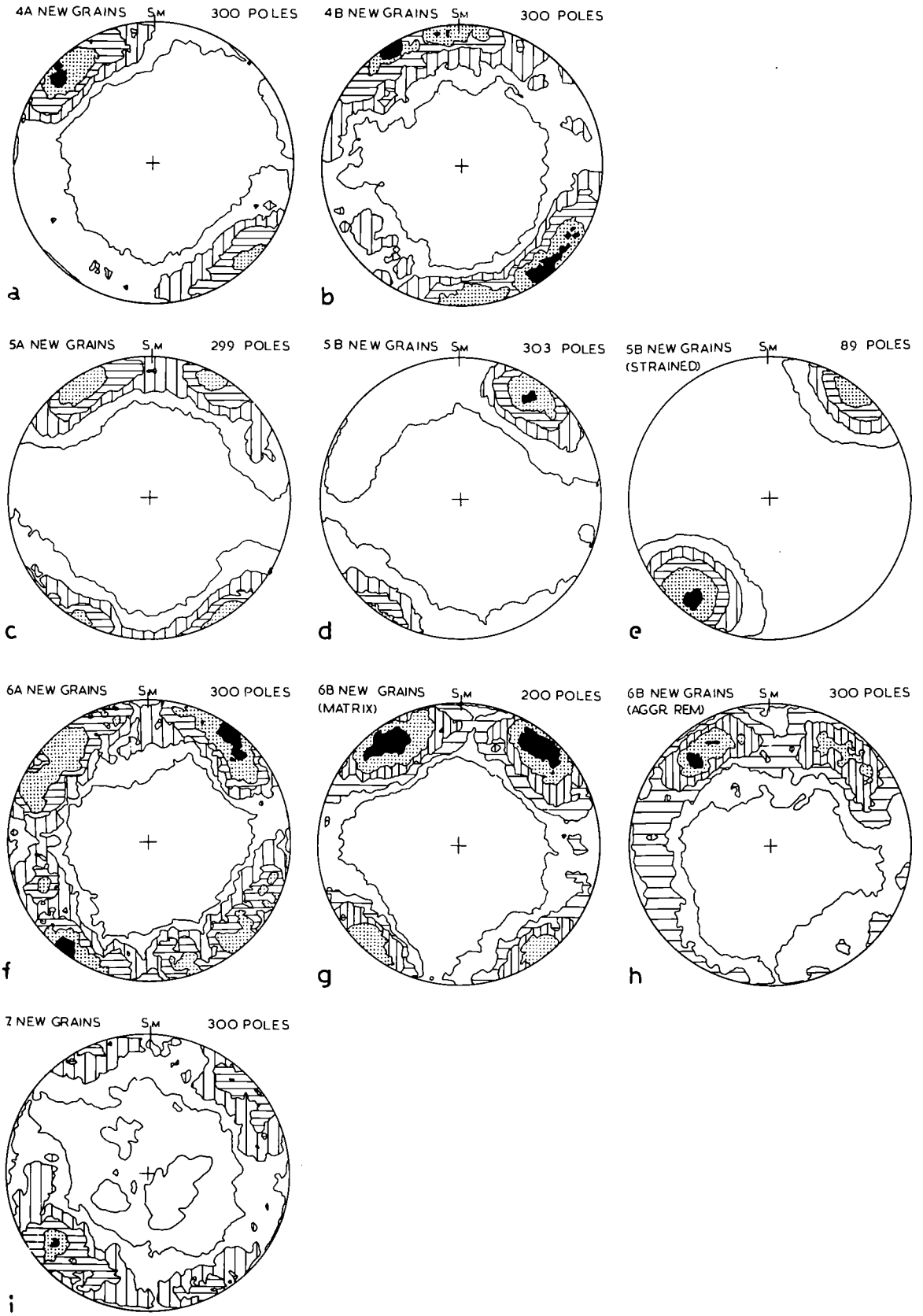
4A NEW GRAINS SM 300 POLES
a
4B NEW GRAINS SM 300 POLES
b
5A NEW GRAINS SM 299 POLES
c
5B NEW GRAINS SM 303 POLES
d
5B NEW GRAINS (STRAINED) SM 89 POLES
e
6A NEW GRAINS SM 300 POLES
f
6B NEW GRAINS (MATRIX) SM 200 POLES
g
6B NEW GRAINS (AGGR REM) SM 300 POLES
h
7 NEW GRAINS SM 300 POLES
i

FIGURE 3.7

(a) Line of minute new quartz grains across a quartz host. Note minute subgrains in the upper half of host grain adjacent to the new grains.

1A

Crossed polars. Width of field: 213 μm

(b) Line of minute opaque inclusions across a quartz host. Note the slight variation in quartz birefringence along this line.

1A

Crossed polars. Width of field: 213 μm

(c) A narrow zone of birefringence variation (vertical). It contains a number of subgrains in the quartz together with some small new mica grains. The lattice on the right hand edge of the upper quartz grain has been rotated slightly.

1A

Crossed polars. Width of field: 213 μm

(d) Line of local variation in birefringence cutting a number of grains including quartz, feldspar and pyroxene from the upper R.H.S. to lower L.H.S. of the photo. It contains some minute new grain growth in most grains. Note the slight displacement of grain boundaries.

1A

Crossed polars. Width of field: 570 μm

a

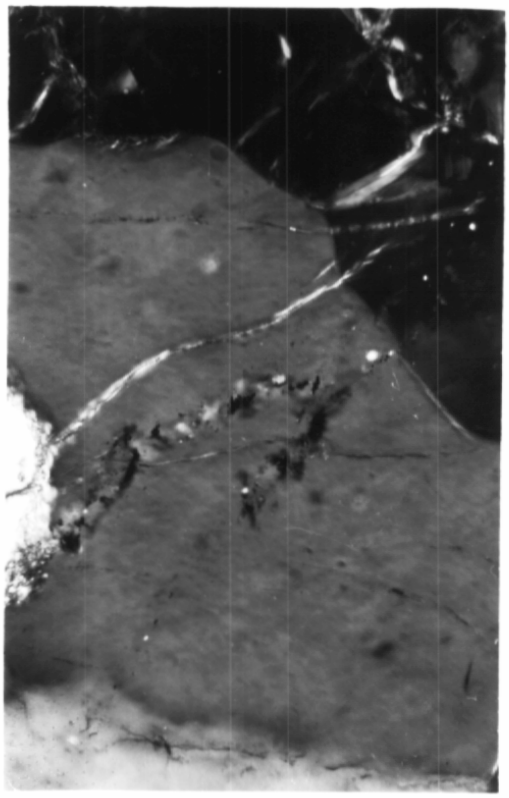

b

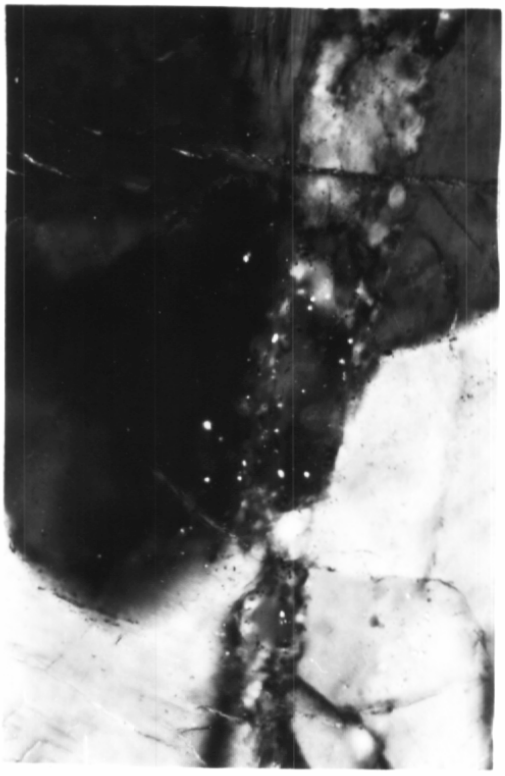

c

d

FIGURE 3.8

(a) Hairline fractures in a quartz grain (upper L.H.S.). The main microstructure passes across the centre of the photo parallel to the hairline fractures. Note the displacement of the quartz-feldspar grain boundary and the feldspar grain left of centre.

1A

Crossed polars. Width of field: 213 μm

(b) Microsheared quartz grain. Note the displacement of the grain and the new grain growth along the microshear. A portion of this is enlarged in C.

1A

Crossed polars. Width of field: 1.4 mm

(c) Strain shadowing, minute subgrain formation and new grain growth along a microshear. The microshear is possibly an intense kink rather than an actual fracture.

1A

Crossed polars. Width of field: 213 μm

(d) The country rock schistosity remnants trend diagonally across the photo from the upper L.H.S. to lower R.H.S. They are defined by a few elongate feldspar grains. S_M trends horizontally across the photo. Defined by elongation of some of the quartz aggregates and aligned deformation bands in quartz hosts.

1B

Crossed polars. Width of field: 7.3 mm

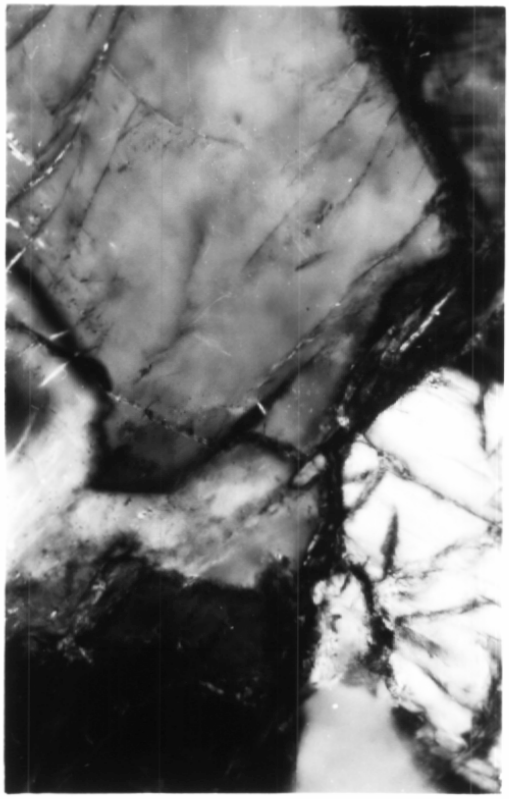

a

b

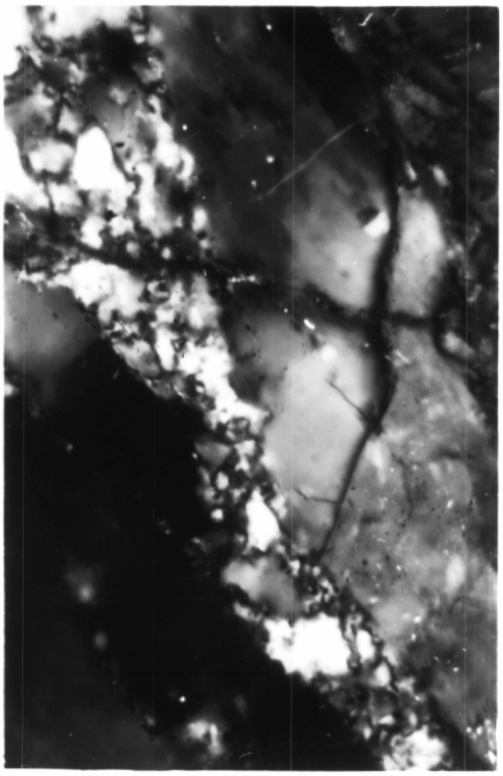

c

d

FIGURE 3.9

(a) Polygonal subgrains within a deformed quartz host grain. Note the new grain growth around the host edge and their larger size, c.f. the subgrains.

1B

Crossed polars. Width of field: 570 μm

(b) New grain growth around the edge of a host quartz grain. Note the rounded new grain boundaries.

1B

Crossed polars. Width of field: 570 μm

(c) Aggregate of new quartz grains. Grain boundaries vary from straight to rounded. Triple point boundaries at 120° occur.

1B

Crossed polars. Width of field: 570 μm

(d) New grains (upper L.H.S.) forming adjacent to subgrains within the host quartz grain remains. Note the polygonal boundaries of the subgrains and the progressive misorientation and size increase into the new grains. Only those grains away from the host remains relative to the white new grains, are new grains. The remainder are subgrains.

1B

Crossed polars. Width of field: 570 μm

a

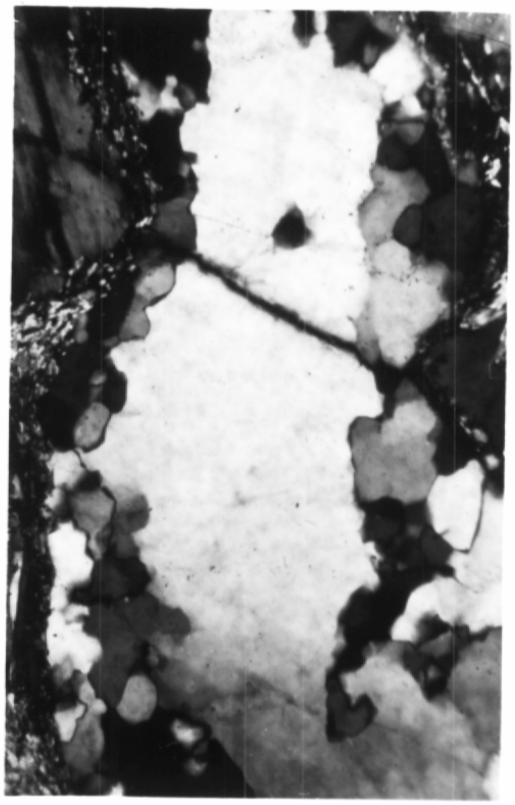

b

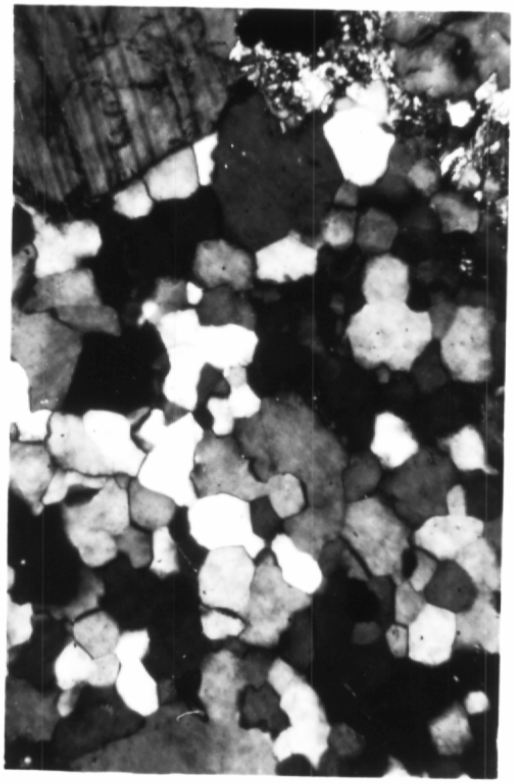

c

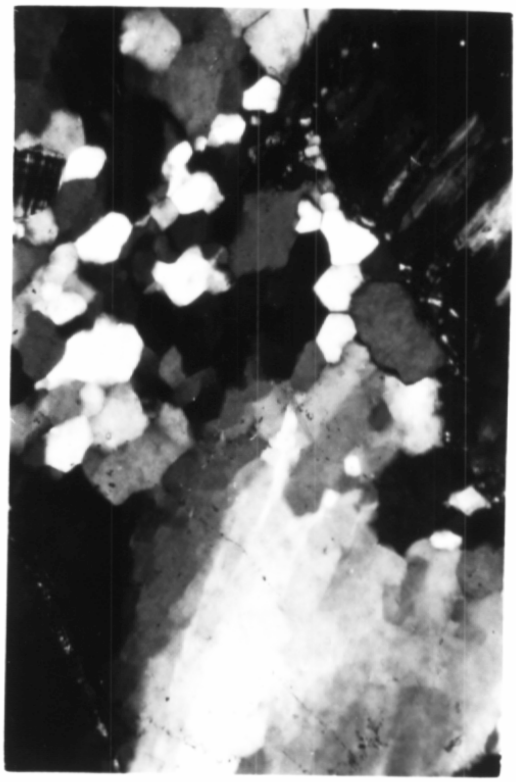

d

FIGURE 3.10

(a) Microfractures with opaque infill in a quartz grain.

2.1A

Crossed polars. Width of field: 570 μm

(b) Slight growth of minute new grains along deformation band boundaries and in recovered host away from the deformation bands. The degree of bulge along the length of a number of the narrow deformation bands has been so great that in places the deformation band has disappeared leaving new grains sitting within its remnants to either side.

2.1A

Crossed polars. Width of field: 213 μm

(c) Strain shadowed quartz grain away from the microshears. Note the fractures infilled with fine grained mica.

2.1A

Crossed polars. Width of field: 570 μm

(d) New grains growing on the edge of a host grain adjacent to subgrains within the host remains. Note the larger size of the new grains relative to the subgrains.

2B

Crossed polars. Width of field: 570 μm

a

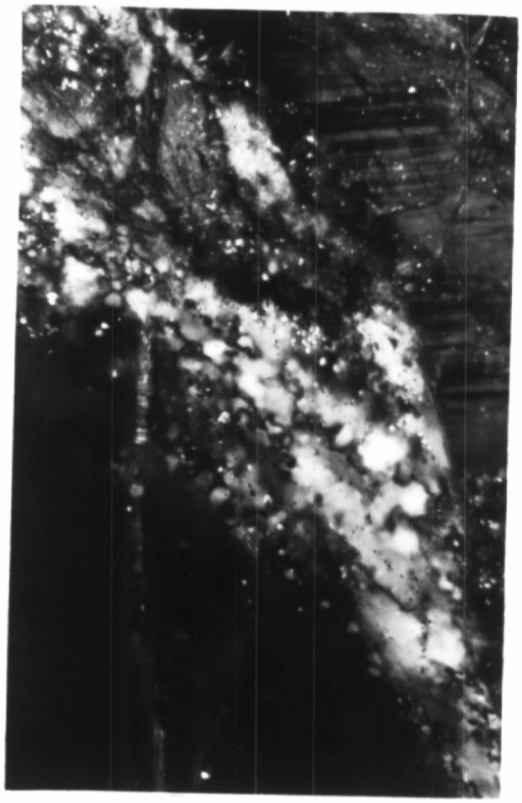

b

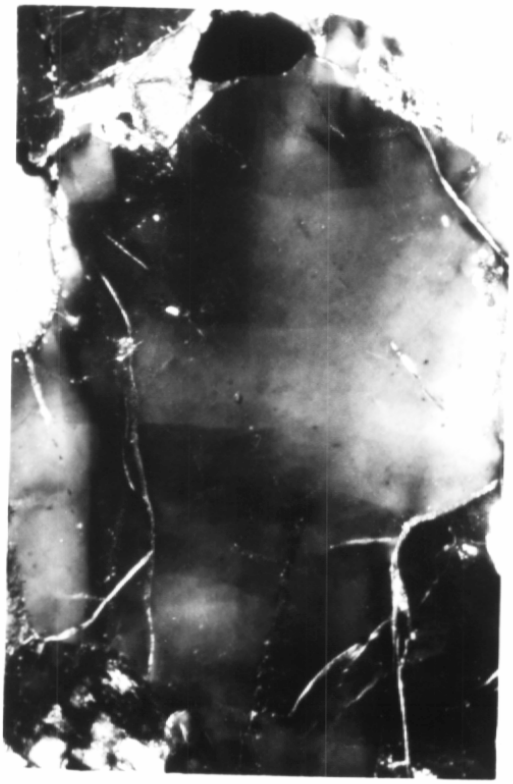

c

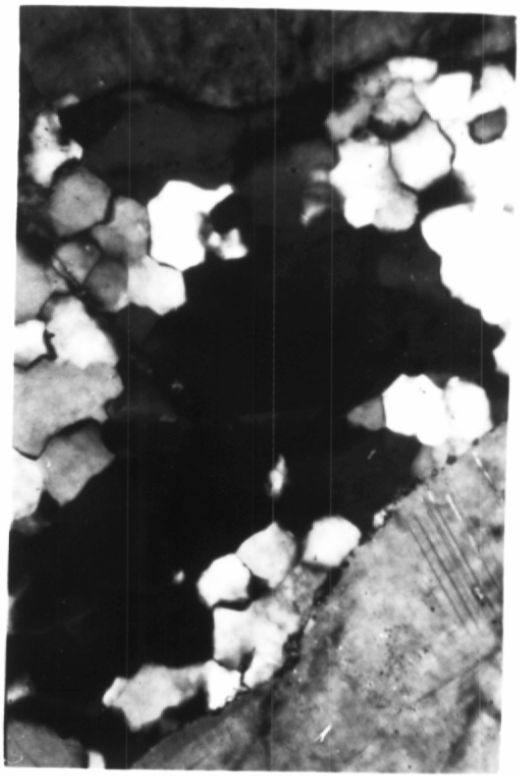

d

FIGURE 3.11

(a) Aggregate of new quartz grains which contains no host grain remains. Grain boundaries range from gently rounded to straight.

2B

Crossed polars. Width of field: 1.4 mm

(b) Streams of pseudotachylite (diagonal). The whitish ellipsoidal mass (lower half, L.H.S.) is a quartz host grain. It is highly deformed and contains a number of small new grains and subgrains. Those directly adjacent to the pseudotachylite are smaller than those in the centre of the host. Note the bubbly nature of the microstructures between the pseudotachylite and this host quartz grain on its upper L.H.S.

2.2A

Crossed polars. Width of field: 138 μm

(c) Fractured quartz grain. The fractures are infilled with opaque.

2.2A

Crossed polars. Width of field: 570 μm

(d) Quartz grain displaced along a microshear.

2.2A

Crossed polars. Width of field: 570 μm

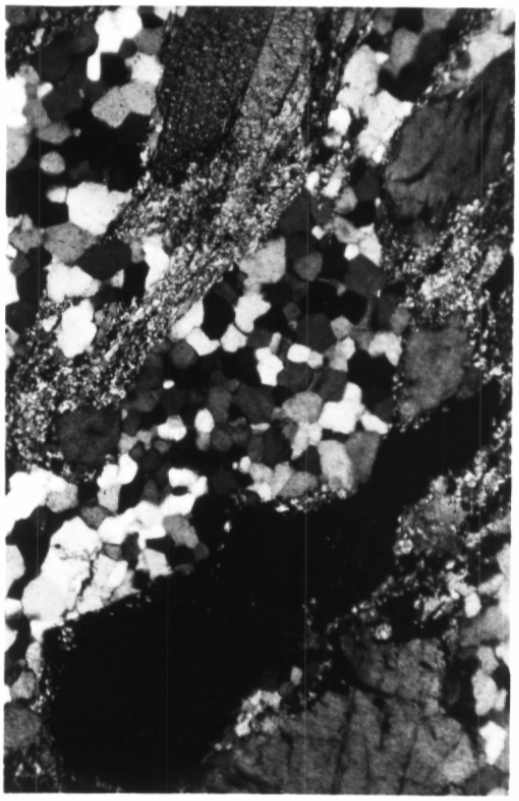

a

b

c

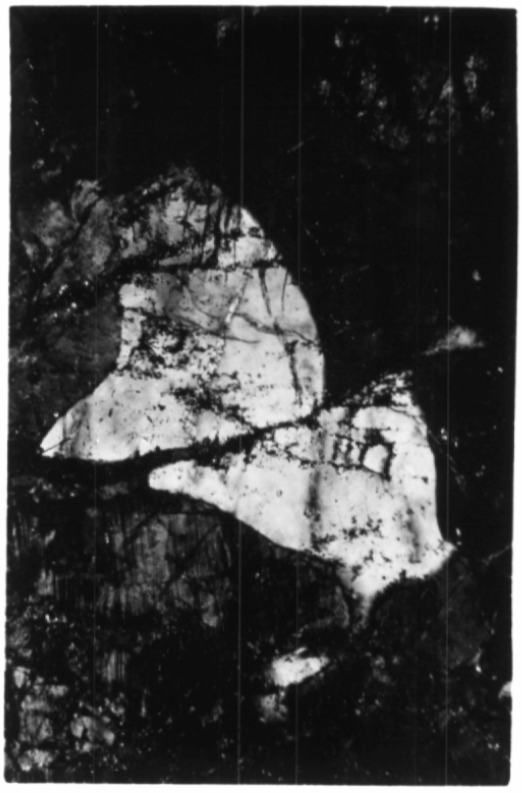

d

FIGURE 3.12

(a) Strain shadowed, deformation banded host quartz grain. Shows growth of new grains along deformation band boundaries.

2.2A

Crossed polars. Width of field: 213 μm

(b) Blind discordant intrusion of pseudotachylite into mylonitic schistosity along a fracture.

3.3A

Crossed polars. Width of field: 570 μm

(c) Strain shadowed, deformation banded quartz host grain. Note the bulge of the deformation band boundaries around subgrains and the new grain growth along them. Note the subgrains in the host grain remains away from the deformation bands and the associated new grain growth on the host edge (R.H.S., lower half).

3.1A

Crossed polars. Width of field: 570 μm

(d) Strain shadowed original quartz grain surrounded by feldspar which exhibits no new grain growth.

3.1A

Crossed polars. Width of field: 213 μm

a

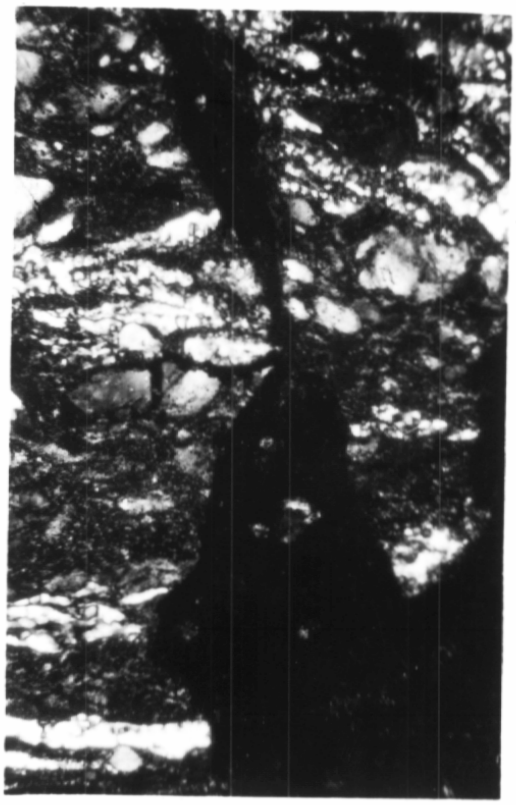

b

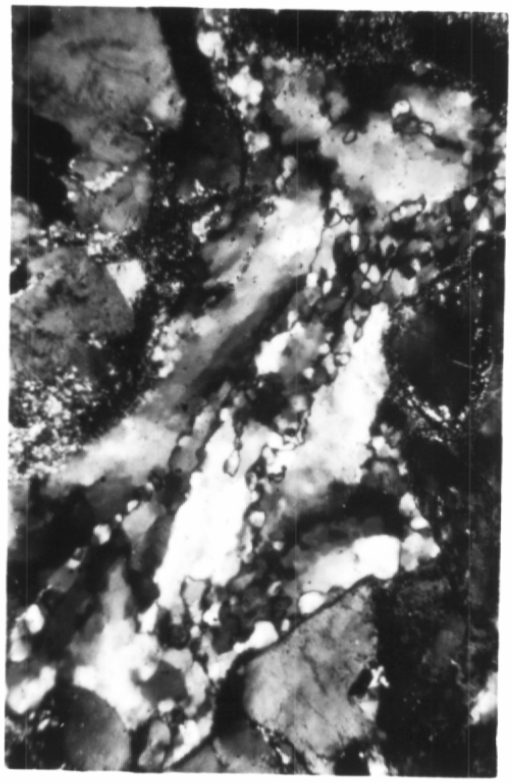

c

d

FIGURE 3.13

(a) Bulge of a deformation band boundary in quartz where it is pinned by subgrain walls. Note the increase in the size of subgrains and the degree of bulge of the deformation band boundary around them, from the bottom to the top of the photo until the latter disappears into new grains. Some of those grains around which the deformation band is bulging are now new grains but most are subgrains.

3.1A

Crossed polars. Width of field: 225 μm

(b) Shows subgrains increasing in size and degree of mismatch towards new grains on the edge of the quartz host. Note the larger size of the new grains relative to the subgrains especially those close to the aggregate edge. The upper quarter of the photo contains deformation band boundary shown in (a).

3.1A

Crossed polars. Width of field: 213 μm

(c) Shows subgrains increasing in size and degree of mismatch towards new grains on the edge of the host. Note the larger size of the new grains relative to the subgrains. Note also the rounded boundaries on the new grains.

3.1A

Crossed polars. Width of field: 213 μm

(d) Quartz aggregate which has almost entirely converted to new grains. Note the curved to straight grain boundaries of new grains surrounded by new grains.

3.1A

Crossed polars. Width of field: 570 μm

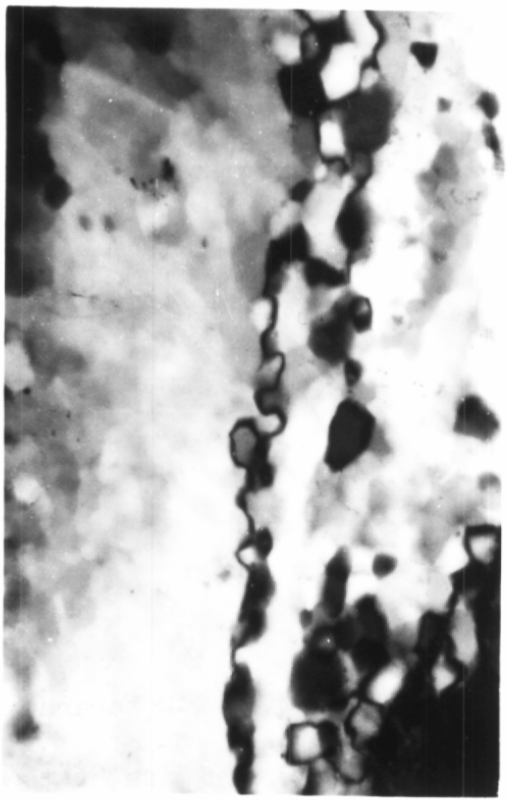

a

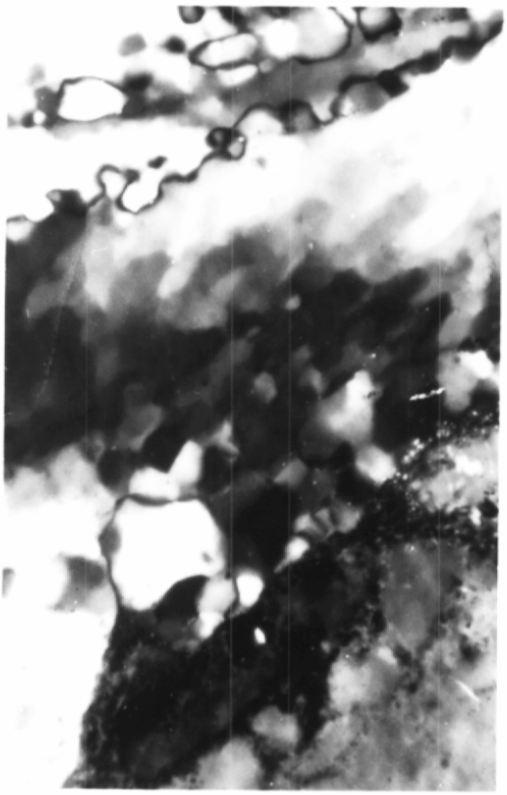

b

c

d

FIGURE 3.14

(a) Deformation banded host grain remains. A few large new grains occur on the host edge.

3B

Crossed polars. Width of field: 570 μm

(b) Quartz aggregate containing no host grain remains. The new grain size is variable and grain boundaries are rounded.

3B

Crossed polars. Width of field: 1.4 mm

(c) Two deformation banded new grains. The deformation bands lie approximately 45° either side of S_M. Note the kinking of the grain boundary between them (left of centre) where it is cut by the deformation bands.

3B

Crossed polars. Width of field: 570 μm

(d) Strain shadowed, deformation banded (kinked) host grain. Note the bulge of the deformation band boundary where it is pinned by small rounded subgrains on the L.H.S. of the photo. Note the larger polygonal subgrains away from the deformation band boundary on the R.H.S. (especially upper R.H. corner).

3.2A

Crossed polars. Width of field: 213 μm

a

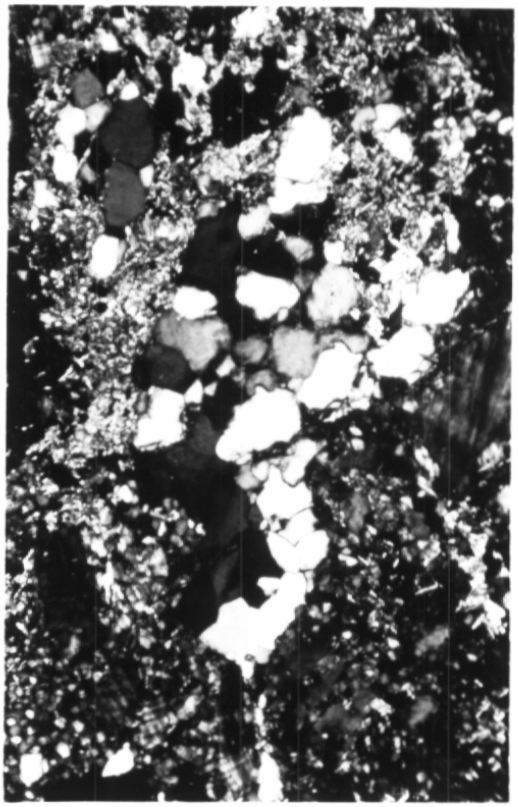

b

c

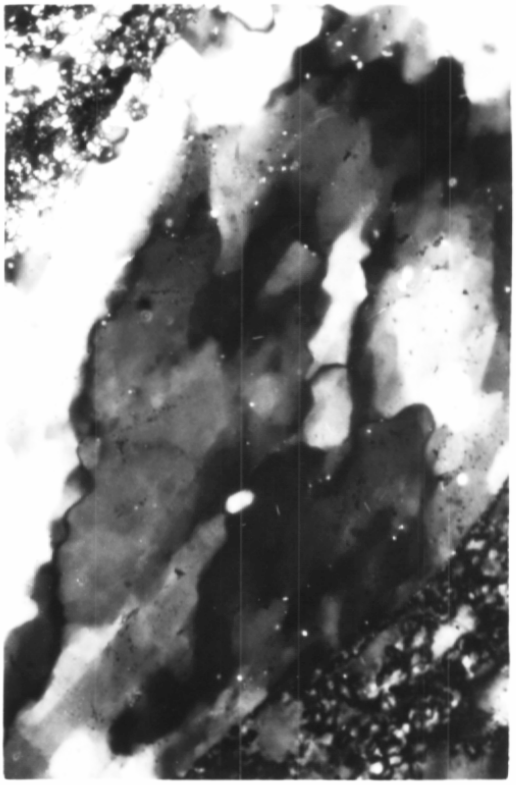

d

FIGURE 3.15

(a) Subgrains and new grains along a deformation band boundary (centre of photo) in quartz. Note their rounded boundaries. The subgrains away from the deformation band boundary to either side are more polygonal.

3.2A

Crossed polars. Width of field: 225 μm

(b) Polygonal subgrains (lower half of photo) merging with new grains in a quartz host. Note the increase in misorientation and size towards the new grains. In the upper half of the photo there are a few polygonal subgrain remains which are merging with new grains around them. Note the increased misorientation as the subgrain size increases.

3.2A

Crossed polars. Width of field: 213 μm

(c) Aggregate of new quartz grains. Grain boundaries are gently curved to straight. Contains only a few triple point boundaries at 120°.

3.2A

Crossed polars. Width of field: 570 μm

(d) Aggregate of new quartz grains. Some are elongate parallel to the aggregate length, that is parallel to S_M trend. Some are also strain shadowed.

3.2A

Crossed polars. Width of field: 570 μm

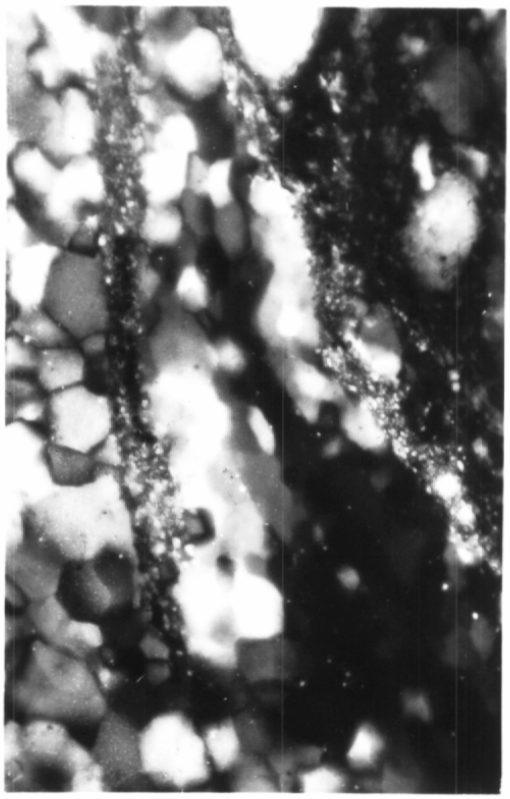

a

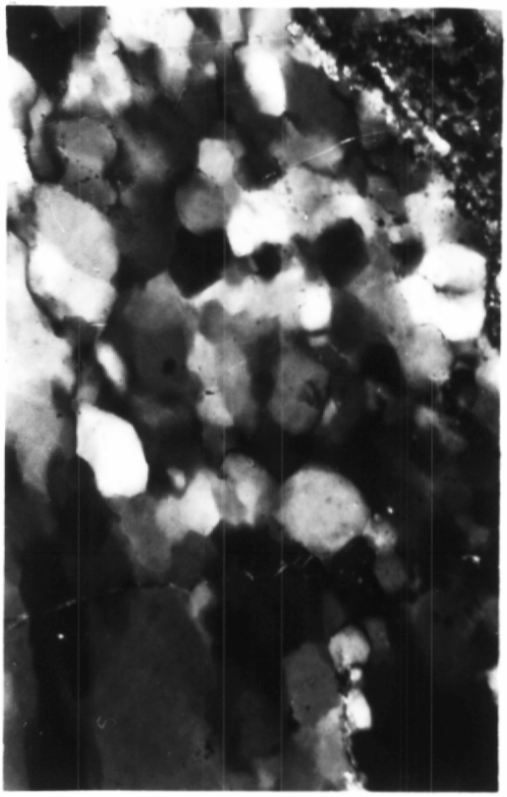

b

c

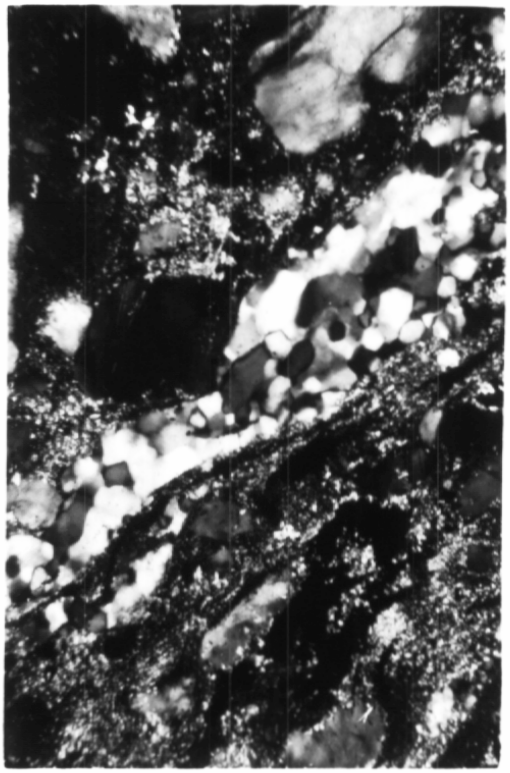

d

Figure 3.16

(a) Strain shadowed and deformation banded quartz host grain which contains subgrains and many small new grains. Note the subgrains merging with new grains in the lower half of the photo and new grains forming long deformation bands in the upper half. The degree of bulge of the deformation band boundaries has in some cases been so great, that they have partly disappeared along their length, leaving new grains sitting within their remnants (centre of photo).

3.3A

Crossed polars. Width of field: 570 μm

(b) Deformation banded portion of a host grain. Shows rounded subgrains along serrate deformation band boundaries and some new grains.

3.3A

Crossed polars. Width of field: 213 μm

(c) Zone of high strain (diagonal) cross cutting S_M (vertical) at a low angle. These zones are associated with the formation of pseudotachylite. Note the thin highly elongate quartz host grains in the high strain zone and the smaller sub and new grains.

3.3A

Crossed polars. Width of field: 1.4 mm

(d) Pseudotachylite occuring as a blind, cross cutting protuberance into undisturbed mylonite (S_M horizontal). Note the long quartz host grain which penetrates into the pseudotachylite in the upper right hand corner.

3.3A

Crossed polars. Width of field: 1.4 mm

a

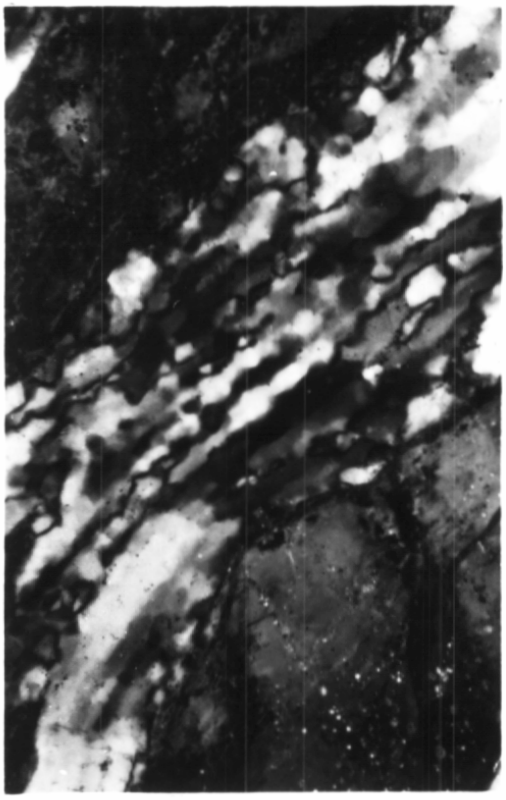

b

c

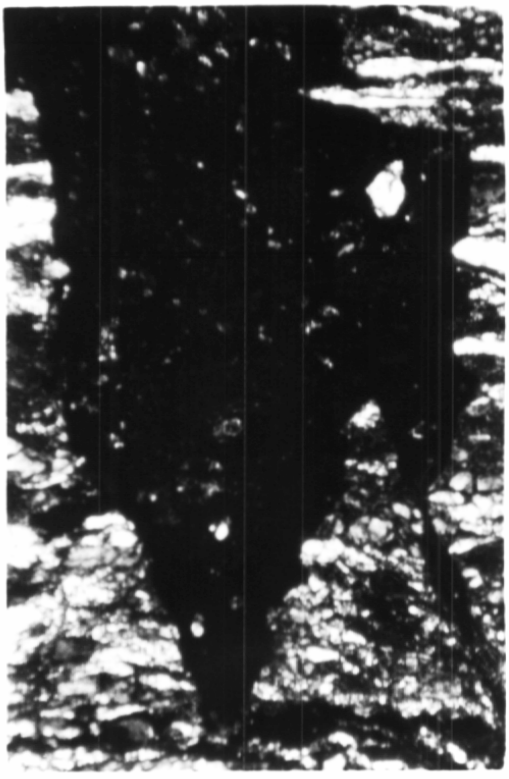

d

FIGURE 3.17

(a) Elongate quartz aggregates of varying width. Note the rectangular grain shape in the narrow aggregates. Granulite facies side.

4A

Crossed polars. Width of field: 570 μm

(b) Elongate quartz aggregates of varying width. Note the rectangular grains in the central thin aggregate. Amphibolite facies side.

4B

Crossed polars. Width of field: 1.4 mm

(c) Elongate quartz aggregates. Note the rectangular grains and four point boundaries in the centre aggregate (bottom half of photo).

5A

Crossed polars. Width of field: 570 μm

(d) Mica and feldspar growth along grain boundaries in a quartz aggregate. Note four point boundaries on L.H.S.

5A

Crossed polars. Width of field: 225 μm

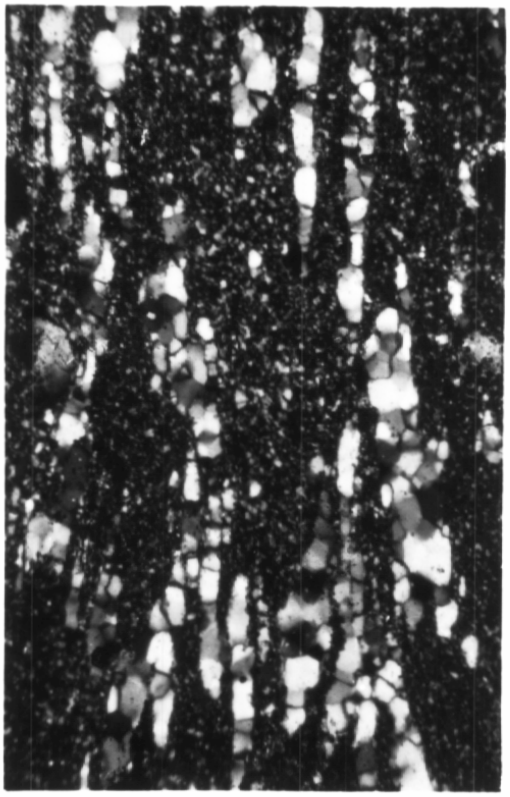

a

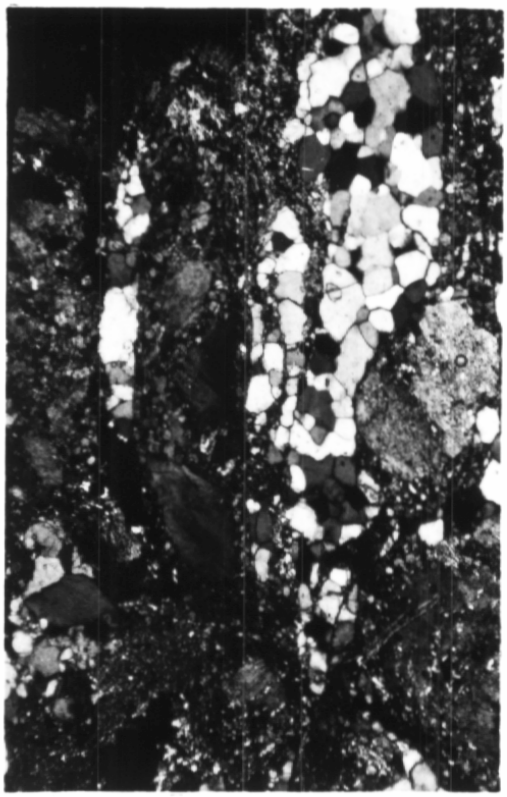

b

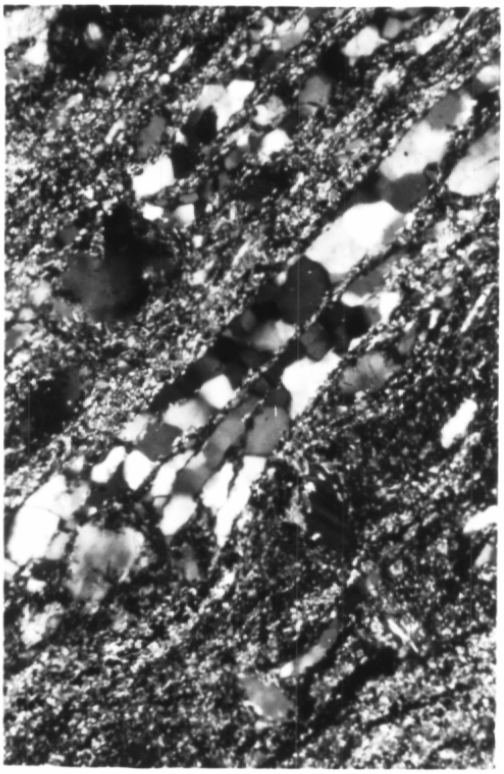

c

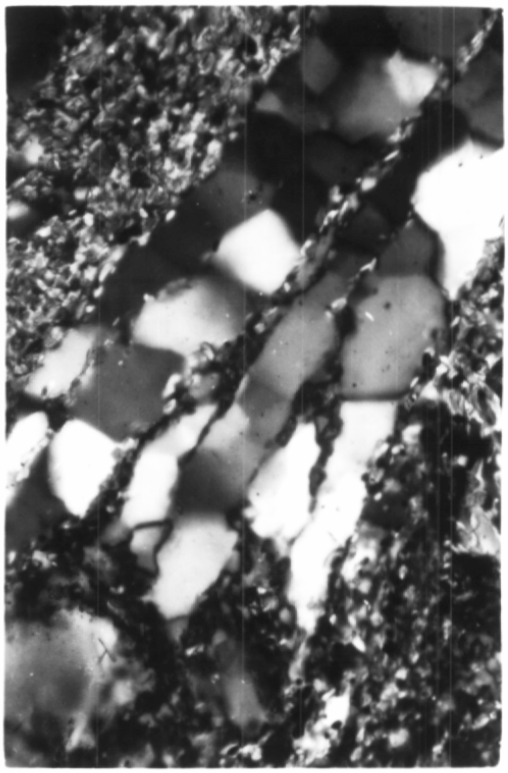

d

FIGURE 3.18

(a) Mica and feldspar growth in a quartz aggregate.

5B

Crossed polars. Width of field: 570 μm

(b) Remains of a quartz aggregate (diagonal across photo). Note the muscovite growth within it and the coarser grain size of quartz within it relative to that in the homogeneous matrix.

6A

Crossed polars. Width of field: 570 μm

(c) Homogeneous quartz-feldspar-mica schist matrix. Quartz and feldspar grains are generally equidimensional.

6A

Crossed polars. Width of field: 570 μm

(d) Quartz aggregate remains. Homogenization stage mylonite on amphibolite facies side. Matrix not as homogeneous, c.f. 3.18(c).

6B

Crossed polars. Width of field: 570 μm

a

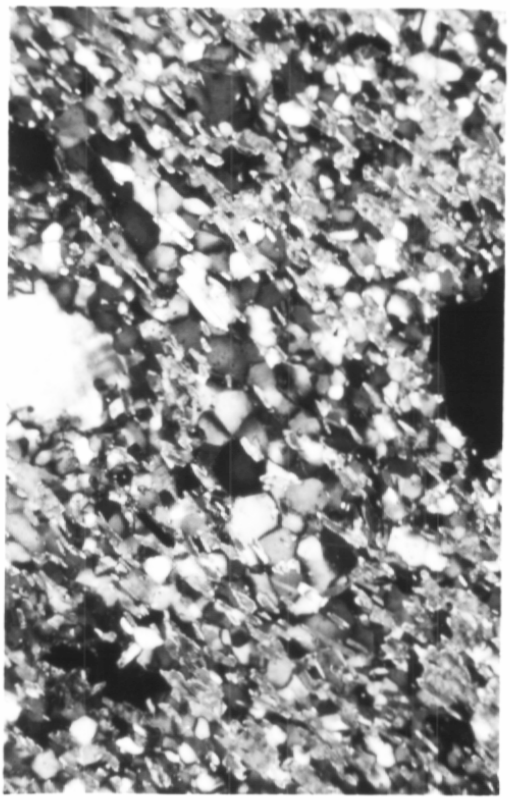

b

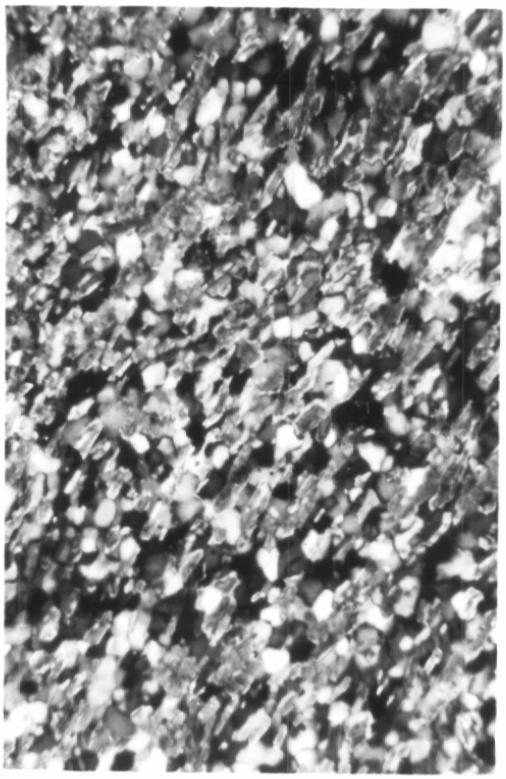

c

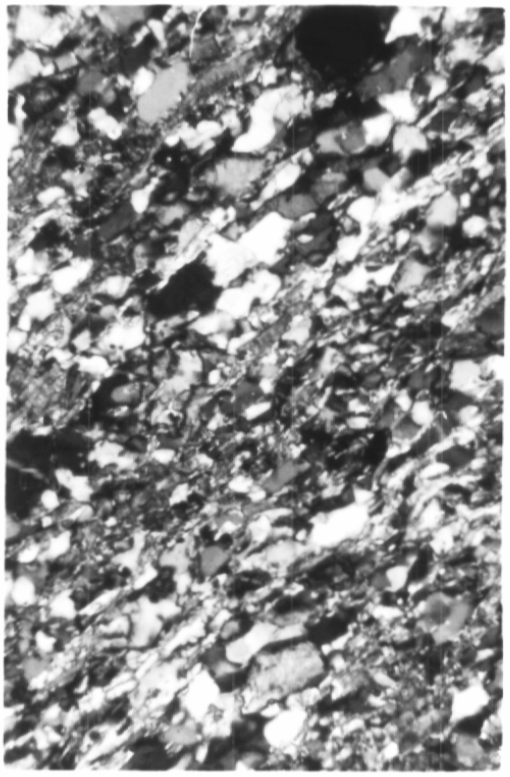

d

FIGURE 3.19

(a) Quartz aggregate remains. Note the mica growth, the strain shadowed quartz grains, and the small strongly rounded new quartz grains within it.

6B

Crossed polars. Width of field: 570 μm

(b) Slaty mylonite: note the strong mica (001) preferred orientation, the equidimensional quartz and feldspar grains, and the strong homogeneity.

7

Crossed polars. Width of field: 1.4 mm

(c) Deformation band boundary in quartz host (the line down the centre of the quartz grain) on the granulite facies side. Note the bulge of the deformation band boundary around subgrains.

3.1A

Crossed polars. Width of field: 570 μm

(d) Deformation band boundary in quartz host on the amphibolite facies side. Note the diffuse nature compared with fig.3.19(c), and the wide zone of bending.

1B

Crossed polars. Width of field: 570 μm

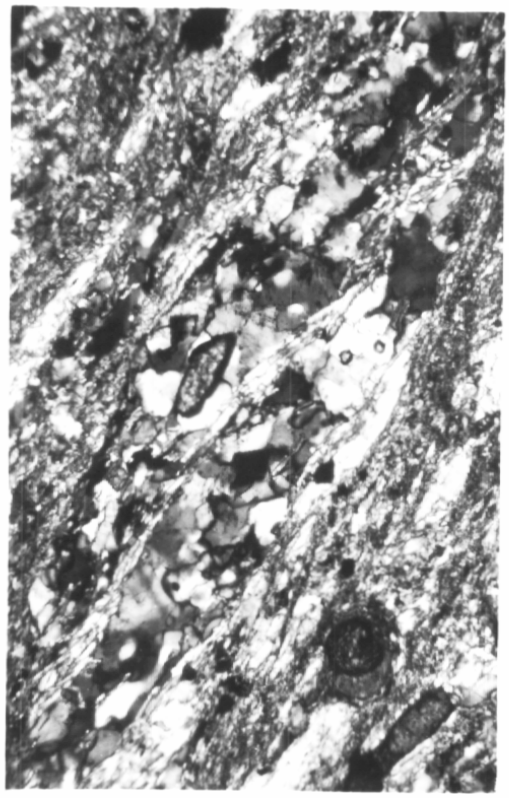

a

b

c

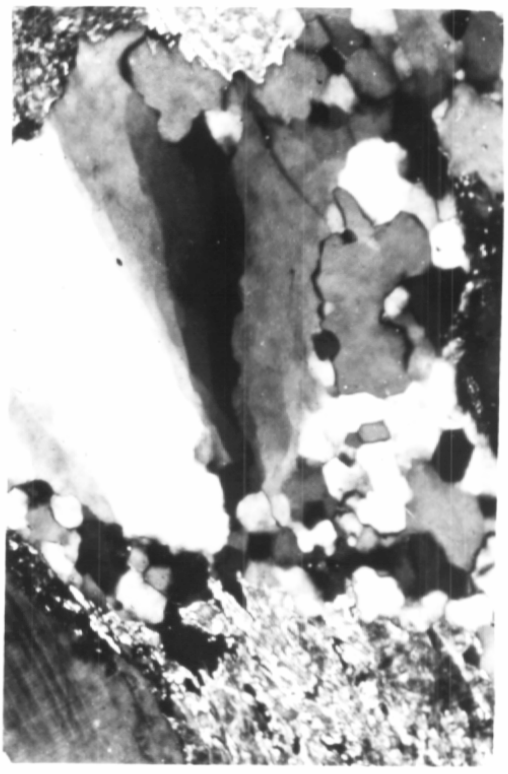

d

FIGURE 4.1

(a) Strain shadowed and kinked original mica.

3.1A

Crossed polars. Width of field: 213 μm

(b) Host mica deformed by slip along (001). Note the new mica growth on its edges and down its centre.

3.1A

Crossed polars. Width of field: 213 μm

(c) Kinked mica host. Note the kink boundary migration down (001) where the angle of kinking is greater (centre of photo).

3.1A

Crossed polars. Width of field: 138 μm

(d) Kinked mica host (kink angle 140°). Note the bulge (serration) of the kink boundary (centre of photo - horizontal). Note the large degree of bulge around the subgrain on L.H.S. It has almost been left sitting in the lattice on the other side of the kink boundary.

3.1A

Crossed polars. Width of field: 55 μm

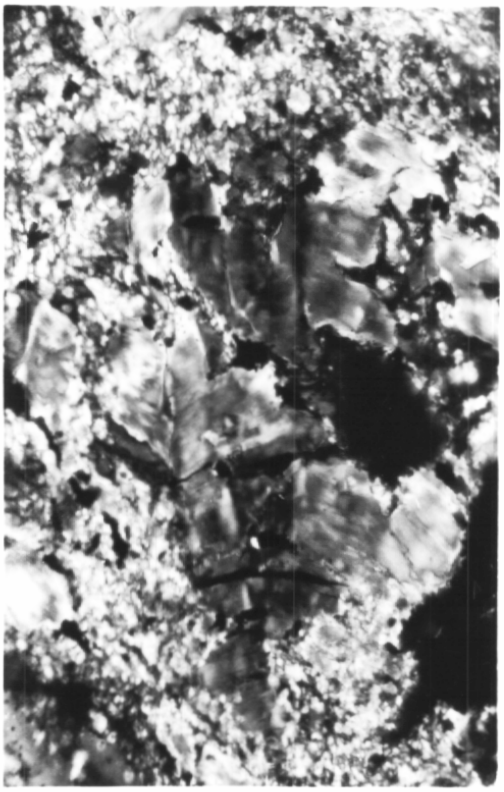

a

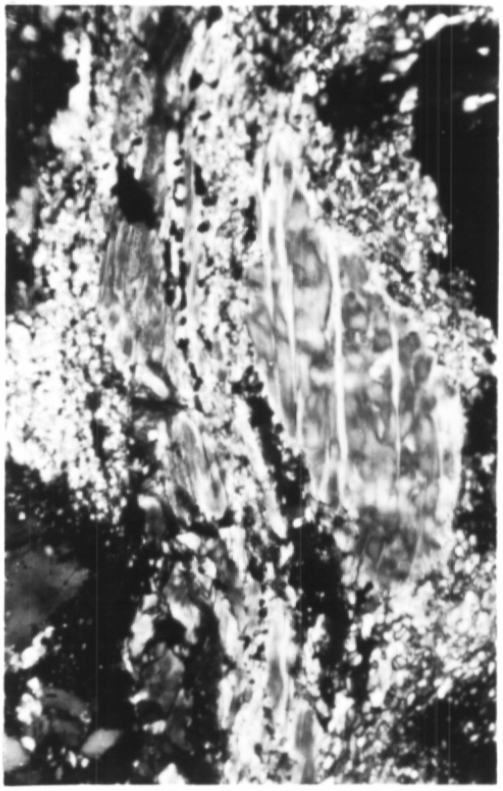

b

c

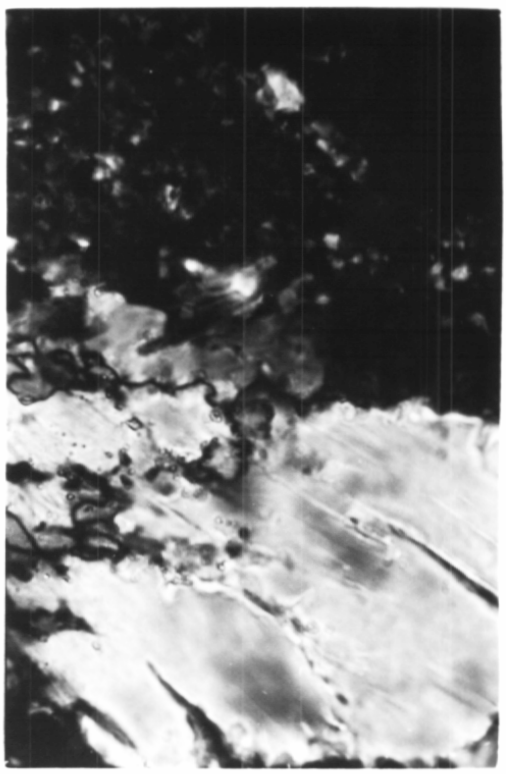

d

FIGURE 4.2

(a) Strongly kink banded mica host grain. The angle of kinking is around 150°. Note the mica subgrains in the exact centre of the photo and the bulge of the kink band boundary around them. The subgrains lie in the deformation band below the bulging boundary. Compare the centre of this photo with the centre of fig. 3.13(a) where a very similar degree of bulge has occurred around subgrains in quartz.

3.1A

Crossed polars. Width of field: 55 μm

(b) Strongly kink banded mica host grain. The centre of this photo is enlarged in figure 4.2(a). The bulge of the kink band boundary around the subgrains can still readily be seen.

3.1A

Crossed polars. Width of field: 138 μm

(c) Mica subgrains and new grains merging together on the edge of mica host grain. The host remnants can be readily seen on the lower L.H.S. Note the progressive increase in misorientation of subgrains towards the top of the photo where there is a mass of new grains. Note the lack of kinking (all the grains are mica). Note the rounded grain boundaries.

3.1A

Crossed polars. Width of field: 55 μm

(d) New mica grains nucleating along a kink in original mica. Some are equidimensional while others are elongate and aligned along the kink.

3.1A

Crossed polars. Width of field: 138 μm

a

b

c

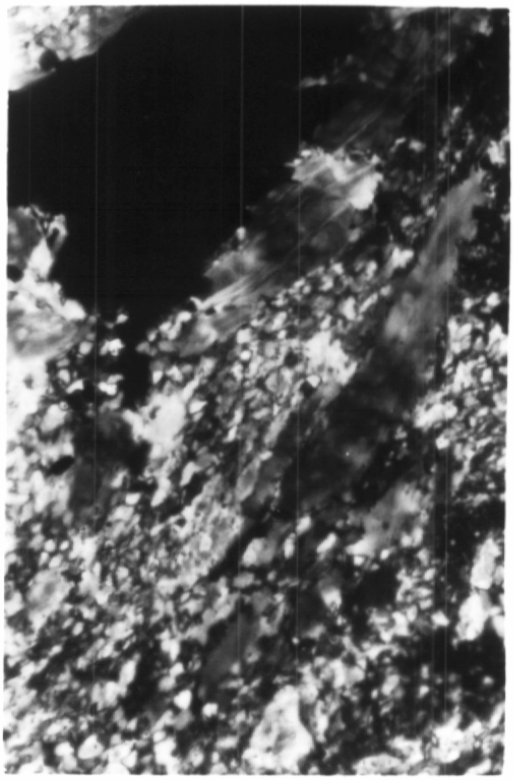

d

FIGURE 4.3

(a) New mica grains nucleating along a kink in, and along the edges of, a deformed mica host. The region of the mica host against the feldspar grain on the lower L.H.S. could contain small subgrains.

3.1A

Crossed polars. Width of field: 138 μm

(b) Mica grains growing within unrecrystallized feldspar.

3.1A

Crossed polars. Width of field: 213 μm

(c) Mica growth within quartz and feldspar aggregates. Note the strong spread of mica in the matrix.

5A

Crossed polars. Width of field: 570 μm

(d) Homogeneous distribution of mica in the homogenization stage mylonite. Note the strong preferred orientation of mica (001).

6A

Crossed polars. Width of field: 570 μm

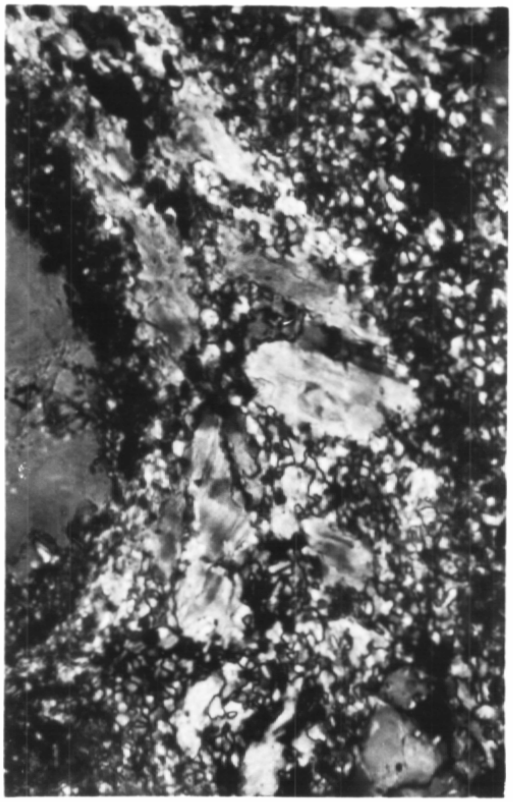

a

b

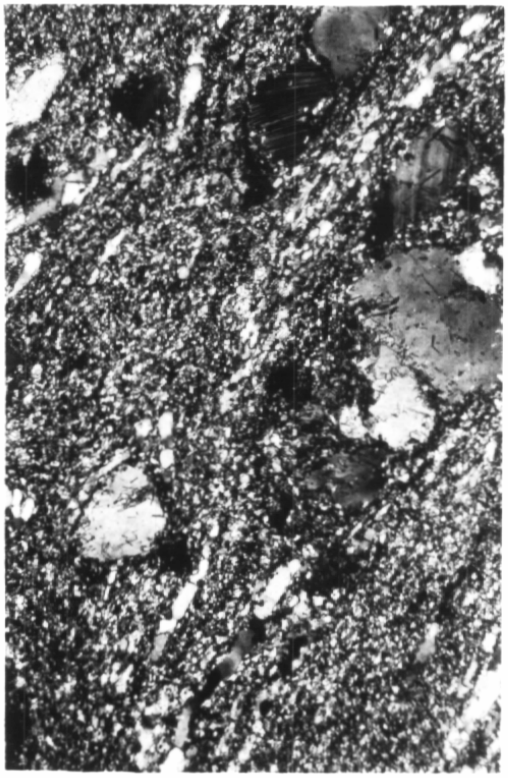

c

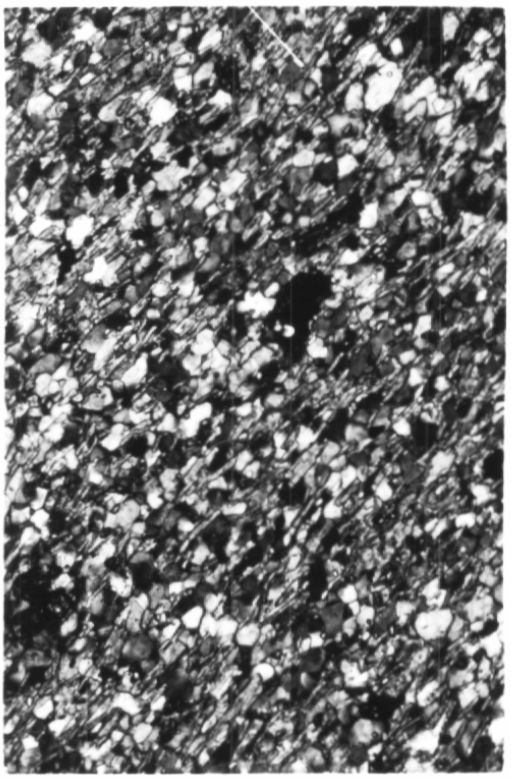

d

FIGURE 4.4

(a) Strain shadowed and kinked original country rock mica.

1B

Plane polarized light. Width of field: 570 μm

(b) Kink banded mica. Note the migration of the kink band boundary (diagonal across photo centre) where the kink angle is slightly more intense. Note the nucleation of small quartz grains on the kink band boundary in this region.

2B

Plane polarized light. Width of field: 213 μm

(c) Interfingering of quartz and mica along mica (001). Note the growth of small micas in the upper half of the photo.

2B

Plane polarized light. Width of field: 570 μm.

(d) An original mica which appears to have deformed considerably by slip along (001).

2B

Crossed polars. Width of field: 1.4 mm

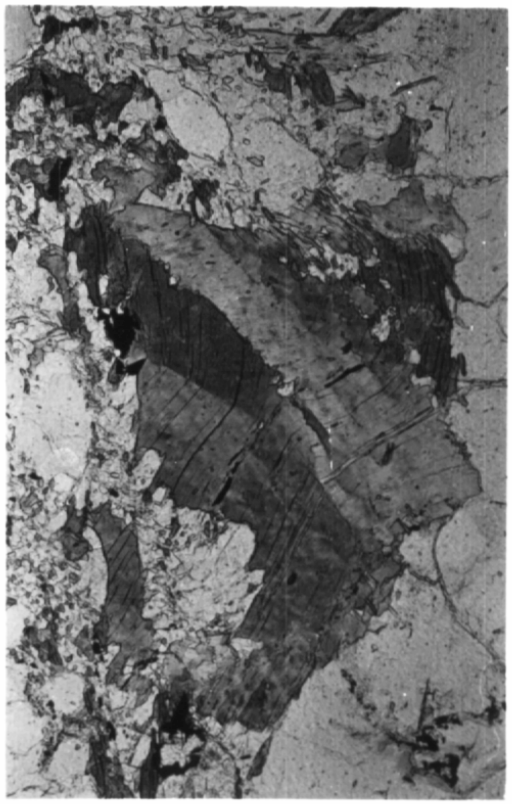

a

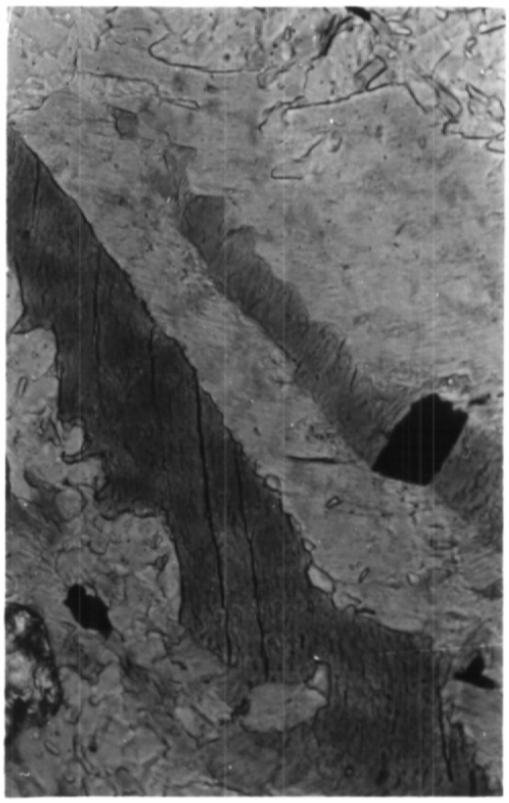

b

c

d

FIGURE 4.5

(a) Deformed host mica grain containing considerable new grain growth along kinks and on its edge. Also contains some quartz and feldspar growth along the kinks. Note the alignment of (001) of the new mica grains along the kinks.

1B

Plane polarized light. Width of field: 570 μm

(b) Kinked host mica containing new grain growth. Note the migration of the kink band boundary (centre of photo, vertical) as the angle of kinking increases and before it disappears into new grains. Note the alignment of new mica grains parallel to the kink band boundary (which is also parallel to S_M)

1B

Plane polarized light. Width of field: 213 μm

(c) Growth of new mica grains along what may be a low angle kink or a narrow kink band. Note the alignment of mica (001) parallel to the zone of new grain growth and across the host (001). Note the growth of quartz and feldspar within this zone.

1B

Plane polarized light. Width of field: 225 μm

(d) New mica grains growing across host mica (001) (the host mica (001) is horizontal). Note the lack of kinking of the host and strong alignment of new grains. They are aligned parallel to the trend of S_M.

1B

Plane polarized light. Width of field: 225 μm

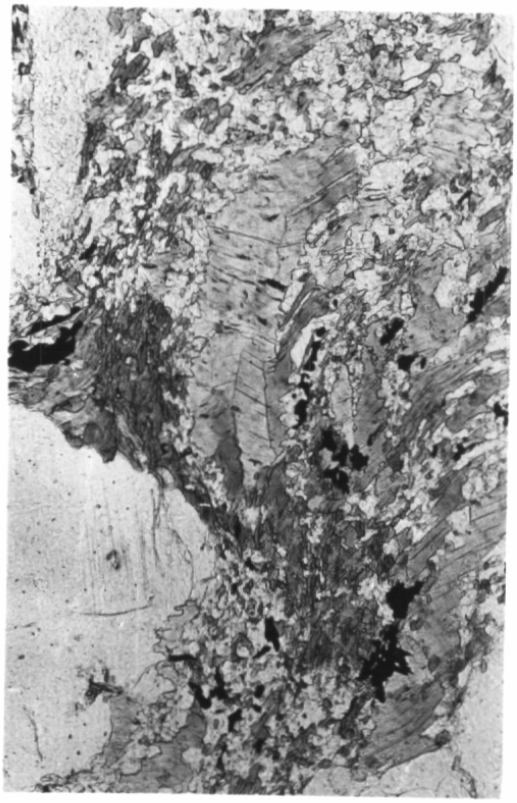

a

b

c

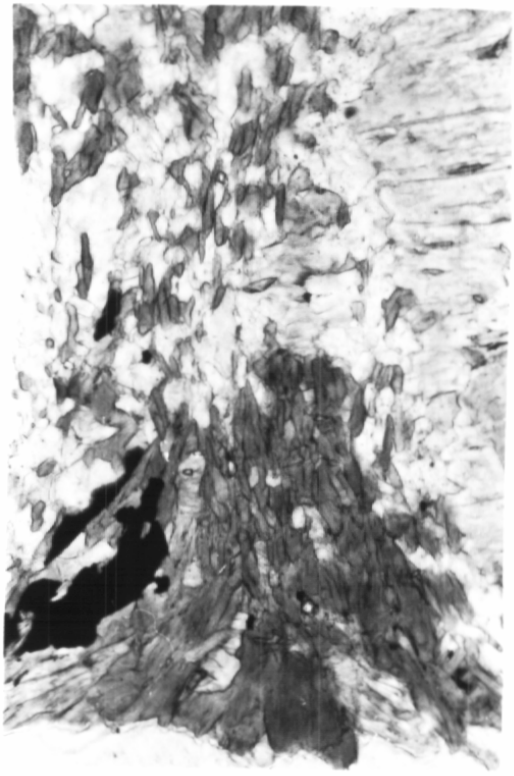

d

FIGURE 4.6

(a) Mica growth stage - amphibolite facies side. Note growth of mica in quartz and feldspar aggregates.

5B

Crossed polars. Width of field: 1.4 mm

(b) Homogenization stage - amphibolite facies side. Note the increased homogenization relative to fig.4.6(a).

6B

Crossed polars. Width of field: 1.4 mm

(c) Slaty mylonite. Note the strong homogeneity and preferred orientation of mica (001).

7

Crossed polars. Width of field: 1.4 mm

(d) This photo shows a biotite which alters along its length (upwards) and recrystallizes as another phyllosilicate. Unfortunately, the strong change in colour along its length as it alters and recrystallizes has not shown up on the black and white photograph. Note the orientation of the new grains across (001) of the old.

4B

Plane polarized light. Width of field: 213 μm

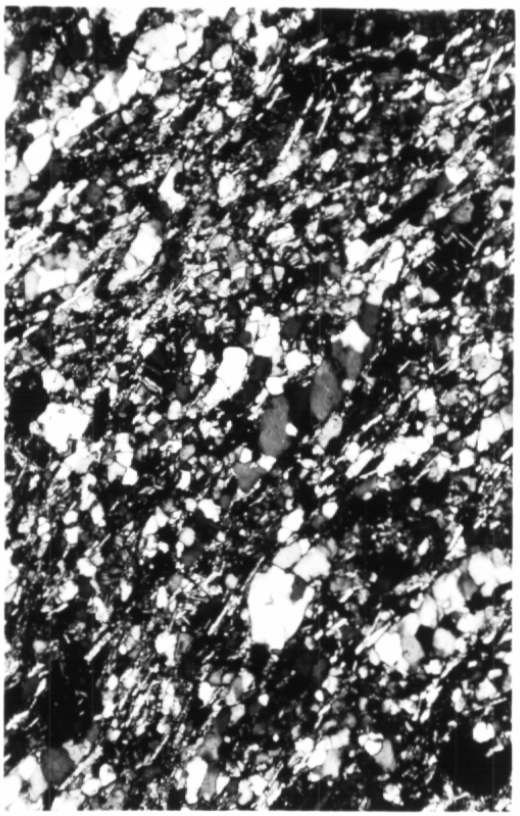

a

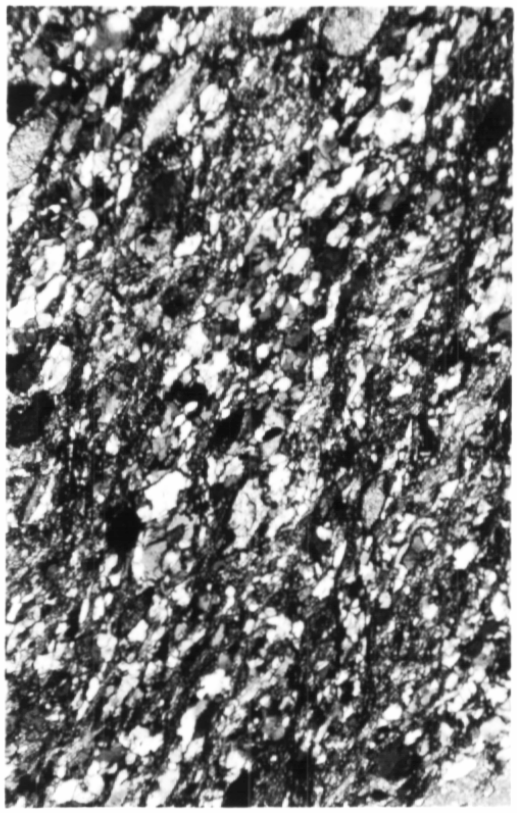

b

c

d

FIGURE 5.1

(a) Strain shadowed, deformation twinned and kinked country rock feldspar. Note the new grain growth along the kinks. Note also the microperthite (lower half of photo).

1B

Crossed polars. Width of field: 570 μm

(b) Strain shadowed, deformation twinned and kinked country rock feldspar. Note the strong birefringence variation near the kink and the microperthite.

1A

Crossed polars. Width of field: 570 μm

(c) Kinked feldspar host. Note the subgrains and new grains along the kink boundary and the bulge of the boundary into the side which shows more strain.

1B

Crossed polars. Width of field: 55 μm

(d) Strongly strain shadowed, deformation twinned and kinked feldspar host grain. Note the new grain growth along the kinks.

4B

Crossed polars. Width of field: 1.4 mm

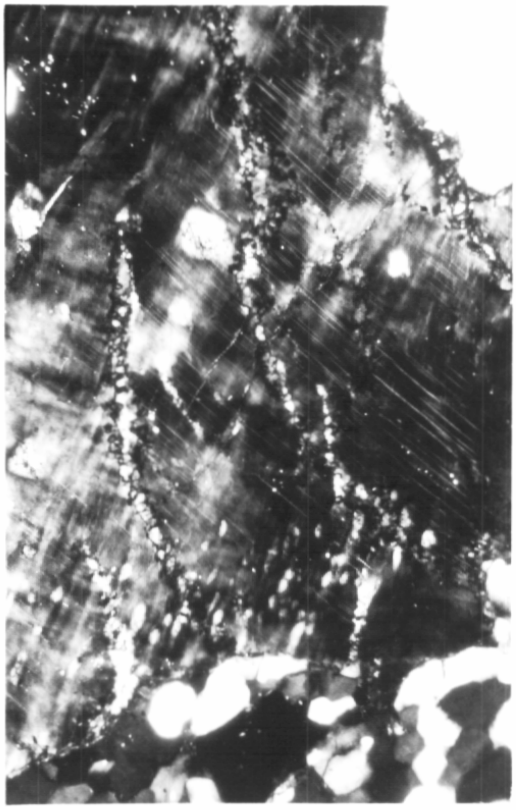

a

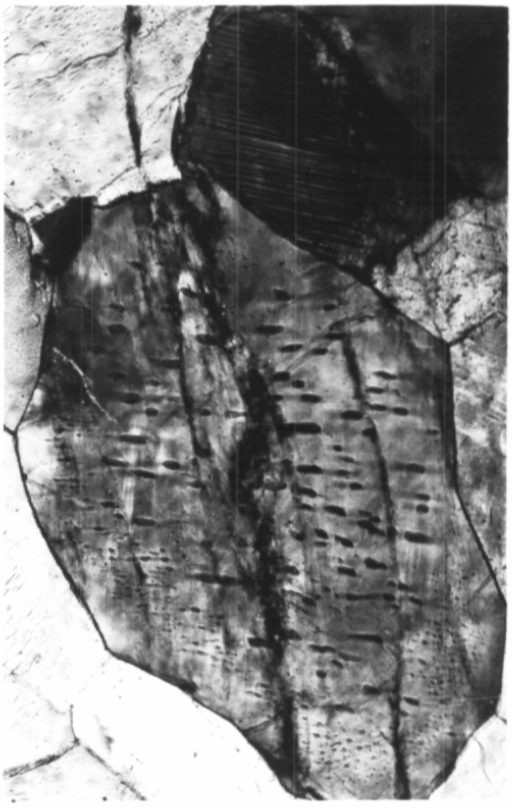

b

c

d

FIGURE 5.2

(a) Strain shadowed, deformation twinned and kinked feldspar host grain. Note the new grain growth along the kinks.

4A

Crossed polars. Width of field: 1.4 mm

(b) Deformation twins aligned symmetrically either side of S_M trend in the remains of a feldspar host grain.

7

Crossed polars. Width of field: 570 μm

(c) Subgrains and new grains within the highly strained edge of a feldspar host. Note the increase in misorientation of subgrains towards the edge (upwards).

1B

Crossed polars. Width of field: 55 μm

(d) Grain boundary bulge between two adjacent feldspar grains, where the boundary is pinned by the walls of subgrains within the host feldspar on either side. Note the increase in the degree of bulge of the boundary from the top of the photo downwards until it runs into new grains near the bottom.

1B

Crossed polars. Width of field: 55 μm

a

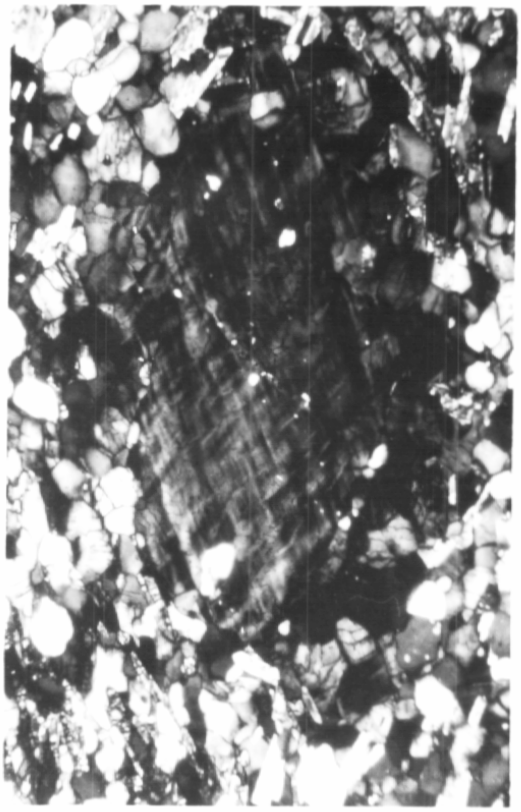

b

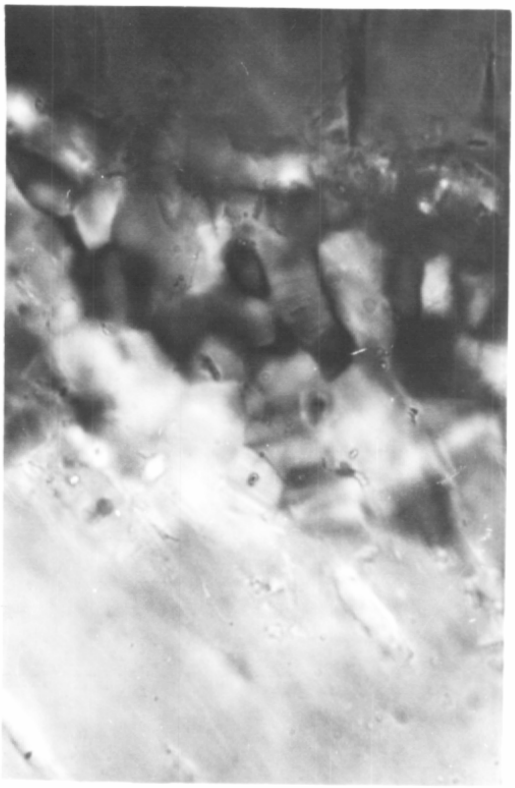

c

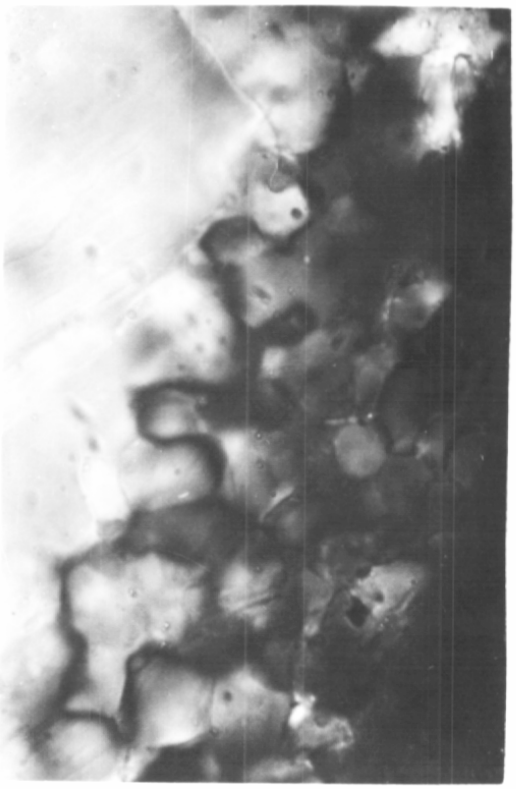

d

FIGURE 5.3

(a) New feldspar grains nucleating along kink boundaries in a feldspar host.

2B

Crossed polars. Width of field: 213 μm

(b) New feldspar grains nucleating along kink boundaries in a feldspar host.

3.1A

Crossed polars. Width of field: 213 μm

(c) New feldspar grains nucleating within a kink band (upper L.H. edge). Note the subgrains (centre, lower R.H. edge).

2B

Crossed polars. Width of field: 55 μm

(d) Subgrains merging with new grains on the intensely strained edge of a feldspar host grain. Note the slightly larger size of the new grains on the R.H. edge.

3.1A

Crossed polars. Width of field: 55 μm

a

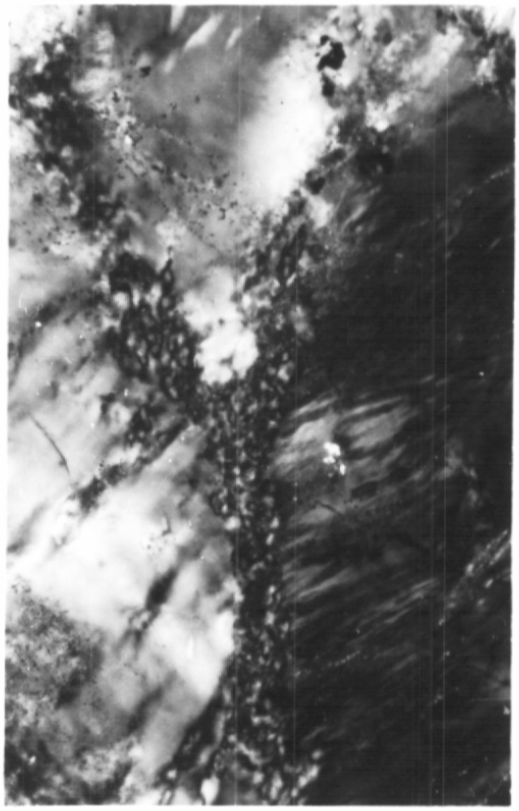

b

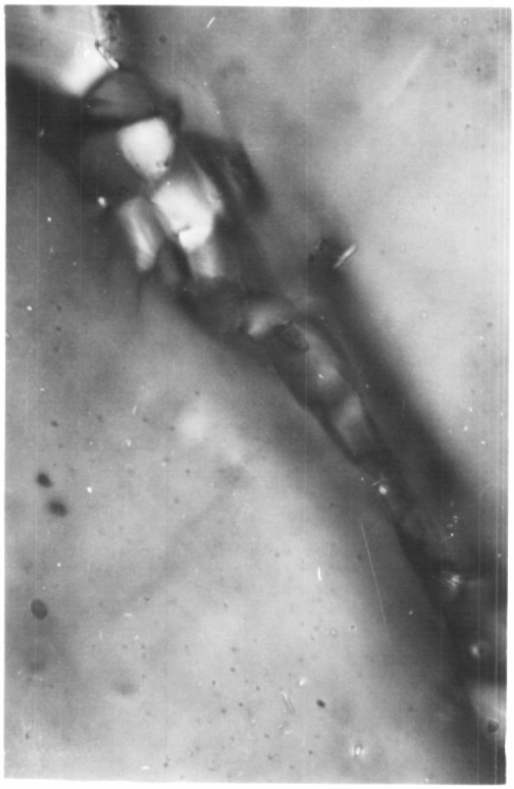

c

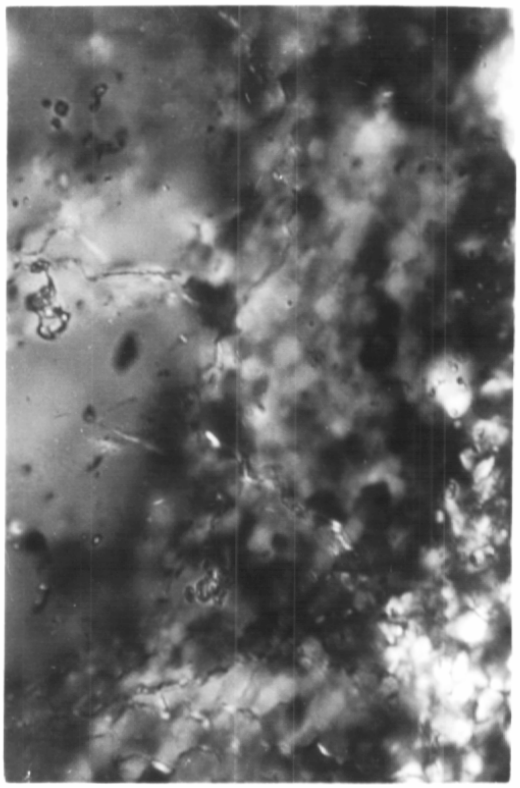

d

FIGURE 5.4

(a) Shows rapid increase in the size of new grains away from the edge of the host grain remains (host remains on L.H.S.).

5B

Crossed polars. Width of field: 138 μm

(b) Shows rapid increase in the size of new grains away from the edge of the host grain remains (host remains on lower R.H.S.).

6A

Crossed polars. Width of field: 213 μm

(c) New grains growing along a deformation twin.

2B

Crossed polars. Width of field: 213 μm

(d) Aggregate of new feldspar grains. Note the rounded to gently curved grain boundaries.

3B

Crossed polars. Width of field: 213 μm

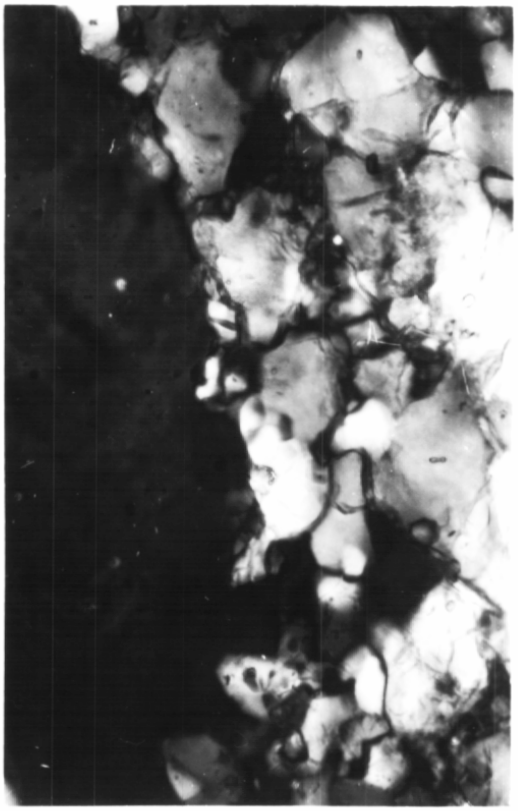

a

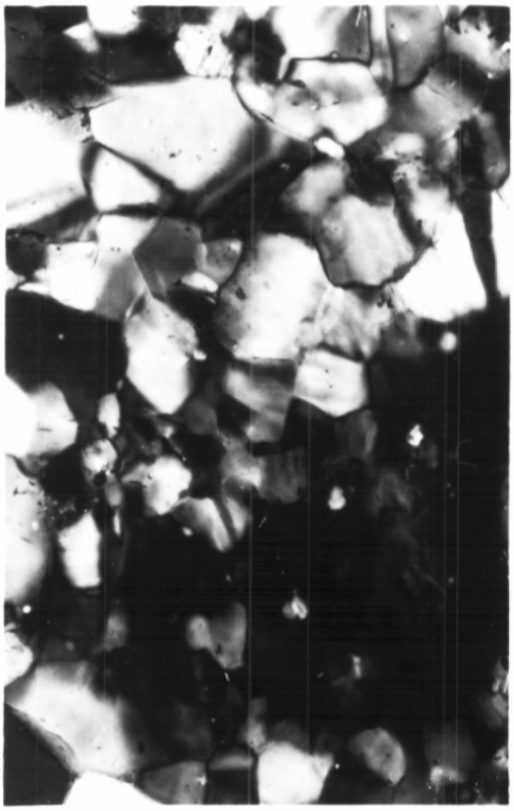

b

c

d

FIGURE 5.5

(a) Aggregate of new feldspar grains. Note the rounded to gently curved grain boundaries.

4A

Crossed polars. Width of field: 138 μm

(b) Aggregate of feldspar grains. Note the mica growth along some of the grain boundaries within the aggregate. Note also the gently curved to straight grain boundaries between adjacent feldspars.

5B

Crossed polars. Width of field: 570 μm

(c) Aggregate of feldspar grains. Note the slight amount of mica growth along grain boundaries within it. Note also the gently curved to straight grain boundaries between adjacent feldspars.

6A

Crossed polars. Width of field: 213 μm

(d) Ellipse shaped feldspar host grain remains in the extremely homogeneous matrix of the slaty mylonite. Note the equidimensional shape of quartz and feldspar grains in the matrix.

7

Crossed polars. Width of field: 1.4 mm

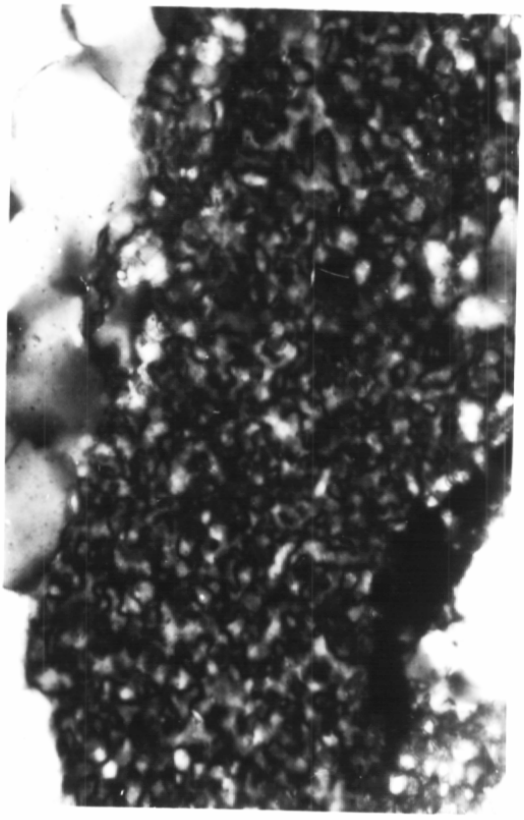

a

b

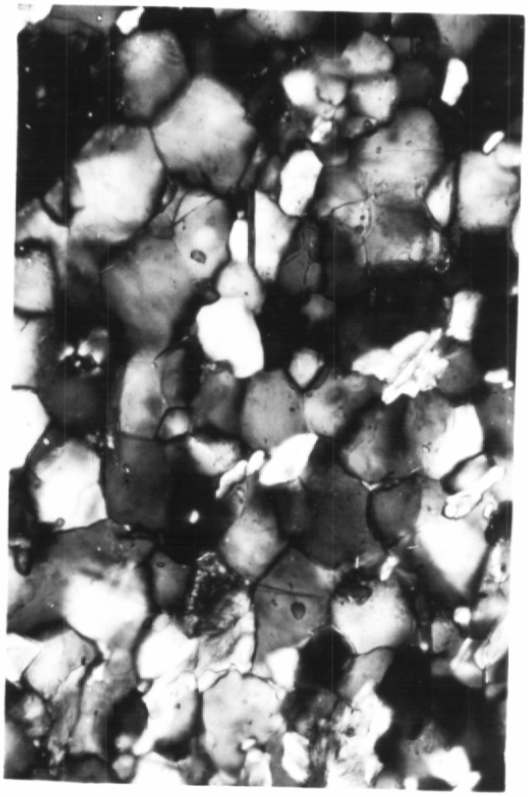

c

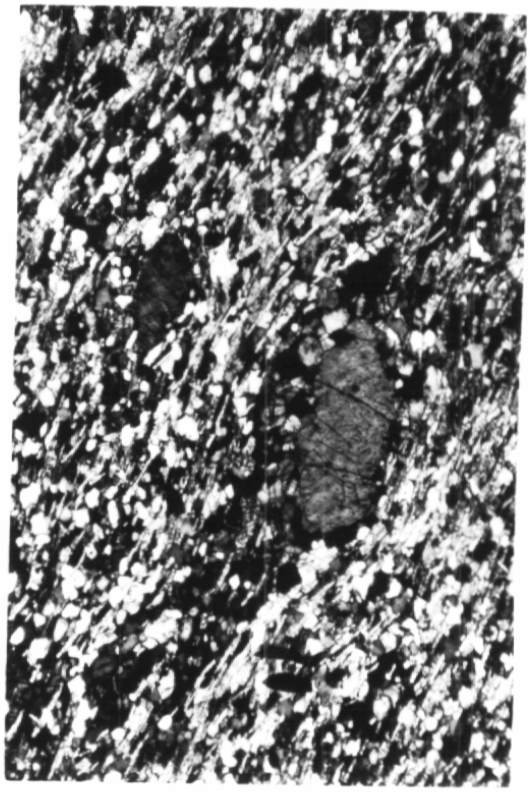

d

THE MAP

A-A is the section from which the specimens for detailed microstructural analysis were collected.

B-B is the section from which the specimens for determining the effect of the $B^{S_3}_{S_M}$ deformation on S_M, were collected.

N.B. The apparent folding of dolerite dykes and much of the bending of geologic boundaries is due to the effect of topographic variation (no topographically contoured maps of the area were available).

STRUCTURAL GEOLOGY BETWEEN ARPARAH AND TOOGUL, MUSGRAVE RANGES